The American Association of Petroleum Geologists Bulletin
V. 60, No. 4 (April 1976), P. 554-565, 9 Figs., 3 Tables

Thickness of Removed Sedimentary Rocks, Paleopore Pressure, and Paleotemperature, Southwestern Part of Western Canada Basin[1]

KINJI MAGARA[2]
Calgary, Alberta T2P OS1, Canada

Abstract The thickness of sedimentary rocks removed by erosion in the geologic past can be evaluated by the use of shale-compaction data, such as the shale transit-time values recorded by sonic logs. The pore pressures in shales also can be calculated using compaction information. Integration of these shale-compaction data with homogenization temperatures of fluid inclusions in quartz infilling of fractures in sandstone, as discussed by Currie and Nwachukwu, makes possible the estimation of the paleotemperature and paleogeothermal gradients in a basin.

Such an integrated study in the southwestern part of the Western Canada basin shows that (1) significant erosion in the geologic past removed as much as 4,600 ft (1,400 m) of the uppermost part of the sedimentary rocks; (2) significant undercompaction and overpressure were present in the deeper part of the Cretaceous section in the past; (3) the *Cardium* sandstone, which has a temperature range of about 140 to 160°F (60 to 71°C) at present, had much higher temperatures of about 300°F (149°C) at the time of maximum burial (before erosion); and (4) the geothermal gradient probably has not changed significantly in the geologic past.

Introduction

Currie and Nwachukwu (1974) recently described a technique to evaluate the subsurface temperature when incipient fractures were made. This technique uses the homogenization temperature of fluid inclusions in quartz infilling of fractures in sandstone. The homogenization temperature is determined by observing the fluid with a microscope while heating the thin section until the fluid bubble disappears. Their study area is in the southwestern part of the Western Canada basin (Fig. 1).

The basic technique used by Currie and Nwachukwu is unique and is probably of practical use in petroleum exploration. Unfortunately, the paleotemperatures and paleogeothermal gradients obtained by them seem to be too low, probably because of their lower estimates of the thickness of eroded sedimentary rocks and pore pressures in the geologic past.

In this paper, an attempt is made to evaluate a more realistic paleotemperature and paleogeothermal gradient for this area, using the homogenization-temperature data, and estimates of erosion and paleopore pressure derived from shale-compaction data obtained from wireline logs. This integrated study may provide useful concepts with regard to hydrocarbon generation, maturation, and migration.

Estimation of Thickness of Erosion

Thickness of sedimentary rocks removed by erosion in the geologic past can be estimated from shale-compaction data. Such estimates are possible because shale compaction is related to overburden load or burial depth, if pore pressure is normal or hydrostatic. Hydrostatic pressure commonly is developed at relatively shallow depths in most sedimentary basins. Therefore, if a shale bed at a given depth within the hydrostatic-pressure zone in an area is compacted significantly more than another shale bed at the same depth in another area where there was no erosion, the former area is interpreted to have been buried more deeply in the geologic past and to have lost some of the uppermost section by erosion. This method cannot apply if the shales are undercompacted, because shale compaction is not a simple function of burial depth in an undercompacted zone.

The level of shale compaction can be determined from the sonic log, because sonic transit time is a function of porosity in a uniform lithology (e.g., shale). The relation between the logarithm of the shale transit time (μs/ft) and depth in the relatively shallow interval of many sedimentary basins, can be approximated by a straight line (Fig. 2A). The pore pressure in this case is known to be hydrostatic. This normal compaction trend extrapolated to the surface, gives a surface transit time value of Δt_o (Fig. 2A), for a situation where there was no significant erosion.

Figure 2B shows a schematic example of the transit time-depth relation where the uppermost section was removed by erosion. The present surface is indicated by a wavy line. If the normal compaction trend in the subsurface is extrapolat-

[1]Manuscript received, March 13, 1975; accepted, August 21, 1975.

[2]Exploration Department, Imperial Oil Limited.

The writer is indebted to Imperial Oil Limited, Canada, and Exxon Production Research Company, U.S.A., for permission to publish this paper, to J. B. Currie of the University of Toronto, Canada, and to F. J. Moretti and D. H. Horowitz of the latter company for important comments. The writer also appreciates the valuable comments made by reviewers for the *Bulletin*.

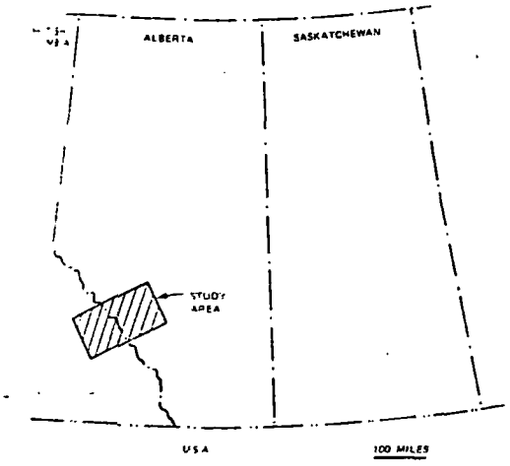

FIG. 1—Map of study area.

ed to the present surface, the surface transit time value ($\Delta t_o'$) will be smaller than the value (Δt_o) for the case in which no erosion occurred. If the normal compaction trend is further extrapolated to Δt_o, the original surface of the sedimentary section can be determined (Fig. 2B). The distance between the present surface and the level at which the extrapolated value equals Δt_o, is the approximate thickness of sedimentary rocks which have been removed by erosion.

In this estimate of erosion, it is assumed that there was no significant rebounding or expansion of sediments during and after erosion, at least not to the extent that such an erosion estimate became erroneous. However, even a minor amount of such sediment expansion may be expected to have a major effect on reducing pore pressure.

The surface transit time value of Δt_o in the case of no erosion, can be determined by two methods. The first method is to determine the normal compaction trends of as many wells as possible in the sedimentary basin in question, and then to extrapolate these trends to the present surface. The maximum transit time value (the least compaction value) among these extrapolated values ($\Delta t_o'$) will be the value closest to Δt_o for no erosion. From extensive studies of the normal compaction trends of the Cretaceous shales in the Western Canada basin, the writer has obtained a maximum surface transit time of about 200 μs/ft in the areas on the northeast, i.e., near the Canadian shield where the amount of erosion is considered to have been small.

The second method is based on the empirical relation between shale porosity and transit time. This relation (Fig. 3) was derived from a study of 14 wells in the Western Canada basin in which both sonic and formation-density logs were run. The shale porosity was calculated from the bulk density, on the basis of shale-grain density of 2.72 gm/cc and water density of 1.02 gm/cc. The porosity-transit time relation for the Cretaceous shales in this area may be expressed as

$$\phi = 0.466 \times \Delta t - 31.7, \qquad (1)$$

where ϕ is the shale porosity in percent and Δt is the shale transit time in μs/ft (Fig. 3). In the earlier paper (Magara, 1973), a different relation was obtained because a grain density of 2.65 gm/cc was used to calculate the porosity. The higher grain density (2.72 gm/cc) seems to be more realistic for shales (Youn, 1974).

The intercept of the thick line with the vertical axis in Figure 3 gives a transit time value of about 68 μs/ft, corresponding to the value for shale grains or matrix. This is the transit-time value where porosity is zero. The line is terminated at the level of 200 μs/ft in the upper right-hand part of Figure 3 because the transit-time values of a clay-water mixture should not exceed the value for water (200 μs/ft). The porosity value corresponding to this termination point is about 62 percent. The relation for porosity values from 62 to 100 percent is shown graphically as a thick horizontal dashed line.

The preceding porosity-transit time relation may be explained in the following manner. The transit time for water, or 100 percent porosity, is about 200 μs/ft. Addition of a small amount (5-10 percent) of clay sediment to the water will produce no significant change in transit time, because the sound essentially will travel through the water, not the clay. The transit-time value will stay at almost the same level until the amount of clay becomes 38 percent of the total bulk volume (or 62 percent porosity). The transit time decreases after this stage as the amount of clay increases (or porosity decreases). This observation in shales is different from that made by Wyllie et al (1956) for sandstones, in which a linear relation is established for the entire range of sandstone porosity (or 0-100 percent).

Figure 4 shows schematic diagrams of shale porosity-depth and transit time-depth relations in the subsurface. The porosity of clay on the sea floor is known to be 70 to 80 percent. The porosity decreases rapidly during the early stages of burial. On the basis of Dickinson's (1953) shale porosity-depth relation in the Gulf Coast area, a porosity of 62 percent would be reached at about 100 ft (30 m). Above this critical depth, the transit time would be about 200 μs/ft as shown in the upper part of Figure 4B. The critical depth, of course, probably will vary in different sedimentary basins. In the interval below this critical depth, the transit time decreases as the shale porosity

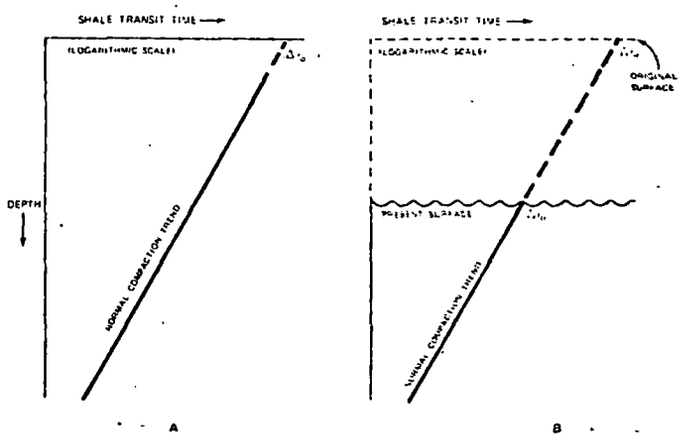

FIG. 2—Schematic diagrams showing normal compaction trends of shale transit time–depth plots in areas of no erosion, A, and with erosion B.

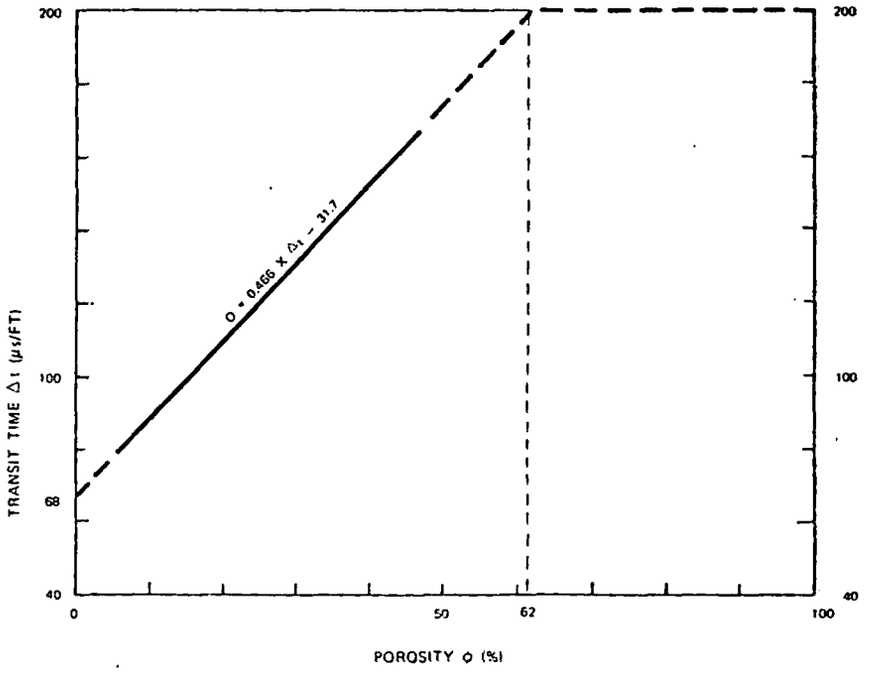

FIG. 3—Empirical relation between porosity and transit time of Cretaceous shales in western Canada.

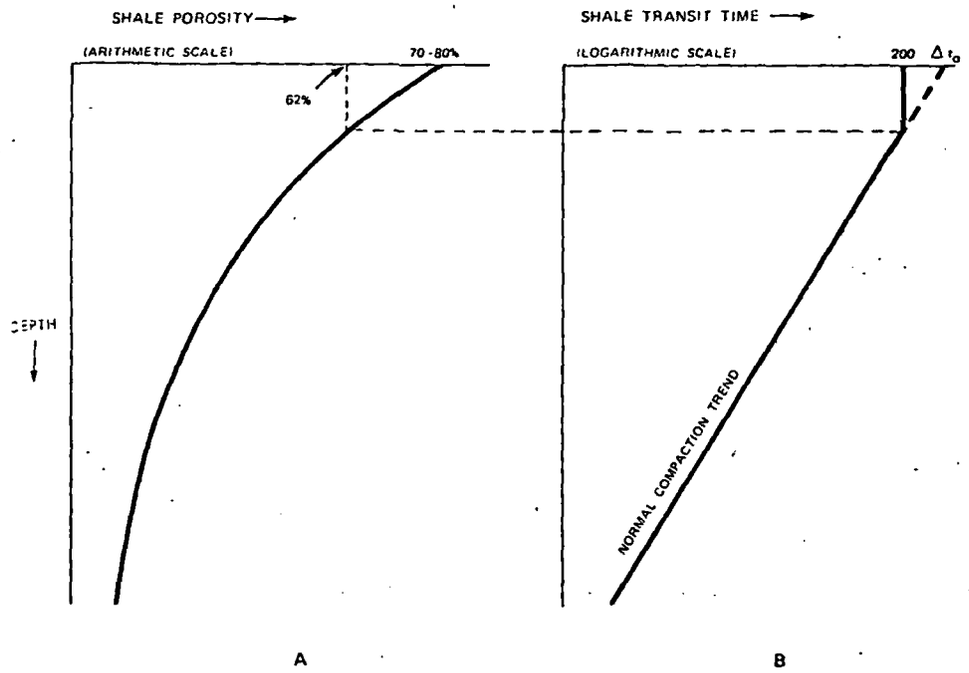

FIG. 4—Schematic diagrams showing shale porosity-depth relation and corresponding shale transit time–depth relation.

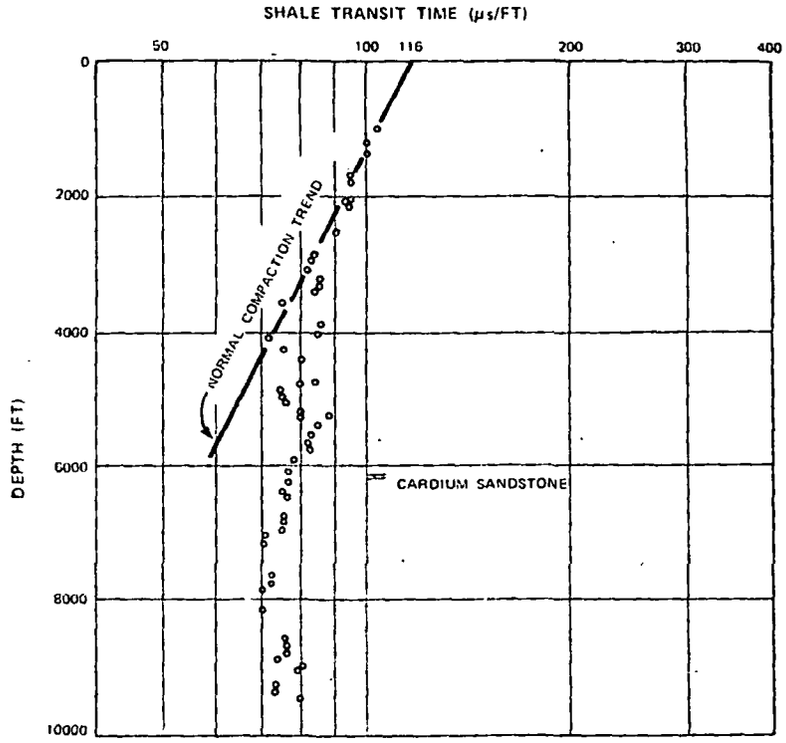

FIG. 5—Shale transit time–depth plot of Pacific Amoco Ricinus 16-29-34-8-W5 well.

decreases (Fig. 4A, B). If the normal compaction trend of transit time established in this deep interval is extrapolated to the surface, we will have a Δt_o value slightly greater than 200 μs/ft. This difference is dependent on the depth of critical compaction (62 percent porosity). From the knowledge of shale compaction in several different basins, the writer believes that the value Δt_o for most basins will not exceed 210 μs/ft.

Therefore, it may be concluded that the value of 200 μs/ft is a good approximation for the surface transit-time value in an area where there was no significant erosion. However, the estimated thickness of erosion using this figure (200 μs/ft) will be the minimum estimate for the reason mentioned previously.

Figures 5-8 show the shale transit time-depth plots on semilog paper for four wells in the Western Canada basin. These are the wells and the adjacent wells in which Currie and Nwachukwu (1974) studied the incipient fractures of the Cardium sandstones. Their results will be discussed later.

Figure 5 is a shale transit time-depth plot for the Pacific Amoco Ricinus 16-29-34-8-W5 well, showing that the shales above about 3,000 ft (910 m) are compacted normally. The normal trend is extrapolated to the surface at 116 μs/ft, suggesting a significant amount of erosion in the geologic past. The thickness of erosion is estimated to be about 4,600 ft (1,400 m), using the technique already discussed (Fig. 2B). The shales below 3,000 ft are undercompacted. This suggests that while the continuous deposition and burial were taking place (before the erosion), the deeper section was undercompacted and overpressured. Most of the overpressure may have disappeared since, because uplift and erosion can be expected to decrease pore pressure. The subsurface temperature will decrease, and the pore space may expand slightly during these events, resulting in the decline of the pore pressure. As a matter of fact, the pressures measured by drill-stem tests in this well are not high. Because of the presence of the undercompacted shales in this well, however, it is evident that there was overpressuring before the erosion.

Figure 6 is a shale transit time-depth plot for the Mobil et al Ricinus 3-5-35-8-W5 well. Based on this plot, 4,200 ft (1,280 m) of erosion is estimated. It was not easy to establish a normal compaction trend for this well because of the lack of a thick shale section at shallow depths. However, the use of the data between 1,500 and 3,500 ft

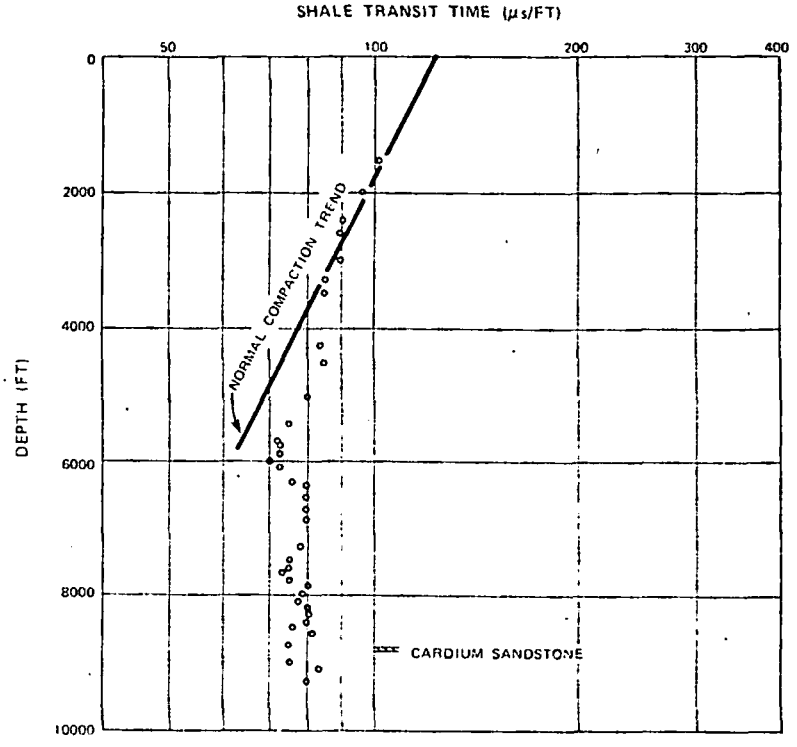

FIG. 6—Shale transit time–depth plot of Mobil et al Ricinus 3-5-35-8-W5 well.

...60 and 1,070 m), and of the slope of the normal ...end established in this general area from data ...om many other wells, made this estimation pos...ible. Shales below about 4,000 ft (1,220 m) are ...ndercompacted so they are considered to have ...een overpressured, at least in the geologic past. The pressure in the deep section at the present ...me is not known.

Figure 7 is a plot of the H.B. Garrington 12-8-36-5-W5 well in which about 3,300 ft (1,010 m) of erosion is calculated. The deeper section is undercompacted only slightly.

Figure 8 shows the plot for the Suptst. Altana H.B. Caroline 10-26-36-6-W5 well which is close to the H.B. Suptst. Altana Garrington 12-24-36-6-W5, one of the five wells studied by Currie and Nwachukwu (1974). The normal compaction trend was determined from the regional knowledge of shale compaction. The calculated thickness of erosion is about 1,700 ft (520 m). The overpressure is known by a drill-stem test of the Cardium sandstone at a depth of 7,200 ft (2,200 m). The pressure of 3,610 psi at 7,200 ft (2,200 m) is about 500 psi in excess of the hydrostatic pressure.

Consider now the possible effect of continental glaciation on the shale-compaction process. If the ice sheet had been added to the sedimentary column as part of the continuous loading history, then its weight certainly will have contributed to additional compaction. If, however, the ice sheet developed after uplift and erosion, shale compaction will not have been affected because the shales already had been "overcompacted" with reference to their depth of burial at that time. The latter is believed to be the case in this area. The fact that the density of ice (0.9 gm/cc) is significantly lower than that of average sediments (approximately 2.3 gm/cc) also must be remembered. In other words, the effect of ice on compaction is believed to be insignificant and is ignored in this study.

Estimation of Paleopore Pressure

As shown in Figures 5-8, there are undercompacted shales in the study area. Within this general area the Cardium sandstones are known to be overpressured at many locations at the present time. However, the degree of pressuring at present is probably less than that in the geologic past. Significant uplift and erosion which took place in this area probably caused a significant decline in pore pressure because of the decrease in

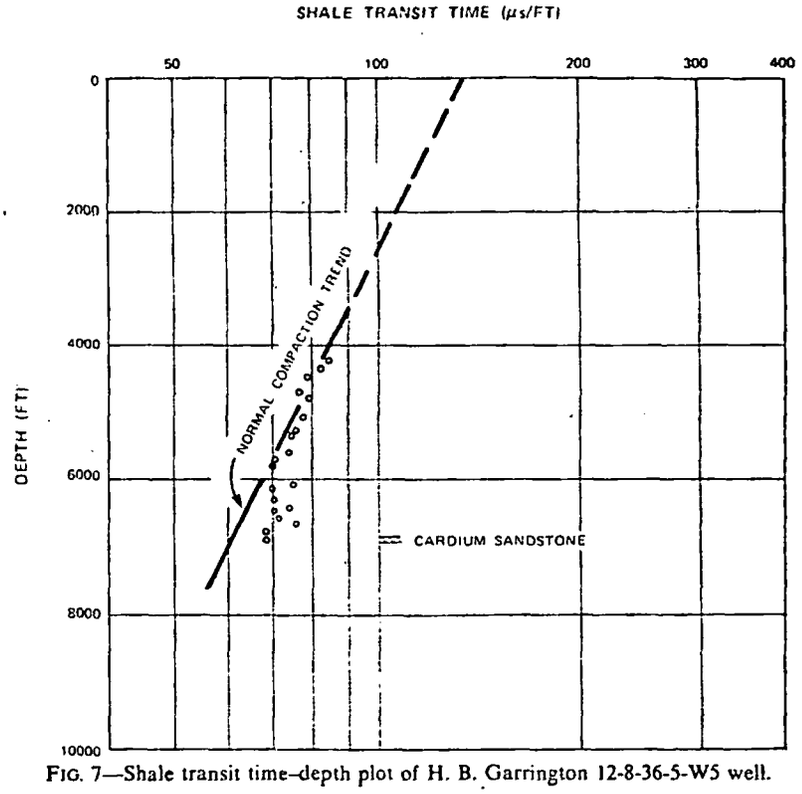

FIG. 7—Shale transit time–depth plot of H. B. Garrington 12-8-36-5-W5 well.

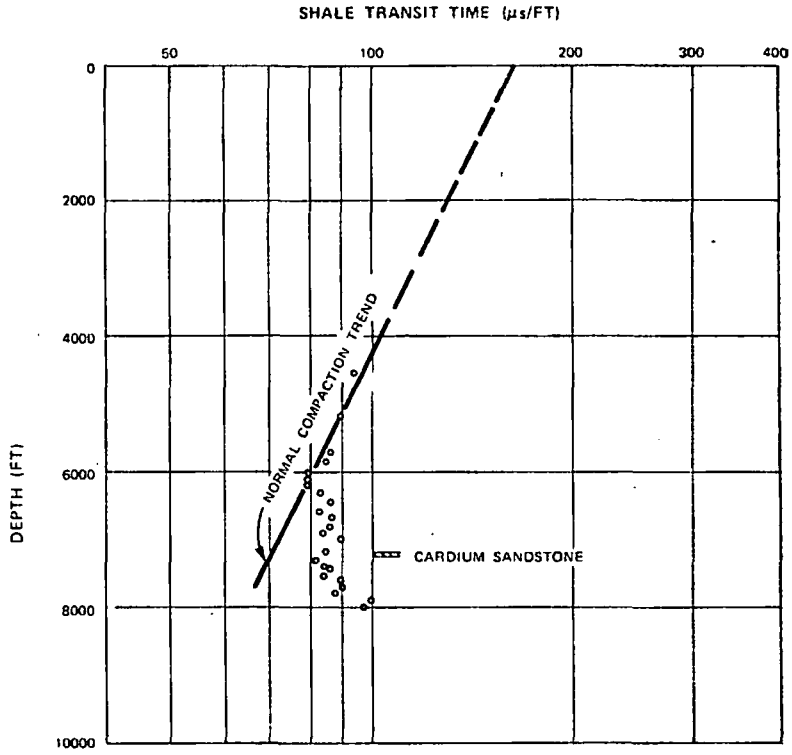

FIG. 8—Shale transit time–depth plot of Suptst. Altana H. B. Caroline 10-26-36-6-W5 well.

temperature and the slight expansion of the pore spaces.

An estimation of the pore pressure in these undercompacted zones before erosion can be made on the basis of knowledge of erosion as discussed previously and on the subsurface transit-time data.

In the well shown in Figure 5, for example, the Cardium sandstone is at a depth of about 6,200 ft (1,890 m). The estimated thickness of erosion is about 4,600 ft (1,400 m). In other words, the Cardium once was buried to a depth of 10,800 ft (6,200 + 4,600 ft) or 3,290 m (1,890 + 1,400 m) before erosion. The shales above and below the Cardium are undercompacted, having a transit time value of about 76 μs/ft. This level of compaction is equivalent to the compaction level at the present depth of about 3,700 ft (1,130 m) in the normal compaction zone. The maximum burial depth of this equivalent level is therefore about 8,300 ft (3,700 + 4,600 ft) or 2,530 m (1,130 + 1,400 m).

From the observations it is possible to make the following burial-compaction model. There was normal compaction during the initial burial from surface to approximately 8,300 ft (2,530 m). Fluid expulsion during this stage was normal. At 8,300 ft the pore-fluids were locked in completely so that there was no further compaction to the maximum burial depth of 10,800 ft (3,290 m). At a later stage the area was uplifted and the uppermost section was removed by erosion. The depth of the Cardium after erosion is about 6,200 ft (1,890 m).

One may ask the following question: what would happen if the generation of these undercompacted shales was "gradual" rather than "abrupt" as assumed in such a model of normal compaction–no compaction? This suggests that fluid expulsion and compaction of these shales may have been continuous during burial with gradual decrease of fluid expulsion and compaction rates with time. The "gradual" model would be quite realistic in many cases. However, the "abrupt" model is simpler and more convenient to use for the estimation of the paleopore pressures. Yet the results obtained by these two different methods are not significantly different. Therefore, the "abrupt" model will be used in this paper.

The pore pressures in the Cardium during the early stages of burial to 8,300 ft (2,530 m) would

TABLE 1. PALEOPORE PRESSURE, MAXIMUM BURIAL DEPTH, AND PALEOPRESSURE/DEPTH OF CARDIUM SANDSTONE AT FOUR LOCATIONS IN WESTERN CANADA

Well	Location	Paleopore Pressure (psi)	Maximum Burial Depth (ft)	Paleopressure/Depth (psi/ft)
A	16-29-34-8-W5 (well shown in Fig. 5)	7,100	10,800	0.66
B	3-5-34-8-W5 (Fig. 6)	10,000	13,000	0.77
C	12-8-36-5-W5 (Fig. 7)	5,200	10,200	0.51
D	10-26-36-6-W5 (Fig. 8)	5,400	8,900	0.61

have been near normal or hydrostatic because the compaction was almost normal. This means that the pore pressure at a depth of 8,300 ft would have been about 3,600 psi using a hydrostatic pressure gradient of 0.44 psi/ft. The rate of increase of pore pressure after this critical stage (or the onset of the restricted fluid expulsion) was discussed by Magara (1975). If there is no aquathermal pressuring effect during burial, the pore pressure would increase at the same rate as that of the overburden pressure, or at about 1 psi/ft. However, this is not the case in most sedimentary basins because the temperature also should increase during burial, resulting in a much higher rate of pressure increase. Magara (1975), in a study of the Gulf Coast shales, estimated the rate of pore-pressure increase since isolation of pore fluids to be about 1.4 psi/ft. Applying this result to the shale in the well being studied, an increased pressure of about 3,500 psi (1.4 × [10,800 − 8,300] psi) above the hydrostatic pressure at the isolation depth (8,300 ft) can be calculated. This means that the Cardium would have been overpressured to about 7,100 psi (3,600 + 3,500 psi) when the maximum burial depth of 10,800 ft (3,290 m) was reached.

The paleopore pressure, the maximum burial depth, and the pressure/depth relation of the Cardium in these four wells were calculated using the preceding method. The results (Table 1) indicate the possible existence of significantly high pressures in the Cardium in the geologic past. The previously mentioned calculation is based on actual shale-compaction data in western Canada and knowledge of aquathermal-pressuring effect obtained in the Gulf Coast area. The validity of applying the aquathermal-pressuring effect observed in the Gulf Coast to western Canada may be a matter for discussion. It is not possible to study such a phenomenon directly in western Canada because of the effect of late-stage disturbance on pore pressure in this area. We can, however, examine the possibility of such a phenomenon on the basis of what is known of the thermal and compaction histories of the area. The pressure generated by the aquathermal effect is a function of at least two important factors: geothermal gradient, and the retention of generated pressure.

Geothermal Gradient

The average geothermal gradient in the Gulf Coast is about 25°C/km (or 1.37°F/100 ft) according to Barker (1972), although it varies widely within this area. The average gradient in the Western Canada basin is about 1.7 to 1.8°F/100 ft (31 to 33°C/km), based on data given by Magara (1973, Fig. 11). This suggests that the aquathermal effect could have been more pronounced in western Canada than in the Gulf Coast because of the higher gradient in western Canada. In other words, applying the results obtained in the Gulf Coast to western Canada would not, at least, cause an overestimation of pore pressures.

The difference of the actual subsurface temperature (not the gradient) in these two areas should not cause a significant difference in generation of aquathermal pressures. This is because the aquathermal pressuring mechanism is related to relative change in temperature since isolation of pore fluids, rather than to actual temperature.

Retention of Generated Pressure

The composition of shales and the level of compaction would be important factors in retaining the generated pressure. Because of lack of data and because both factors probably vary widely within each area, it is not easy to evaluate these factors.

It is assumed that there was no significant compaction of undercompacted shales during and after erosion. Therefore, the paleopore pressure can be calculated from the present compaction data. However, this may not be true always because the pore pressures in these shales probably dropped during and after erosion mainly because of a cooling effect. The decreasing pore pressure would have caused the late-stage compaction of the shales.

In other words, the undercompacted shales at present are more compacted than those in the geologic past (especially before erosion). It follows that the calculated paleopore pressure using the present compaction data and the estimated

TABLE 2. RANGES OF HOMOGENIZATION TEMPERATURE OF CARDIUM SANDSTONE AT FIVE LOCATIONS IN WESTERN CANADA*

Well	Location	Homogenization Temperature °C (°F)
A	16-29-34-8-W5	45-108C (113-226F)
B	3-5-35-8-W5	45-100C (113-212F)
C	12-8-36-5-W5	50-85C (122-185F)
E	12-24-36-6-W5	51-84C (124-183F)
F	10-5-36-5-W5	49-88C (120-190F)

*Determined by Currie and Nwachukwu (1974).

amount of erosion may be the possible lowest estimate.

Therefore the calculated paleopore pressures in the Cardium may be lower than the pressures which actually existed in the geologic past, but may be quite reasonable estimates with our current knowledge of shale compaction. These estimated paleopressures based on shale compaction data are at least more realistic than those by Currie and Nwachukwu (1974). They simply assumed hydrostatic pressures throughout geologic time.

Estimation of Paleotemperature

Currie and Nwachukwu (1974) discussed the results of their research on the homogenization temperature of liquid-gas (or vapor) inclusions in the mineral filling which now occupies some of the fracture openings in the Cardium sandstone. Their objective was to determine the temperature at which fluid inclusions were formed in fracture-filling material (mainly quartz).

They first made thin sections of these quartz fillings which contain fluid inclusions. The thin sections were heated under a petrographic microscope by using a Leitz heating stage, until the bubble in each inclusion disappeared. The temperature when the bubble disappeared was measured and was called the "homogenization temperature."

The same measurement was made for many samples from a single reservoir to obtain a range of temperatures. Then this range of homogenization temperature was introduced into the pressure-temperature-specific volume diagram for water to obtain the range of temperature under subsurface conditions (or under high pressure). The maximum temperature in this subsurface range may be assumed to be close to the temperature when the sedimentary deposits reached the maximum burial depth. In other words, this temperature seems to indicate the temperature of the deposits immediately before significant erosion took place. The minimum temperature in this range would be close to the present subsurface temperature. In this discussion, the fractures and infillings are assumed to have been caused mainly by the changes of the subsurface stress field associated with uplift and unloading.

The ranges of the homogenization temperatures of the Cardium section determined by Currie and Nwachukwu (1974) are shown in Table 2.

Wells A, B, and C in Table 2 are the same as those in Table 1. Well E in Table 2 is only a few miles away from well D shown in Table 1. Well F in Table 2 is not far from well C. Because of their proximity, the latter two sets of wells may be combined to study the subsurface temperature at the time of maximum burial.

As mentioned previously, estimation of the paleotemperatures may be made by using the pressure-temperature-specific volume diagram for water (Fig. 9). The vertical axis shows the pressure in bars and psi, and the horizontal axis shows the temperature both in Celsius and Fahrenheit. The thin diagonal lines indicate the specific volumes (cc/gm) which are reciprocals of the densities (gm/cc) of water.

In well A, for example, the maximum homogenization temperature was 226°F or 108°C (Table 2). This value is shown as A on the bottom horizontal axis of Figure 9. It is assumed in this case that the pressure in the inclusion when the homogenization temperature is determined is zero psi. The estimated paleopore pressure in the Cardium is about 7,100 psi (Table 1). Therefore, point A on the horizontal axis is moved parallel with the equal-specific-volume lines to a new point shown as A′ in Figure 9 corresponding to pressure of 7,100 psi.

The reason for moving point A parallel with the isospecific volume lines is that the volume of the fluid inclusion should be unchanged under subsurface conditions and under the homogenization stage under the microscope. The temperature of point A′ is about 280°F (138°C), which is considered to be the paleotemperature when the Cardium sandstone was buried to the maximum burial depth (10,800 ft, 3,290 m). Assuming that the surface temperature was about 50°F (10°C) at that time, a geothermal gradient of about 2.1°F/100 ft (38°C/km) is calculated.

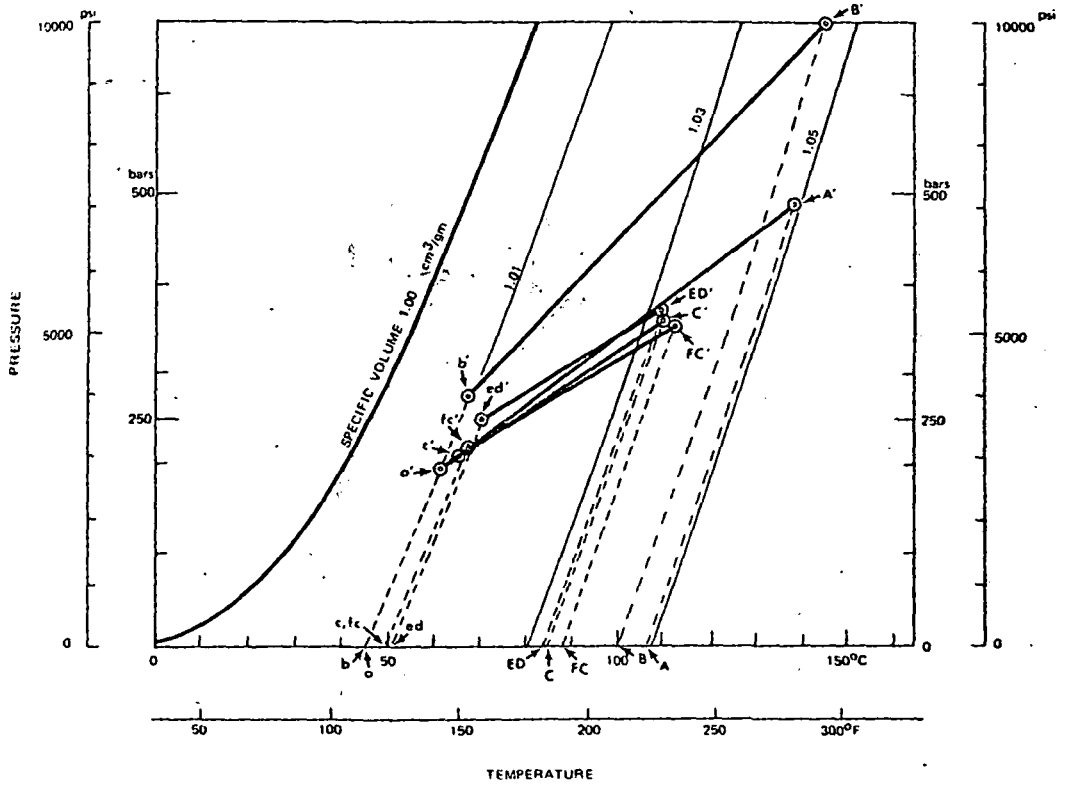

FIG. 9—Graph showing ranges of homogenization temperature of Cardium sandstone and interpreted ranges of temperature and pressure under subsurface conditions at five locations in western Canada. Alphabets refer to wells shown in Tables 1-3.

The minimum homogenization temperature for this well is marked *a* on the bottom axis of Figure 9. The point corresponding to the subsurface condition after erosion is labelled *a'*, which has a temperature of about 142°F (61°C). This temperature is slightly higher than the present temperature of this section. The geothermal gradient is calculated to be about 1.8°F/100 ft (33°C/km) using the average surface temperature of 32°F (0°C), which seems to be a reasonable figure. This gradient is in agreement with the general geothermal gradient observed in this general area (Magara, 1973).

The points for the other wells are also shown in Figure 9 such as indicated by *B-B'*, *b-b'* and so on. In the case of each of the last two wells in Table 2, a combination of the two wells, as mentioned previously, is used for the study, shown as *ED-ED'*, *ed-ed'*, etc., in Figure 9. The calculated temperatures and geothermal gradients are summarized in Table 3.

The results in Table 3 suggest that the Cardium sandstone reached temperatures as high as 300°F (149°C) at the time of maximum burial. Its present temperatures range from 140 to 160°F (60 to 71°C), which is about one-half of the maximum. These estimated paleotemperatures are higher than those given by Currie and Nwachukwu (1974). The reason for this difference is that in their estimate they ignored the importance of the presence of undercompacted shales in this area. They assumed that the pore pressure was hydrostatic at the time of maximum burial. Their method of estimating the thickness of erosion is also quite interpretive, based on an average denudation rate (Currie and Nwachukwu, 1974). The values given in the present paper are believed to be more realistic.

The estimated geothermal gradient in Table 3 shows that the gradient generally was higher at the time of maximum burial than that at present. In this calculation an average surface temperature of 50°F (10°C) was used for the time of maximum burial. (This suggests that the average temperature of the sediments at the time of sedimentation was higher than the present surface

TABLE 3. ESTIMATED TEMPERATURE AND GEOTHERMAL GRADIENT OF CARDIUM SANDSTONE AT TIME OF MAXIMUM BURIAL AND AT NEAR PRESENT***

	At Maximum Burial Depth		Near Present	
Well	Temperature °F	Gradient* °F/100 ft	Temperature °F	Gradient** °F/100 ft
A	280	2.1	142	1.8
B	293	1.9	153	1.4
C	230	1.8	154	1.8
ED	230	2.0	160	1.8
FC	234	1.8	151	1.7

*Based on the surface temperature of 50°F.
**Based on the present average surface temperature of 32°F.
***For locations of wells A, B, ...F, refer to Tables 1 and 2.

temperature.) If, however, the surface temperature was higher than 50°F (10°C), the geothermal gradient must have been lower. The other important factors affecting the interpretation of the geothermal gradient are the estimates of eroded thickness and the paleopore pressure, discussed previously. If the thickness of erosion was greater than estimated, the paleogeothermal gradient would have been lower than estimated. This is because the burial depth would have been greater but yet the paleotemperature would not have been much higher. However, if the paleopore pressure was higher than estimated, because of the possible late-stage compaction of undercompacted shales and the possible underestimation of aquathermal pressuring effect as discussed previously, the actual paleotemperature and, therefore, the paleogeothermal gradient would have been higher than the writer's estimate (see Fig. 9).

Although estimates of thickness of erosion and on paleopressure made in this paper are believed to be more accurate than those made by Currie and Nwachukwu, the estimated geothermal gradients at the time of maximum burial shown in Table 3 may include both positive and negative errors. In any case, there seem to be more factors possibly causing positive errors on the paleogeothermal gradient than factors causing negative errors. Thus, it appears that the actual paleogeothermal gradient would have been lower than the preceding current estimates.

From these observations and interpretation, it appears that the geothermal gradient probably did not change very much in the geologic past. Currie and Nwachukwu's estimate showed the changes of the gradient from 1.9 (maximum burial) to 1.1 (near present) °F/100 ft (35 to 20°C/km) in some wells (see their Fig. 6). These differences are probably caused by their lower estimation of erosion and pore-pressure. Their interpreted near present geothermal gradient of 1.1°F/100 ft (20°C/km) is considerably different from the present geothermal gradient of 1.7 to 1.8°F/100 ft (31 to 33°C/km) in this area (Magara, 1973). This lower value (1.1°F/100 ft) seems to have resulted from the use of the high surface temperature value of about 59°F (15°C). The present surface temperature extrapolated from the subsurface data in this area is approximately 32°F or 0°C (see Magara, 1973, Fig. 11). In their Figure 6, Currie and Nwachukwu indicated the geothermal gradient lines to be straight lines, on the assumption that the pore pressure has been hydrostatic (or that pore pressure is a linear function of depth). If the pore pressure was abnormal and its abnormality varied in the geologic past, the geothermal gradient lines must be curved rather than straight lines.

Conclusions and Comments

1. The maximum burial depth of a section can be estimated by using shale-compaction data. In this paper, sonic logs were used for this study.

2. The difference between the estimated maximum burial depth and the present burial depth of a section gives the thickness of erosion which occurred in the geologic past. The calculated thickness of eroded sediments in the current study area of the Western Canada basin is as much as 4,600 ft (1,400 m).

3. The pore pressure at the time of maximum burial may be evaluated using the shale-compaction data and the current knowledge of the effect of aquathermal pressuring. In the deeper section of the Cretaceous formations in this area, shales are undercompacted in comparison with the overlying normally compacted section. This suggests that, at least in the geologic past, the deeper sections were overpressured. The amount of such paleo-overpressure in the shales above and below the Cardium sandstone is estimated to have been as high as 10,000 psi for the maximum burial depth of 13,000 ft (3,962 m). The corresponding pressure/depth value, therefore, may have been about 0.77 psi/ft.

4. The homogenization temperatures of fluid inclusions in quartz infillings of Cardium fractures determined by Currie and Nwachukwu

(1974) are reexamined in this paper to obtain more realistic paleotemperatures of this sandstone by using the data on thickness of erosion and paleopore pressure. The result suggests that the temperature of the Cardium was as high as 300°F (149°C) at the time of maximum burial.

5. The paleogeothermal gradient evaluated from the previously mentioned information shows that the gradient at the time of maximum burial may have been slightly higher than that at present. Because most of the possible errors involved in this calculation tend to increase the geothermal gradient of the past, the estimated gradient may be too high. Therefore, it is believed that the geothermal gradient has been relatively unchanged. This conclusion is different from that of Currie and Nwachukwu who interpreted that the gradient changed significantly in the past. Their assumption that pore-fluid pressures in the geologic past were hydrostatic seems to be unrealistic because of the presence of the undercompacted shales in this area. Their estimation of thickness of eroded sedimentary rocks based on average denudation rate also may be unrealistic.

6. Evaluation of such factors as the maximum burial depth, the thickness of erosion, the paleopore pressure, and the paleotemperature and paleogeothermal gradient, as discussed in this paper, may provide useful information for petroleum exploration because these factors can be related to generation, maturation, and migration of hydrocarbons.

References Cited

Barker, C., 1972, Aquathermal pressuring; role of temperature in development of abnormal-pressure zones: AAPG Bull., v. 56, p. 2068-2071.

Currie, J. B., and S. O. Nwachukwu, 1974, Evidence of incipient fracture porosity in reservoir rocks at depth: Canadian Petroleum Geology Bull., v. 22, p. 42-58.

Dickinson, G., 1953, Geological aspects of abnormal reservoir pressures in Gulf Coast Louisiana: AAPG Bull., v. 37, p. 410-432.

Magara, K., 1973, Compaction and fluid migration in Cretaceous shales of western Canada: Canada Geol. Survey Paper 72-18, 65 p.

——— 1975, Importance of aquathermal pressuring effect in Gulf Coast: AAPG Bull., v. 59, p. 2037-2045.

Wyllie, M. R. J., A. R. Gregory, and L. W. Gardner, 1956, Elastic wave velocities in heterogeneous and porous media: Geophysics, v. 21, p. 41-70.

Youn, S. H., 1974, Comparison of porosity and density values of shale from cores and well logs: Master's thesis, Univ. Tulsa.

GEOTHERMAL ENERGY: AN UNDEVELOPED CANADIAN RESOURCE?

by

G.D. GARLAND

University of Toronto

INTRODUCTION

That the earth itself is a reservoir of thermal energy has been recognized for centuries. The increase in temperature with depth, observed in mines and boreholes, is evidence of an internal heat source, from which heat is escaping to the earth's surface. Most of this heat is believed to be produced by radioactive elements in the outer part of the earth, but a portion may represent residual original heat. However, while the total rate of energy loss is very large: 3.2×10^7 megawatts, much greater than the rate of energy expended in earthquakes, the density of the thermal flux is, except in unusual regions, very small. Through more than 99% of the earth's surface, the heat flux is of the order of 1 microcalorie per cm^2 sec, far too small to be of use to man. It is only in the remaining 1% of the area that unusual conditions combine to give a much higher flux. These areas of higher density of geothermal energy have been utilized for many years in Iceland and Italy, and in more recent times in New Zealand, the United States and other countries. There has not yet been a commercial development of geothermal sources in Canada, except, of course, for medicinal hot-water baths.

The purpose of this paper is to assess the possible importance of geothermal sources upon the Canadian energy situation. Even if geothermal energy is not utilized in this country for some years, the extension of developments in the western United States and Mexico will change the continental energy balance, with implications for this country. In order to show the natural conditions that are required to produce a geothermal field, and the installations that are involved in harnessing it, brief descriptions of fields in Italy, New Zealand and Iceland will be given and the possibility of similar conditions existing in Canada will be discussed. A description will also be given of a newly-proposed process, which involves the artificial circulation of water into areas that are not natural geothermal fields.

EXAMPLES OF GEOTHERMAL AREAS

Larderello, Italy Natural steam wells were known in this area, south of Volterra, at least as early as the eighteenth century. In 1777 the wells were developed for their boric acid content, and borax was extracted. The first use of the thermal energy came in 1904, when a steam-driven generator producing 40 h.p. was installed. Today, about 160 wells are drilled into the field, to a maximum depth of 1600 m., and these produce steam at the rate of almost 3,000,000 kg. per hour (Burgassi 1964). A most important feature of the Larderello field is that the steam is dry, many wells producing superheated steam at temperatures of the order of 200°C. The steam is used to drive the turbines of generators, producing electric power at the rate of 380,000 kw.

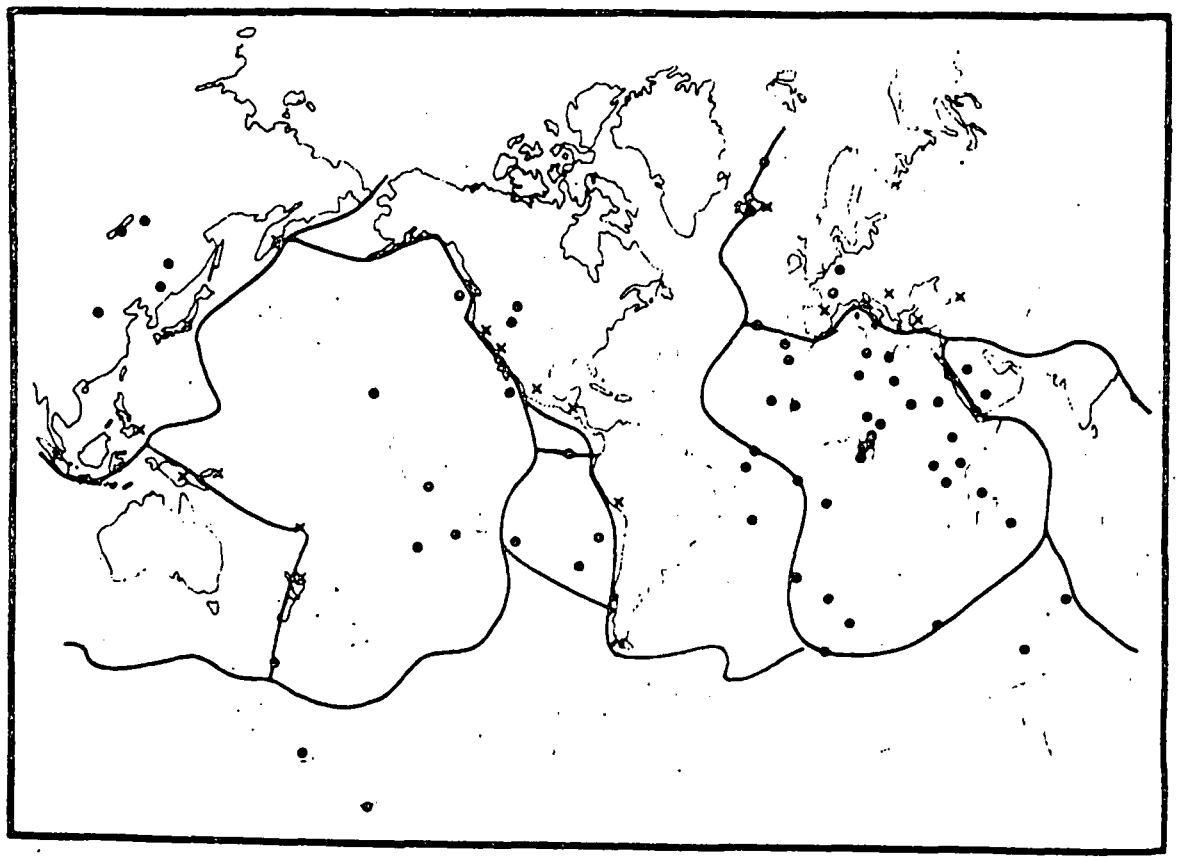

Fig. 1. Developed geothermal areas of the world (crosses) in relation to plate boundaries and hot spots (circles).

Geologically, the area is one generally associated with young volcanism, although volcanic rocks are not exposed in the immediate vicinity of Larderello. The field itself is located on a upfaulted block within a sedimentary basin. This basin contains a thick sequence of permeable anhydrite overlain by an impermeable clay, and it is believed that this combination is of great importance in determining the nature of the field.

Wairakei, New Zealand The Wairakei field is located within a zone of active volcanoes, which extends for 300 km. across North Island. (Healy, 1964). Development of the field began in 1950, and about 100 wells have now been drilled. Electric power is in production at the rate of about 150,000 kw., to be increased eventually to 250,000 kw.

Geologically, the field is located on a local upfaulted block within an area of subsidence. The aquifer is a pumice breccia, capped by a relatively impervious mudstone, which is itself overlain by young volcanic rocks. One deep well has passed through the aquifer into underlying young volcanic rock, which is believed to be related to the source of heat.

The most striking difference between the Larderello and Wairakei fields is that while the former produces superheated, dry steam, the Wairakei wells produce fluids of varying thermal quality, ranging from hot water to saturated steam. This property is believed to be related to the lateral extent of the porous reservoir rock, which, in the case of the Wairakei field, allows cold ground water to mix with the steam in various proportions.

Iceland Iceland is an island formed entirely of volcanic rock, lying on the axis of the mid-Atlantic Ridge. Hot water springs and natural outlets of steam have been known for many years, and have been utilized for domestic heating for decades. Application of geothermal energy for power production began with the design of a 15,000 kw. generating station in the Hengill area near Reykjavik.

Heat sources in Iceland are divided into low temperature and high temperature types (Bodvarsson 1964). Low temperature sources are characteristically hot-water springs, producing water at a temperature of 100°C, and often arranged in linear patterns, suggestive of structural control along faults. High temperature sources, which produce steam, are restricted to the neo-volcanic zone of most recent volcanic activity. There is evidence, from the isotopic content of the water, that it is of surface origin, rather than juvenile water released in the volcanic process. In this regard, the fields are similar to others, and a reservoir, capable of permitting fluid circulation, must be present. As sedimentary rocks are not present, the reservoir porosity must be provided by fractures in the volcanic rocks.

Bodvarsson has estimated the total potential of the Icelandic thermal areas at 300 megawatts. The present utilization of geothermal energy for heating is equivalent to 60,000 tons of coal per year.

Descriptions of other geothermal areas of the world may be found in Ruiz Elizondo (1964) and McNitt (1965).

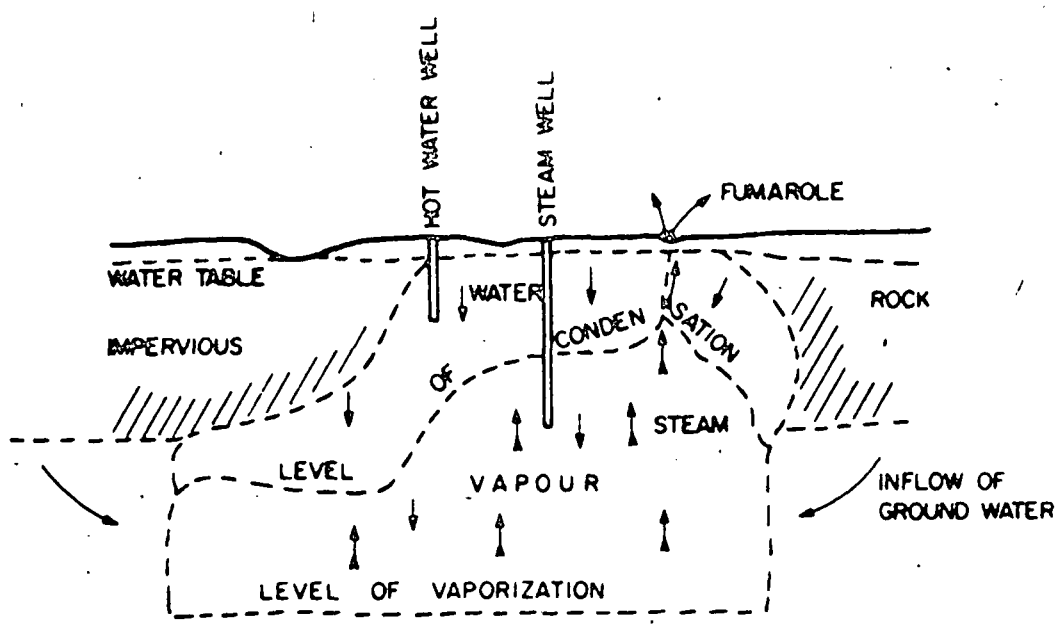

Fig. 2. A vapour-dominated geothermal system (after White et al).

PHYSICS OF GEOTHERMAL AREAS

The above examples have shown some common features, which are typical of all geothermal areas: proximity to geologically young volcanism, transport of heat to the surface by hot water or steam produced from surface water, the presence of a porous aquifer to permit the circulation of the water and to provide the reservoir.

The global distribution of regions of young volcanism is now rather well understood in terms of plate tectonics (Fig.1). Most volcanic areas occur near the boundaries of the rigid plates, into which the outer part of the earth appears to be divided. Very often, these regions are also areas of high seismic activity. Plate motion is believed to be controlled by some system of convection in the mantle of the earth, the currents rising and spreading under oceanic ridges, and drawing the plates down under subduction zones. Recently, however, it has been proposed (Wilson and Burke 1972) that the convection system is complicated by the presence of plumes, which carry heat and material to the surface, and whose relation to a general convection system is not yet understood. Plumes may be recognized by the outpouring of unusual volumes of volcanic rock, as in the case of Iceland, a plume on a ridge, or Hawaii, the result of a plume beneath the interior of a single plate. Potential geothermal areas are therefore to be expected either near plate boundaries, or in conjunction with plumes beneath the interiors of plates.

The surface expression of these areas varies greatly in intensity, from springs of moderately hot water, to outpourings of steam. White et al (1971) have discussed the mechanics of geothermal reservoirs with the aim of clarifying the distinction between vapour-dominated (i.e. steam), and fluid dominated fields. Figure 2 shows their model of a vapour-dominated system. Heat is carried upward from hot rock by a water convection system. Closer to the surface, the reduction in pressure permits water to boil. This depth forms the lower margin of the main body of the reservoir. In the main reservoir, steam and water coexist. Closer to the surface, steam condenses and heat is carried by both water and steam. Steam may escape to the surface along major channels. If the supply of surface or ground water is too great, the large vapour-dominated region of the reservoir may not develop. The difference in type of field is therefore determined by the effectiveness of the cap rock, and the extent of porosity in the reservoir. In fields such as Larderello, and also the Geysers, California, the inflow of water relative to the heat supply is controlled, so that steam predominates.

An alternative representation of a geothermal reservoir is by means of a "pipe model", in which the cross-sectional areas and velocities are indicated. Figure 3, adapted from Elder (1965) shows such a model for Wairakei. A notable feature is the range of times involved in the recharge and recirculation systems. While the figures shown represent estimates only, there is evidence from isotopic studies on the time required for water to circulate (Hulston 1964). Measurements on Wairakei water show that 92% of the water from the field is meteoric, and the tritium content of this water is so low that the time it has spent in the earth must be considerably

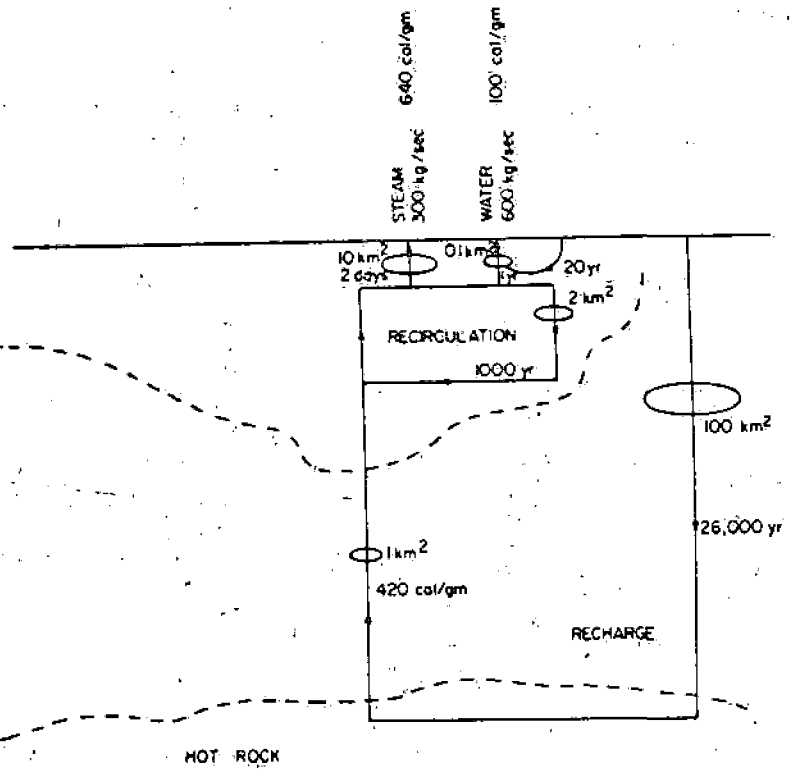

Fig. 3. Pipe model representation of circulation in a geothermal system (after Elder).

greater than one half-life of tritium (125 years). The total volume output of the Wairakei field would be provided by only 5% of the present annual rainfall in the catchment area of the field.

EXPLORATION AND PROVING

While the distribution of young volcanic rocks gives a broad guide to the regions in which to explore for geothermal fields, it is necessary to have methods to localize the search. Fortunately, a number of the methods of geophysical prospecting are immediately adaptable, since the reservoirs are nothing more than regions of anomalous physical properties. Measurements of the electrical conductivity of the crustal rocks, which can be made from the earth's surface, from a powerful exploration tool. The conductivity of rocks increases with temperature, so that the elevated temperature of a geothermal area can be detected directly. Early experiments were conducted in Iceland (Bodvarsson 1964), and electrical methods of exploration are now widely employed. In some regions, there is a correlation between minor seismic activity and geothermal areas. The monitoring of seismic noise by networks of portable seismographs will, in those cases, indicate the most promising locations. In the United States about $50 million per year are currently spent on the geophysical search for geothermal areas.

However, as in the search for oil and minerals, the location of a geothermal anomaly does not mean that a commercial resource is present. It is necessary to evaluate the total rate of output of heat from the area, and also to consider the thermal quality of the fluids (temperature of water, and energy content per unit mass, or enthalpy, of the steam). Within the bounds of a potential field, heat is discharged by conduction through the soil, by convection from water surfaces, in steam from steam vents (fumaroles), in hot water from springs, and by seepage to streams. Methods have been developed, particularly in New Zealand (Dawson 1964) for assessing the importance of each of these, using only shallow augur holes. The potential of a new area may be estimated before more expensive drilling is undertaken.

THE HARNESSING AND ECONOMICS OF GEOTHERMAL POWER

Electrical production at the major fields is by means of steam-driven turbines. In the case of a dry-steam field such as Larderello, the design of suitable generators is relatively straightforward. The more common situation is that typified by Wairakei (Armstead 1964), where different wells in the field produce steam at different pressures and of different degrees of saturation, or simply hot water. In these cases, the generating plant must be carefully designed to optimize the utilization of the different fluids. At Wairakei, hot water is only used if, when its pressure is reduced to an intermediate level, it boils ("flashes") to produce steam. The plant (Fig. 4) has been designed to handle natural steam at two pressures, or the steam produced by flashing.

In considering the economics of geothermal power generation, a number of factors, not encountered in other systems, must be considered.

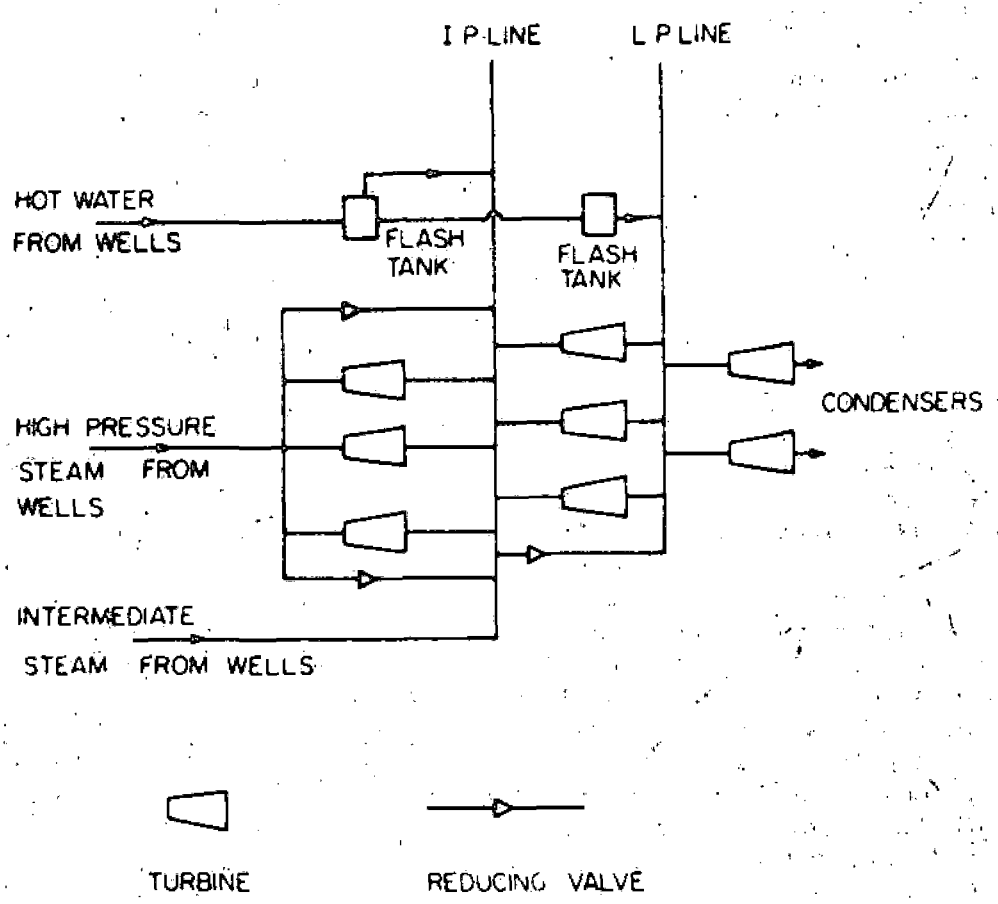

Fig. 4. Utilization of fluids of differing thermal quality, in New Zealand (after Armstead).

These include the estimated lifetimes of the field, and of individual wells, the deterioration of the fluid-handling system by dissolved substances, the cost of disposal of waste hot water, and the possible income to be derived by separation of valuable dissolved substances.

Geothermal fields, like all exploitable sources of resources, must have finite lifetimes, but because all known fields are still in production, there is very little evidence on the time scale. There is evidence, from Maori legends (Healy 1962) that no gross changes in temperature have occured at Wairakei in one thousand years, and the geological evidence would support the existence of hydrothermal activity there for the past million years. Much more serious is the finite lifetime of individual wells, since the drilling of new wells constitutes a recurring charge in the exploitation of a given field. Decrease in the productivity of a well is believed to result from a decrease in the porosity of the surrounding rocks, provoked by the deposition of dissolved substances in the pores. The experience at Larderello (Chierici 1964) has been that the flow of a well decreases as an inverse power of time; for the average well, the production is reduced to 10% of the initial value in 20 years. Taking this rate of decrease, and estimating the cost of re-drilling, Chierici gave the costs of geothermal power production in Italy as follows (30 megawatt geothermal plant; 300 megawatt fuelled plant; 1960 prices).

	Geothermal	Fuelled Electrical
Installation per kw	\$130. - \$150.	\$110. - \$120.
Operation per kwh.	0.12 - 0.13 ¢	0.06 - 0.07 ¢
Fuel or steam " "	0.08 - 0.09 ¢	0.50 - 0.55 ¢

While initial installation and operation costs are higher, the freedom from fuel costs makes the geothermal operation very attractive, in this case. Similar figures are available for the Geysers area in California, where the installation this year will reach 412 mw. (two-thirds of the requirements of San Francisco) and thereby surpass Larderello. Installation costs are quoted as \$110/kw, and total operation, including steam, as 0.35¢/kwh. The installation at the Geysers is projected to be increased to 1300 mw. by 1980. It must be emphasized that both installation and operation costs would be higher for the "wet" type of field, as at Wairakei. In Iceland, the cost of energy for domestic heating has been given as 0.35 cents per kwh. (Bodvarsson and Zoëga 1964).

It will be seen that the experience of those countries advanced in the use of geothermal power shows that installations in the range of 60 -220 megawatts are effective and efficient. The required production rate of steam or hot water to provide the energy for this is indeed impressive. For example, the experience at Larderello shows that 9 kg. of steam are utilized to produce 1 kwh of electrical energy. The required production rate for a 100 mw. installation is thus 1×10^6 kg. per hour of steam equivalent to 24000 tons per day. For a field producing hot water (at 200°C) instead of steam, approximately three times as much water would be required, because of its lower enthalpy.

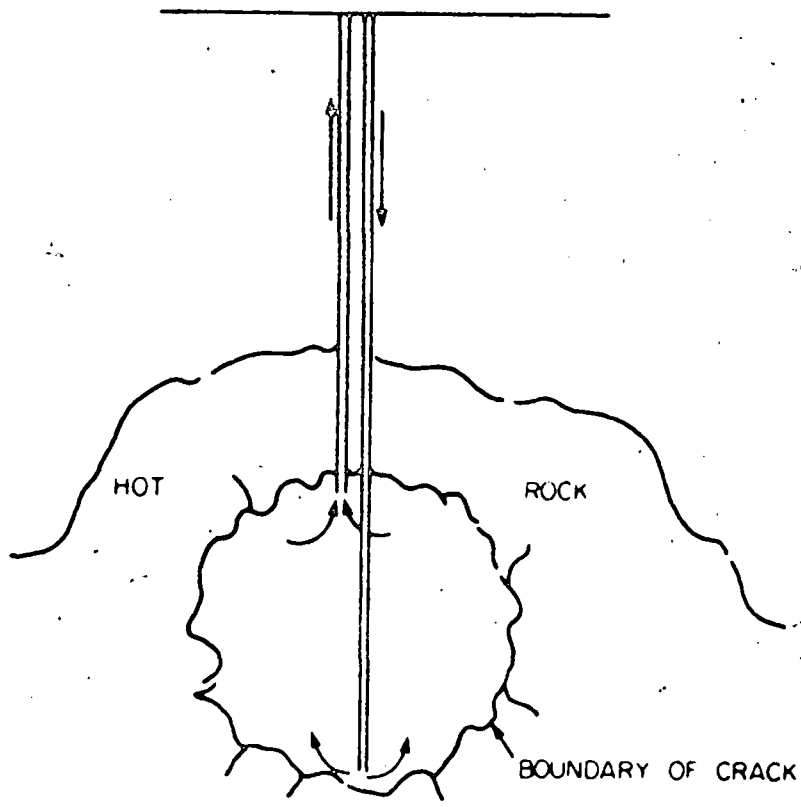

Fig. 5. Proposed artificial recharge system.

The output mentioned for the Larderello plants corresponds to an overall efficiency of about 16%, in terms of the energy content of the steam. It is interesting to note that this is just about one half of the efficiency of an ideal engine operating between the input and exhaust temperatures of 250°C and 80°C respectively.

To date, the disposal of waste hot water has probably not been a major factor of expense, but with increasing consciousness of the problems of thermal pollution, it could well be a factor in the future. Obviously, large volumes of hot water, often heavily charged with dissolved substances, cannot be discharged into fish-bearing streams. Geothermal plants are, of course, free of other forms of pollution.

A PROPOSED SYSTEM USING ARTIFICIAL RECHARGE

It is evident from the descriptions of natural geothermal areas that special, and fortuitous, combinations of circumstances are required: a source of heat near the earth's surface, and the correct combination of porosity and impervious cap rock to provide a reservoir. The utilization of geothermal energy would be much more widespread if the earth's heat could be extracted from other regions, where these conditions do not all exist. For example, there are numerous areas in western North America, where the outflow of heat is greater than the worldwide average, presumably because of recent igneous activity, but the reservoir conditions do not exist. A recent proposal (Robinson et al 1971) is based on the idea of producing an artificial reservoir system in such areas. Imagine a large-diameter (40 cm.) hole bored into a region of relatively hot rock, at a depth of perhaps 5 km. (Fig. 5). The average geothermal gradient is about 30°C per km., but in regions where the heat flow is twice normal, temperatures of the order of 300°C would be reached at this depth. Water at high pressure (1500 psi) is forced into this hole, to produce, according to preliminary experiments, a thin, circular crack lying in a vertical plane. A second large-diameter hole is drilled to reach the crack at a higher level, and water is circulated between the deep and shallower hole. Calculations show that heat could be extracted at the rate of approximately 90 megawatts for 20 years, before cooling of the rock rendered the source inefficient. However, during this time cooling of the rock could well produce subsidiary fractures, which would increase the area of contact between water and rock, actually rendering the system more efficient with time. Energy could be extracted at the rate of 90 megawatts by the circulation of 2 million gallons of water per day, assuming an input temperature of 50°C and an output temperature of 250°C. Once circulation is begun, it is expected to continue, requiring only the pressure resulting from the different densities of hot and cold columns. The hot water would return to the surface at a pressure above atmospheric and could be flashed to produce steam.

The possibility of achieving such an artificial recharge system depends principally on two critical factors: the development of economic systems for the drilling of deep, large-diameter holes, and the effectiveness of the pressure-induced cracking process. There is hope for the first, in

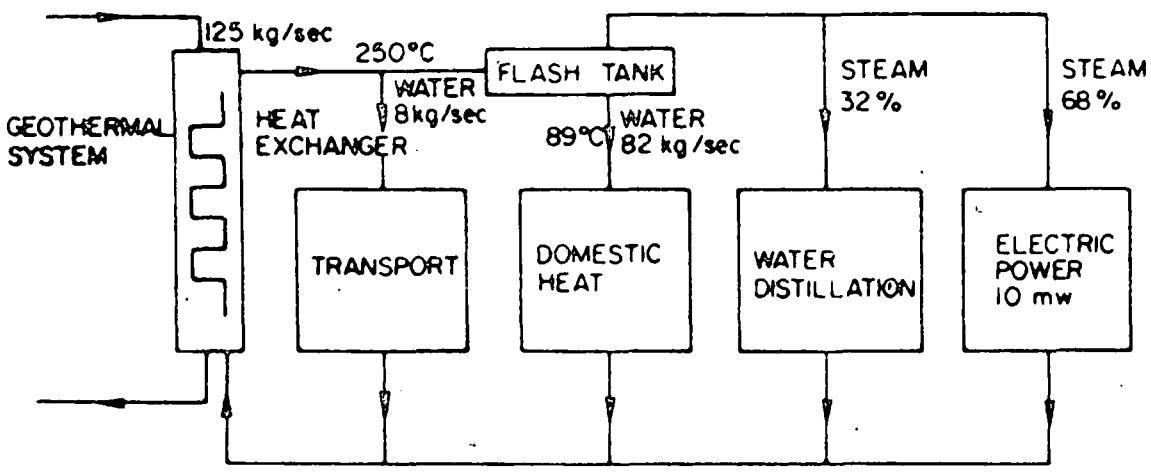

Fig. 6. Use of natural steam to provide total energy requirements for a community (after Robinson et al).

the form of a nuclear-powered electric melting drill. While the second problem has been studied on the laboratory scale it appears impossible to be certain of the outcome in the real earth before deep holes are drilled, and the technique tried. Further theoretical studies (Harlow and Pracht 1972) support the validity of the assumptions, in particular the importance of secondary thermal fracturing of the rock.

If the system is feasible, Robinson et al propose that the hot water be flashed, to produce steam for a generator of 10 megawatts (Fig. 6). The remaining water could be used for domestic heating, and possibly even to power vehicles driven by steam - turbine engines. (The flow of hot water shown in Fig. 6 for Transport is that required to power 10,000 vehicles for 30 miles per day). The complete installation, from the two wells, could provide the energy requirements for a community of 10,000 people.

THE PROSPECTS IN CANADA

The experience from other countries shows that active geothermal areas are invariably associated with geologically recent volcanism. As we have noted, the latter activity is usually related to plate boundaries, or to intra-plate plumes. In Canada, young volcanism is characteristic of the western Cordillera, near the western limit of the Americas plate (Fig. 1). Isolated plumes have not yet been recognized in this country. Before turning to the Canadian possibilities in detail, let us note again that future geothermal developments along the western margin of the Americas plate, are almost certain to have an impact on the continental energy resource picture, and there an indirect effect on the Canadian situation.

In the Canadian Cordillera the volcanism has been discussed by Souther (1970). Of great significance to possible sources of geothermal energy is his recognition of belts of Quaternary (i.e. younger than approximately one million years) volcanoes (Fig. 7). Most of these volcanoes are small cinder cones, whose active life was apparently short. The youth of some of them is remarkable. A flow and cone at Aiyansh, B.C. west of Hazetton, has been dated at 220 ± 130 years, while Mt. Edziza, southeast of Telegraph Creek, is known to have erupted at least three times in the past 1800 years. The structure in the vicinity of Mt. Edziza suggests that a situation favourable to a geothermal field may exist, with faults and fractures providing the porosity. According to Souther, the region is one which was first subject to compressive stresses, producing thrust faults. A change in the stress system led to a condition of tension, permitting the formation of a downfaulted block, on which the volcanic cone is situated.

Measurements of heat flow in the Canadian Cordillera are in progress, by the Earth Physics Branch, Department of Energy Mines and Resources. Jessop and Judge (1971) have reported the relatively high value of 1.86×10^{-6} cal/cm^{2}sec for Penticton in southern British Columbia. The extension of heat flow measurements into the neo-volcanic zones will be most important. Even if natural geothermal fields are not located, the outlining of regions of high heat flow (approximately 2×10^{-6} cal/cm^{2}sec or greater) will indicate the possible locations of future artificial-recharge instal-

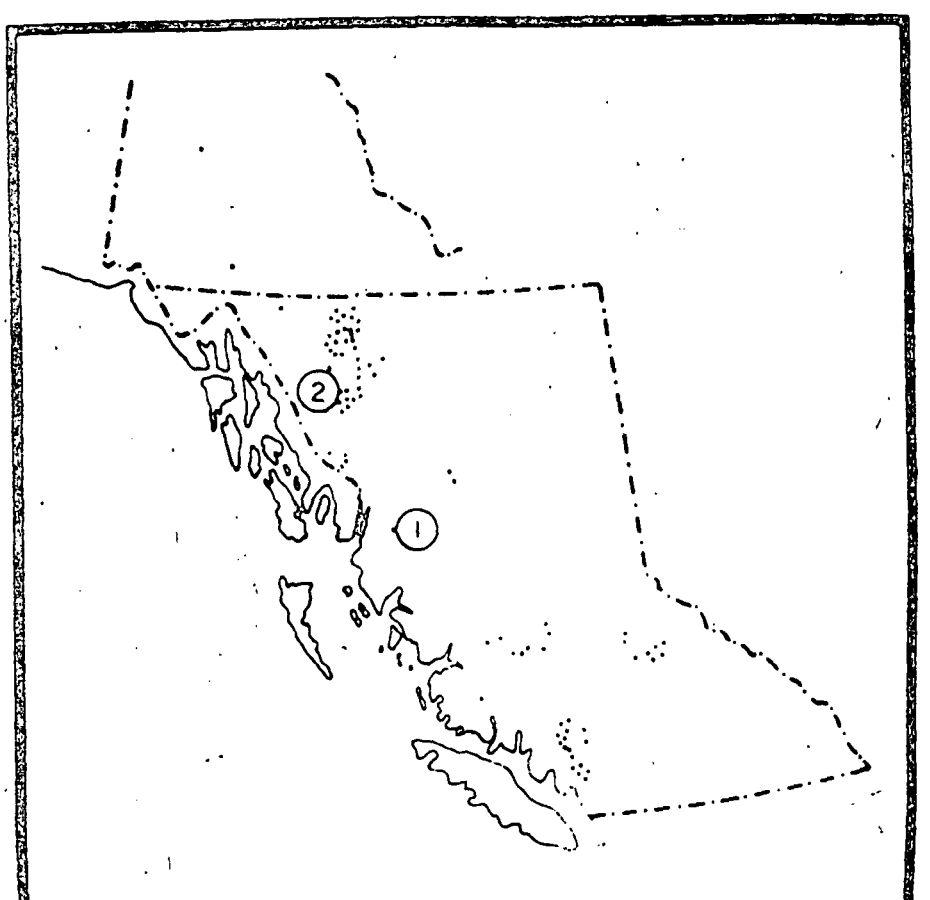

Fig. 7. Location of Tertiary and younger volcanic rocks in British Columbia (after Souther). The positions of Aiyansh (1) and Mt. Edziza (2) are indicated.

lations, if that technique becomes a reality. More detailed geophysical investigations of other types, including electrical conductivity and micro earthquake studies also appear to be called for in the neo-volcanic belts. It is known that the western Cordillera is a general region of high electrical conductivity (Caner, Auld, Dragert and Camfield 1971), but the detailed mapping of the conductivity in the vicinity of the young volcanoes will require many more measurements.

The occurrence of hot springs is, of course, evidence of some source of geothermal energy. Harrison Hot Springs, and the springs near Terrace, both occur close to the neo-volcanic belts, and would appear worthy of detailed study. In contrast, the hot springs of the Rocky Mountains (Warren 1927, Pickering 1954) hold little promise for geothermal energy production. The water temperature is low: on the average, about 115°F, and there is no nearby source of volcanic heat. The explanation given by Warren for the Banff springs appears correct, that surface water circulates to depth, along fractures, in a region of normal geothermal gradient. If this is the case, there is no possibility of obtaining steam, or water sufficiently hot to flash to steam.

Throughout most of the remainder of Canada, evidence of geothermal sources, and of high heat flow (Jessop 1968) is lacking. Geothermal possibilities appear limited to British Columbia and the Yukon. As has been shown, steam fields certainly can produce electrical power at competitive costs to other types of generation, and hot water fields, if of sufficient thermal quality, probably can. The method compares favourably, in its impact on the environment, with either large hydro-electric installations, and with plants using fossil fuels. Furthermore, the seismicity of the western Cordillera may well argue against hydro-electric dams in certain areas. The search for geothermal fields would therefore appear to be well worthwhile, although, until the development of the artificial recharge system, the necessity of proving substantial flows of thermal fluids, as discussed above must always be kept in mind.

References

Armstead, H. Christopher H., 1964, Geothermal power development at Wairakei, New Zealand, U.N. Conference on New Sources of Energy, 3, 274-282.

Bodvarsson, Gunnar, 1964, Physical characteristics of natural heat resources in Iceland. U.N. Conference on New Sources of Energy 2, 82-89.

Bodvarsson, Gunnar and Johannes Zoëga, 1964, Production and distribution of natural heat for domestic and industrial heating in Iceland. U. N. Conference on New Sources of Energy 3, 449-455.

Burgassi, Renato, 1964, Prospecting of geothermal fields and exploration necessary for their adequate exploration, performed in various regions of Italy. U.N. Conference on New Sources of Energy, 2, 117-133.

Caner, B., D.R. Auld, H. Dragert and P.A. Camfield, 1971, Geomagnetic depth sounding and crustal structure in western Canada. Journ. Geophys. Res. 76, 7181-7201.

Chierici, Averardo, 1964, Planning of a geothermal power plant; technical and economic principles. U.N. Conference on New Sources of Energy, 3, 299-311.

Dawson, G.B., 1964 The nature and assessment of heat flow from hydrothermal areas. N.Z. Journ. of Geol. and Geophys. I. 155-171.

Elder, John W. 1965, Physical processes in geothermal areas. In Terrestrial Heat Flow (William H.K. Lee, Editor). American Geophysical Union, Monograph 8.

Harlow, Francis H. and William E. Pracht, 1972, A theoretical study of geothermal energy extraction. Journ. Geophys. Res. 77, 7038-7048.

Healy, J., 1962, Structure and volcanism in the Taupo volcanic zone, New Zealand. Amer. Geoph. Un. Monograph 6, ed. G.A. Macdonald and H. Kuno, 151-157.

Healy, J., 1964, Geology and geothermal energy in the Taupo volcanic zone, New Zealand. U.N. Conference on New Sources of Energy 2, 250-256.

Hulston, J.R., 1964, Isotope geology in the hydrothermal areas of New Zealand, U.N. Conference on New Sources of Energy, 2, 259-262.

Jessop, A.M., 1968, Three measurements of heat flow in eastern Canada. Can. J. Earth Sciences 5, 61-68.

Jessop, Alan M. and Alan S. Judge, 1971, Five measurements of heat flow in southern Canada. Can. J. Earth Sciences 8, 711-716.

McNitt, James R., 1965, Review of geothermal resources. In Terrestrial Heat Flow (William H.K. Lee, Editor). American Geophysical Union, Monograph 8.

Pickering, B.J., 1954, Principal hot springs of the southern Rocky Mountains of Canada. Alberta Society of Petroleum Geologists, Guidebook, Fourth Annual Field Conference.

Robinson, E.S., J.C. Rowley, R.M. Potter, D.E. Armstrong, B.B. McInteer, R.L. Mills, M.C. Smith, 1971, A preliminary study of the nuclear subterrene, Los Alamos Scientific Laboratory, Report LA - 4547.

Ruiz Elizondo, Jésus, 1964, Prospection of geothermal fields and investigations necessary to evaluate their capacity. U.N. Conference on New Sources of Energy 2, 3-23.

Souther, J.G., 1970, Volcanism and its relationship to recent crustal movements in the Canadian Cordillera. Can. J. Earth Sciences, I, 553-568.

Warren, P.S., 1927, Banff Area, Alberta. Geol. Surv. Can. Memoir 153.

White, D.E., L.J.P. Muffler and A.H. Truesdell, 1971, Vapor-dominated hydrothermal systems compared with hot-water systems, Economic Geology, 66. 75-97.

Wilson, J.T. and Burke ,Kevin,1972, Two types of mountain building. Nature,239, 448-449.

MINERAL DEVELOPMENT MAP OF SOUTH
SASKATCHEWA

SHOWING

DESIGNATED OIL AND GAS POOLS, WELL SPACING AREAS, COMMERCIAL POTASH AREAS, OIL AND GAS PIPE LINES, REFINERIES, POTASH MINES, SODIUM SULPHATE PLANTS AND DEPOSITS, AND SALT PLANTS

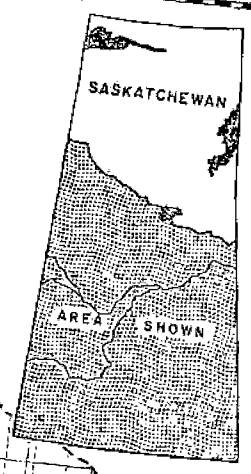

LEGEND

- Oil Pools
- Gas Pools
- Well Spacing Areas (AREA - 4)
- Commercial Potash Areas
- Oil Pipe Lines
- Gas Pipe Lines
- Oil Refineries
- Gas Conservation Plants
- Potash Shaft Mine
- Potash Solution Mine
- Sodium Sulphate Plants
- Sodium Sulphate Deposits
- Salt Plants

Kilometres 10 0 10 20 30 40 50 Kilometres
Miles 5 0 10 20 30 40 50 Miles

Prepared by Department of Mineral Resources, Province of Saskatchewan
Survey to December 31, 1975

PRECAMBRIAN SHIELD

AREA RESERVED FOR MILITARY USE

AREA - A
AREA - B
AREA - C
AREA - D
AREA - E
AREA - F
AREA - G
AREA - H

PRINCE ALBERT NATIONAL PARK

NORTH BATTLEFORD

MOOSE JAW

REGINA

SWIFT CURRENT

ESTEVAN

MONTANA — NORTH DAKOTA

Uranium and thorium in the Precambrian basement of western Canada. I. Abundance and distribution

R. A. BURWASH
Department of Geology, University of Alberta, Edmonton, Alberta T6G 2E1
AND
G. L. CUMMING
Department of Physics, University of Alberta, Edmonton, Alberta T6G 2E1

Received 29 July 1975
Revision accepted for publication 23 October 1975

Delayed neutron activation analyses of 182 core samples from the basement of the western Canada sedimentary basin give mean values of 4.13 ppm U and 21.1 ppm Th. These values are almost twice the published values for the Shield as a whole. Replicate analyses of a composite sample of all cores indicates an analytical precision of ±1% for uranium and ±7% for thorium.

Histograms of number of samples *vs*. U and Th values indicate a negatively skewed frequency distribution. Analysis of composite samples prepared from a large number of hand specimens may tend to conceal this skewed nature. Mean abundance values will also be influenced by the form of the U and Th frequency distributions.

Trend surface analysis, with smoothing to reduce the effect of high or low single sample values, indicates two 'highs' common to both U and Th. The helium-producing area around Swift Current, Saskatchewan is associated with a high U–Th plutonic complex. A linear belt trending northeast from Edmonton appears to be a Hudsonian metamorphic belt in which U and Th have been concentrated. Several local concentrations of U or Th are found in the Peace River Arch of northern Alberta.

Des analyses par activation neutronique retardée de 182 échantillons de forage provenant du socle du bassin sédimentaire de l'Ouest Canadien, donnent des valeurs moyennes de 4.13 ppm pour l'uranium et de 21.1 ppm pour le thorium. Ces valeurs sont presque le double des valeurs publiées pour l'ensemble du Bouclier. Des analyses répétées d'un échantillon composite de tous les forages indiquent que la précision analytique est de ± 1% pour l'uranium et de ± 7% pour le thorium.

Dans des histogrammes où nous avons représenté le nombre d'échantillons en fonction des teneurs en U et Th, on obtient une courbe de fréquence asymétrique négative.

L'analyse d'échantillons composites préparés à partir de plusieurs échantillons macroscopiques tend à masquer cette asymétrie. Les teneurs moyennes seront aussi influencées par la forme des distributions de fréquence.

L'analyse de la surface de courbure adoucie pour réduire l'effet causé par des échantillons ayant des valeurs extrêmes, montre deux maximums communs à l'U et au Th. La région productrice d'hélium aux environs de Swift Current, en Saskatchewan, est associée à un complexe plutonique à haute teneur en U et Th. Une ceinture linéaire de direction nord-est à partir d'Edmonton semble être une ceinture métamorphique Hudsonienne dans laquelle l'U et le Th ont été concentrés. Plusieurs concentrations locales de U et Th sont situées dans l'arche de Peace River dans le Nord de l'Alberta.

[Traduit par le journal]

Introduction

The search for areas of uranium mineralization in the Canadian Shield has been greatly expedited by the development during the past ten years of readily portable, highly sensitive gamma-ray detectors for use in prospecting and ground surveys. In the last 6 years, airborne gamma spectrometers have been used to define areas a few miles to a few tens of miles wide and up to several hundred miles long with above average uranium and thorium contents (Darnley *et al.* 1971). The geometry of these belts suggests that they are related to regional zones of folding, shearing, and metamorphism. If such belts are widespread in the Canadian Shield, it is possible that they may also be recognized in the Precambrian basement underlying the western Canada sedimentary basin. Neither ground nor airborne gamma-ray

detectors have proved useful for crystalline rock buried below a sedimentary cover. For basement uranium and thorium values, we must thus rely on cores from deep drill holes.

A collection of drill cores of unweathered rock from below the Precambrian–Paleozoic unconformity, covering an area of approximately 400 000 sq. mi (1 000 000 sq. km) has already been the subject of detailed petrologic and geochemical studies (Burwash and Krupička 1969, 1970; Burwash *et al.* 1973). In view of the fact that less than 200 samples are available to represent this large area of Precambrian crust, it seemed desirable to use a method of analysis for uranium and thorium that would give the highest degree of analytical precision and accuracy consistent with reasonable cost. The method chosen was delayed neutron activation analysis.

From the analyses carried out in this program it was hoped to determine: (1) the average uranium and thorium content of this area of the crust; (2) the nature of the frequency distribution within the sample population; and (3) the location and extent of areas of anomalously high and low uranium and thorium values, as defined by trend surface analysis of our data. The more difficult question of the relationship of uranium and thorium concentrations to other chemical and petrologic variables in this suite of samples will be considered in a subsequent paper.

Method

The method of delayed neutron activation analysis described by Gale (1967) was adapted by Cumming (1974) for use with the facilities of the McMaster Nuclear Reactor. The theory underlying the method is given in these two papers. In our work, 5.000 g aliquots of powdered samples from basement cores, previously analyzed for all major elements by X-ray fluorescence analysis, were sealed in polythene vials. Each vial was irradated for two 30 s intervals, once without cadmium shielding and once with shielding. Twenty-five seconds after ejection from the reactor, the neutrons emitted during a 64 s counting period were recorded.

The uranium and thorium contents were calculated by comparison with standard samples prepared by addition of known weights of pure uranium or thorium salts to an inert matrix. The uranium salt was checked for normal isotopic composition by H. Baadsgaard. The standard samples were usually run several times each day to detect changes in neutron flux within the reactor as control rods were inserted or withdrawn. For most of the determinations, the reactor was operating at a power of 5.0 MW. However, during one work session in August 1973, excessive atmospheric temperature and humidity caused daily changes between 5.0 and 4.75 MW, requiring calibration of standards at both power levels. The content of uranium and thorium in each rock sample was calculated using the formulas given by Cumming (1974). A single standard uranium sample prepared in 1970 was used in this program until June 1974, when it was found, by comparison with a new set of replicate standards, to give results systematically high by 3%. All values quoted in this paper have been recalculated to conform to the 1974 standards.

The precision and accuracy of our method was tested by making replicate analyses of two aliquots of a powder prepared from core from Mobil Oil Woodley Sinclair Cantuar 2-21. The aliquots were taken from a 25 g split of material, analyzed 5 times by Rosholt *et al.* (1970), using the isotope dilution technique. Since delayed neutron activation analysis is nondestructive, the same two samples were run a total of 15 times during the course of 3 working sessions at the reactor (over a period of 18 months). The results of these replicate analyses are given in Table 1. The 95% confidence intervals for U and Th as determined for the two methods of analysis overlap and hence, the mean values are not significantly different at the 95% confidence level.

Results

The results of the individual analyses of 182 cores from the Precambrian basement of the western Canada sedimentary basin are given in Table 3 (Addendum). Means are 4.13 ppm uranium and 21.1 ppm thorium. Replicate analyses ($n = 13$) of the composite sample of all basement cores (Burwash and Krupička 1969, p. 1382) gave 4.16 ± 0.04 ppm uranium (95% confidence interval) and 20.91 ± 1.50 ppm thorium (95% confidence interval), in excellent agreement with the means of the individual analyses. These values are compared with those of Shaw (1967) and Eade and Fahrig (1971) in Table 2. Our data suggests that the mean uranium and thorium content of the western Canadian basement is approximately twice the average of the Canadian

TABLE 1. Ninety-five percent confidence intervals for delayed neutron activation analyses and isotope dilution analyses of standard sample 3633[a]

	Uranium (ppm)	Thorium (ppm)
Delayed neutron activation analysis Burwash and Cumming (this work) (N = 15)	23.46±0.20	81.55±5.51
Isotope dilution Rosholt *et al.* (1970) (N = 5)	23.36±0.48	81.97±2.29

[a]U of A Sample No. 3633; Mobil Oil Woodley Sinclair Cantuar 2-21, Lsd: 2-Sec. 21- Twp. 16- Rge. 17- W. 3; Depth 7305 ft (2226.6 m).

TABLE 2. Uraniam and thorium content of Canadian Shield areas

	U ppm	Th ppm
Western Canada Basement (mean of 182 determinations, this paper)	4.13	21.1
Canadian Shield, mean (Shaw 1967)	2.45	10.3
Canadian Shield, average weighted according to size of structural province	2.1	13.0
Bear Province	8.1	35.7
Slave Province	1.7	8.4
Churchill Province	2.6	15.5
Superior Province (Eade and Fahrig 1971)	1.2	9.7

Shield as a whole. In terms of the regional averages given by Eade and Fahrig (1971), our values are intermediate between those of the Churchill and Bear provinces. As will be shown later, our maximum concentrations can be spatially related to features lying within the southwestward extension of the Churchill province.

Rigorous statistical comparisons of our data with previously published averages are probably unwarranted, due to: (1) different criteria for collection of samples, (2) different criteria for selection of samples to be analyzed, and (3) single rock as opposed to composite sample analysis.

An important difference between our work and that of Shaw (1967) and Eade and Fahrig (1971) is that our 182 analyses are on individual rock samples. Only one composite of all core samples was prepared for replicate analysis to assess precision of our methods. Shaw (1967) used 32 composites prepared from 330 individual rock specimens. Eade and Fahrig (1971), in an attempt to extend coverage of the Shield as widely as possible, used several thousand hand specimens from 26 areas to yield 78 composites. The preparation of composites has the disadvantage that high and low values from individual specimens are suppressed, and the analytical values reported tend to cluster toward the mean.

A histogram of number of samples *vs.* uranium content in parts per million (Fig. 1) shows a skewed frequency distribution, with a bias toward values less than 1 ppm. The histogram of number of samples *vs.* thorium content (Fig. 2) has the same shape as that for uranium. The slightly irregular profile of the histogram for thorium values <12 ppm may reflect in part the lower accuracy of the method of delayed neutron activation analysis for low thorium contents, probably no better than ±10% for concentration less than 10 ppm on a single determination.

Comparison of Figs. 1 and 2 with the histograms of uranium and thorium content of silicic igneous rocks published by Clark *et al.* (1966, figs. 24-8 and 24-9) indicate that a complex metamorphic terrain has both a greater range and a more highly skewed distribution than an entirely igneous population. This result should be anticipated in view of the diverse sedimentary as well as metamorphic processes acting on some of the rock units sampled in our study.

Uranium Distribution

The results of applying a surface-smoothing procedure to the areal distribution pattern of U are shown in Fig. 3. The procedure involves obtaining grid values for contouring by interpola-

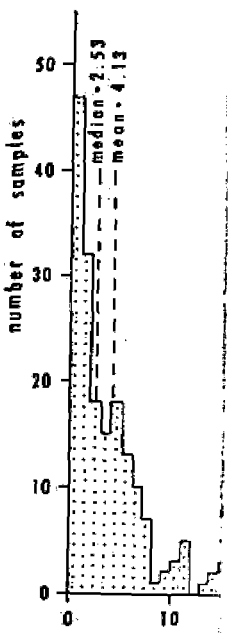

FIG. 1. Histogram of Basement core samples (n = 182).

tion from samples i
square. This techniq
vidual high values
coverage of sample l
line was used to ass
and valleys in the co
the methods used is
bert (1976). In areas
less than one well
longitude), a single
produce a recogniz
surface. The overa
basement core samp
3 and 4.

Since the purpose
was to locate uraniu
regional igneous an
moderate depths, r
cumulations, we d
sedimentary and
rocks, volcanic rock
(diabase). To the S
three wells from N
ternational Bound
nos. 184, 185, and
given in Table 3 wer
tours shown in Fig.

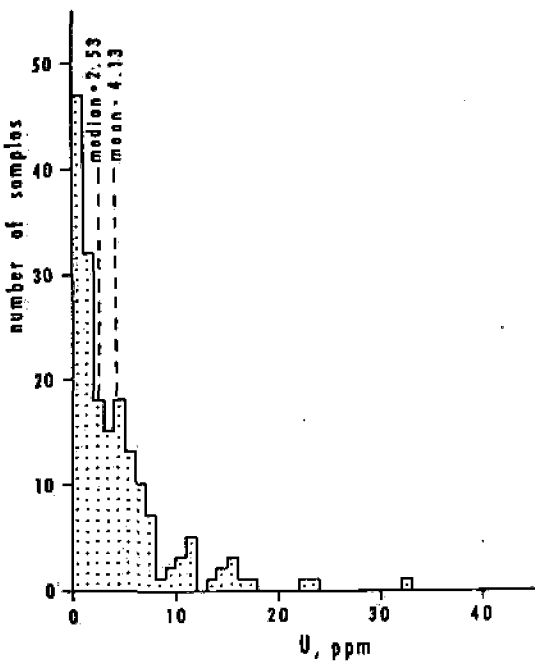

FIG. 1. Histogram of uranium content of Precambrian Basement core samples from the Western Canada Basin (n = 182).

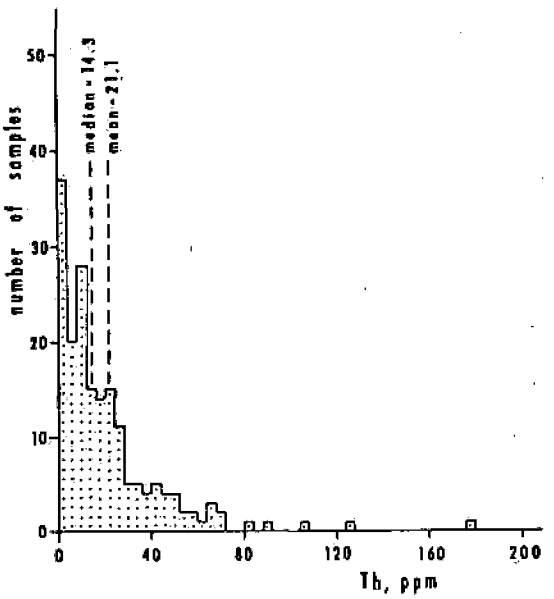

FIG. 2. Histogram of thorium content of Precambrian Basement core samples from the Western Canada Basin (n = 182).

tion from samples in the vicinity of each grid square. This technique reduces influence of individual high values in areas with a reasonable coverage of sample locations. An additional routine was used to assure the continuity of ridges and valleys in the contours. Further discussion of the methods used is given in Burwash and Culbert (1976). In areas of sparse well control (*i.e.*, less than one well per degree of latitude and longitude), a single high uranium value will still produce a recognizable anomaly on the trend surface. The overall distribution of analyzed basement core samples is shown by dots on Figs. 3 and 4.

Since the purpose of the trend surface mapping was to locate uranium concentrations related to regional igneous and metamorphic processes at moderate depths, rather than supracrustal accumulations, we deleted from the data base sedimentary and low-grade metasedimentary rocks, volcanic rocks, and hypabyssal dike rocks (diabase). To the Canadian locations we added three wells from North Dakota close to the International Boundary (Table 3 (Addendum), nos. 184, 185, and 186). The use of all analyses given in Table 3 would probably modify the contours shown in Fig. 3.

The map of uranium distribution shows two main positive anomalies. In southwestern Saskatchewan, a roughly equidimensional anomaly includes an area of uranium-rich epizonal plutons belonging to the closing phases of the Hudsonian orogeny. Two core samples (20 and 22, Table 3) strongly influence the trend surface. The commercial accumulation of helium in Lower Paleozoic strata of this area has been linked to basement petrology and topography (Burwash and Cumming 1974).

A linear anomaly trending northeastward from Edmonton toward the western margin of the exposed Shield contains the highest values on the trend surface (>24 ppm U). Four core samples (nos. 42, 54, 56, and 60) in a linear array are primarily responsible for this anomaly. It is probably significant that the strike of the anomaly corresponds closely to the regional structural fabric of the Churchill geologic province in northern Saskatchewan. It also lies very close to the southern limit of strong post-crystalline deformation in the Athabasca mobile zone (Burwash and Krupička 1969). The Kasba Lake – Edmonton gravity low, chosen by Burwash and Culbert (1976) as one of the major structural boundaries in the western Canadian basement, is parallel to and slightly north of the uranium anomaly. If some of the major lithologic units

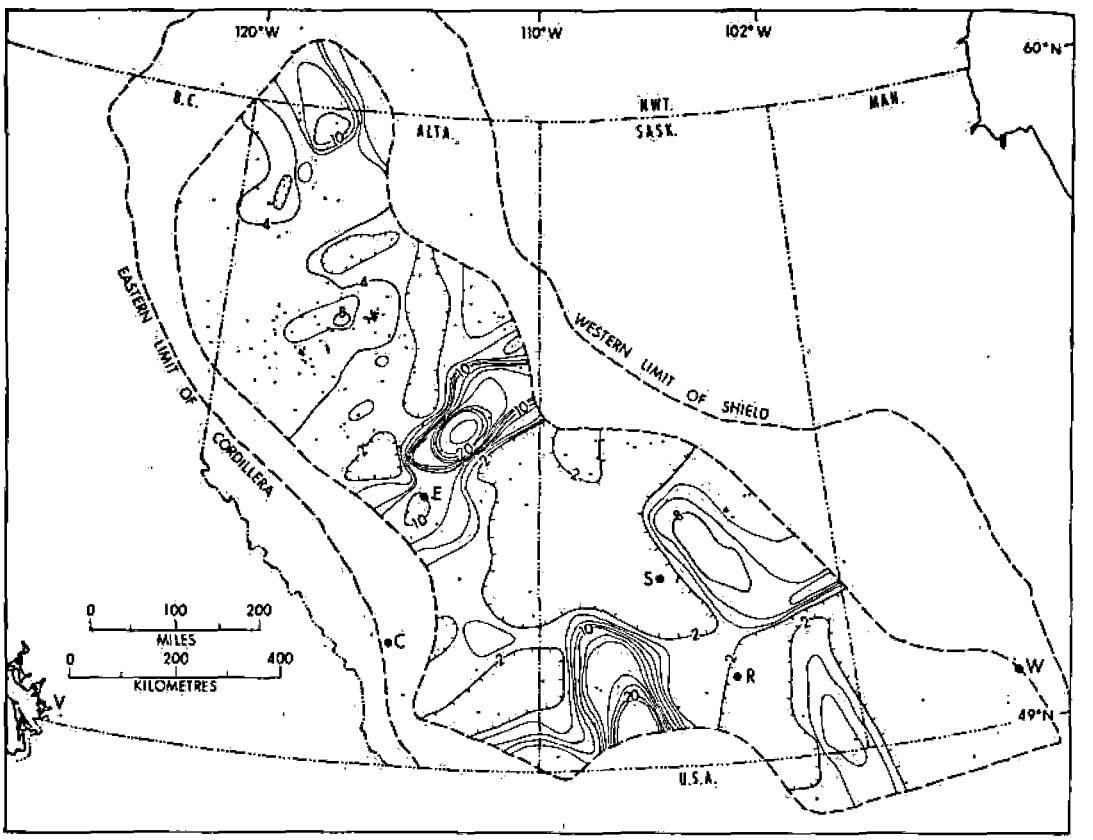

FIG. 3. Smoothed trend surface for uranium in the Precambrian Basement of the Western Canada Basin. Contour interval 2 ppm. Depressions shown by hachures. A few data points used by the computer lie outside the contoured area.

exposed in the Virgin River belt in northern Saskatchewan (Wallis 1970) extend southwestward into the subsurface, the uranium concentrations may be present in highly metamorphosed sedimentary rocks or in igneous rock bodies in which these were assimilated.

Four core samples from northern Alberta (nos. 85, 132, 138, and 155) with uranium contents >15 ppm lie within the major concentration of basement wells penetrating the Peace River Arch (Burwash and Krupička 1970, figs. 1 and 7). The smoothed trend surface shows only a broad positive uranium feature for this area, with values between 4 and 8 ppm U. In a very general fashion, the 4-ppm contour conforms to the shape of the Peace River Arch.

Near the northern and southern limits of the area of study, several contours have shapes suggesting regional trends. However, with the limited sample coverage in these areas, the confidence level of these contours is low and no firm judgement can be made of their significance.

Thorium Distribution

The trend surface map for thorium (Fig. 4) shows several of the same general trends as the uranium map. In southwestern Saskatchewan, high uranium and thorium are associated with a late Hudsonian igneous event. The equidimensional anomaly on the thorium map is associated with the same two drill cores as is the uranium anomaly.

The well defined linear anomaly trending northeast from Edmonton, shown in Fig. 3, is present but less well defined on Fig. 4. It is probably associated with three values in the range 40 to 60 ppm Th (samples 54, 56, and 64). An isolated anomaly in north-central Alberta is due to a single sample (no. 59) with 128 ppm Th. In the vicinity of the Red Earth oil field, approximately

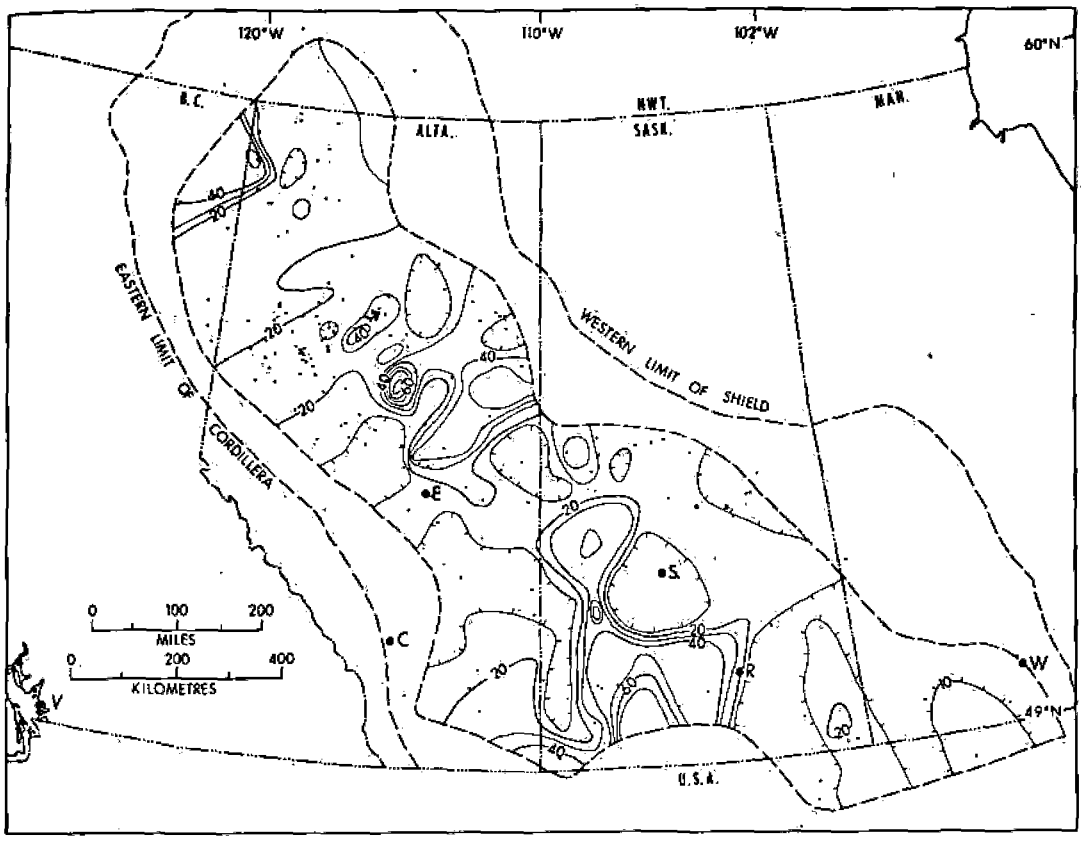

FIG. 4. Smoothed trend surface for thorium in the Precambrian Basement of the Western Canada Basin. Contour interval 10 ppm. Depressions shown by hachures.

220 mi (350 km) north-northwest of Edmonton, a cluster of data points contains 5 samples (nos. 116, 120, 121, 122, and 124) with thorium values greater than 60 ppm. On the trend surface map, this area is represented by an elliptical 40 ppm Th contour.

The areas on Fig. 4 with low thorium values are also areas of sparse sample control. The low values found in southeastern Saskatchewan and southwestern Manitoba correspond to the inferred subsurface extension of the Superior Province. The low thorium values associated with the west half of central and southern Alberta are at present unexplained.

Conclusion

The mean concentrations of uranium and thorium of the western Canadian basement, as determined from delayed neutron activation analysis of core samples from deep drill holes, are higher than the average values for the whole Shield published by Shaw (1967) and Eade and Fahrig (1971). In terms of the regional averages given by Eade and Fahrig (1971), our area conforms most closely to the pattern of other areas of the Canadian Shield last affected by the Hudsonian orogeny (the Churchill and Bear Provinces).

The frequency distribution of both U and Th in our sample population is definitely not a distribution symmetrical about the mean, but is highly skewed toward lower values, as is shown by the separation of the mean and the median. In this circumstance, a few high values greatly alter the mean. In establishing a regional sampling program, a careful selection of a limited number of sampling sites for single rock analysis will provide a better clue to anomalous areas than composites from multiple rock specimens.

Trend surface analysis of uranium and thorium content, when combined with petrographic criteria for recognition of rocks of plutonic igneous

or metamorphic origin, can aid in the interpretation of regional crustal units. Anomalously high uranium and thorium values may identify discrete areas of plutonic activity (essentially equidimensional) or linear belts of probable metamorphic origin. Examples of uranium and thorium enrichment in both igneous and metamorphic settings are shown on our maps.

Acknowledgments

The authors wish to express their appreciation to the many oil companies who supplied the core samples on which this project depended. The cooperation of the staff of McMaster Nuclear Reactor made possible the delayed neutron activation analyses. Trend surface analysis was done by R. R. Culbert. D. A. Taylor assisted with final compilation of graphical material. Financial support for the project was given by grants from the National Research Council of Canada and the Department of Energy, Mines and Resources. The assistance of R. W. May as a critical reader is greatly appreciation. The manuscript was typed by V. Stephansson.

Addendum

TABLE 3. Precambrian Basement core sample locations, depths, and uranium–thorium analyses (ppm)

Index No.	Location					Elevation (feet asl)	Total depth (ft)	PC depth (ft)	Sample depth (ft)	U (ppm)	Th (ppm)
	Lsd.	Sec.	Twp.	Rge.	Mer.						
1	7—	29—	12—	2—	E1	800	1009	708	1009	0.93	5.0
2	3—	1—	5—	2—	W1	787	1150	1042	1150	0.75	12.0
3	3—	1—	8—	18—	W1	1364	3826	3816	3825	0.94	6.8
4	9—	1—	37—	28—	W1	1186	2047	2035	2045	0.18	0.9
5	16—	4—	3—	32—	W1	1617	8329	8315	8328	7.97	24.9
6	3—	27—	8—	8—	W2	2058	8834	8680	8830	0.37	2.0
7	2—	11—	15—	26—	W2	1937	7740	7682	7738	2.01	41.8
8	1—	15—	48—	17—	W2	1425	2595	2543	2594	8.84	17.7
9	11—	3—	50—	18—	W2	1370	3501	—	3056	0.28	0.4
10	12—	3—	50—	18—	W2	1423	3269	—	2170	0.32	0.8
11	12—	3—	50—	18—	W2	1423	3269	—	3170	0.29	1.5
12	8—	9—	50—	18—	W2	1433	2437	2393	2378	1.77	11.4
13	13—	18—	52—	13—	W2	1215	1619	1586	1615	3.91	11.5
14	12—	15—	52—	14—	W2	1210	1790	1704	1785	3.19	17.2
15	2—	5—	61—	24—	W2	1721	1825	1763	1820	1.01	4.5
16	4—	31—	3—	26—	W3	3072	7339	7240	7335	0.47	2.9
17	9—	32—	6—	22—	W3	3458	8858	8808	8820	11.76	48.5
18	2—	4—	10—	19—	W3	3051	8777	8510	8774	3.31	6.8
19	9—	20—	12—	2—	W3	2421	7785	7779	7785	4.60	23.7
20	2—	21—	16—	17—	W3	2411	7312	7281	7305	23.46	82.3
21	1—	9—	17—	14—	W3	2387	6755	6706	6755	4.80	21.0
22	15—	3—	17—	18—	W3	2440	7260	7246	7260	15.25	46.4
23	1—	31—	18—	28—	W3	2521	7440	7420	7440	0.12	0.5
24	4—	16—	37—	1—	W3	1833	5415	5383	5410	1.28	26.3
25	8—	15—	52—	2—	W3	1771	3297	3250	3290	0.54	1.9
26	7—	14—	56—	17—	W3	2351	4333	4325	4332	0.33	40.2
27	13—	21—	61—	15—	W3	1543	2773	2755	2767	0.28	6.4
28	8—	11—	62—	22—	W3	1708	3461	3452	3460	3.38	34.5
29	1—	36—	63—	5—	W3	1830	1923	1915	1921	0.44	2.2
30	9—	21—	63—	8—	W3	1722	2061	2035	2061	1.43	5.2
31	8—	8—	64—	2—	W3	2085	2028	2003	2009	0.41	1.8
32	8—	8—	64—	2—	W3	2085	2028	2003	2026	1.97	8.6
33	8—	30—	64—	15—	W3	1564	2435	2399	2435	1.45	31.7
34	12—	14—	12—	12—	W4	2488	6981	6930	6975	4.58	21.9
35	4—	12—	15—	27—	W4	3309	11836	11793	11815	0.50	17.5
36	5—	1—	17—	14—	W4	2466	7281	7270	7276	0.15	0.3
37	13—	22—	20—	12—	W4	2442	6155	6147	6147	n.d.	n.d.
38	6—	9—	31—	1—	W4	2409	7189	7168	7174	5.44	19.0
39	13—	36—	35—	2—	W4	2667	7231	7229	7229	0.74	2.0
40	1—	6—	38—	15—	W4	2746	8373	8345	8370	1.33	3.7
41	16—	17—	48—	20—	W4	2479	8266	8105	8150	3.64	14.5
42	8—	17—	50—	26—	W4	2373	8995	8984	8985	17.70	35.1
43	8—	17—	50—	26—	W4	2373	8995	8984	8990	0.40	3.0
44	14—	29—	52—	2—	W4	2089	5502	5468	5485	1.52	15.8
45	1—	11—									
46	8—	17—									
47	14—	14—									
48	7—	14—									
49	7—	14—									
50	6—	36—									
51	9—	29—									
52	10—	13—									
53	1—	27—									
54	16—	19—									
55	13—	17—									
56	4—	3—									
57	7—	24—									
58	7—	24—									
59	6—	10—									
60	12—	27—									
61	14—	9—									
62	7—	28—									
63	7—	11—									
64	5—	32—									
66	8—	36—									
66	8—	20—									
67	10—	14—									
68	9—	34—									
69	12—	23—									
70	5—	29—									
71	10—	20—									
72	5—	35—									
73	6—	36—									
74	5—	31—									
75	9—	20—									
76	9—	20—									
77	16—	12—									
78	8—	11—									
79	3—	5—									
80	11—	18—									
81	11—	11—									
82	6—	6—									
83	12—	16—									
84	15—	16—									
85	14—	15—									
86	5—	1—									
87	12—	33—									
88	15—	21—									
89	12—	11—									
90	16—	9—									
91	1—	12—									
92	1—	16—									
93	10—	20—									
94	2—	25—									
95	16—	25—									
96	14—	34—									
97	8—	17—									
98	13—	18—									
99	5—	3—									
100	10—	6—									
101	7—	5—									
102	16—	13—									
103	13—	24—									
104	6—	11—									
105	6—	31—									
106	2—	15—									
107	1—	22—									
108	11—	3—									

TABLE 3 (*Continued*)

Index No.	Location Lsd.	Sec.	Twp.	Rge.	Mer.	Elevation (feet asl)	Total depth (ft)	PC depth (ft)	Sample depth (ft)	U (ppm)	Th (ppm)
45	1—	11—	53—	12—	W4	2282	6437	6435	6437	7.57	7.1
46	8—	17—	53—	15—	W4	2380	7801	7790	7800	3.61	4.2
47	14—	14—	55—	15—	W4	2078	6534	6430	6533	1.03	3.3
48	7—	14—	57—	6—	W4	1984	5212	5207	5210	4.06	39.2
49	7—	14—	57—	6—	W4	1984	5212	5207	5210	0.96	9.9
50	6—	36—	58—	23—	W4	2074	7357	7162	7336	0.85	2.1
51	9—	29—	59—	24—	W4	2065	7527	7340	7527	0.07	0.7
52	10—	13—	60—	4—	W4	1973	4714	4700	4714	0.19	0.7
53	1—	27—	60—	26—	W4	2133	7519	7507	7518	7.59	7.9
54	16—	19—	62—	19—	W4	2323	6604	6590	6604	16.88	57.1
55	13—	17—	67—	23—	W4	2066	6406	6390	6405	2.74	5.1
56	4—	3—	69—	10—	W4	2515	5033	5019	5024	22.52	50.5
57	7—	24—	76—	18—	W4	2054	4641	4628	4633	0.67	15.6
58	7—	24—	76—	18—	W4	2054	4641	4628	4639	0.97	9.4
59	6—	10—	77—	25—	W4	2616	6120	6103	6120	3.15	127.7
60	12—	27—	78—	4—	W4	1857	2570	2557	2567	15.75	53.8
61	14—	9—	86—	7—	W4	1622	1793	1773	1792	1.27	22.3
62	7—	28—	87—	12—	W4	1540	2304	2299	2302	2.47	43.9
63	7—	11—	87—	17—	W4	1445	2863	2850	2860	0.55	15.9
64	5—	32—	88—	8—	W4	810	789	785	789	11.20	45.1
66	8—	36—	88—	8—	W4	831	936	906	929	0.68	21.4
66	8—	20—	89—	9—	W4	792	1142	1125	1141	1.75	41.9
67	10—	14—	91—	14—	W4	1560	2414	2408	2414	1.14	8.1
68	9—	34—	94—	14—	W4	1379	2000	1991	2000	2.55	179.5
69	12—	23—	98—	21—	W4	2259	3840	3836	3840	0.85	24.0
70	5—	29—	62—	1—	W5	2086	7575	7505	7575	0.63	2.1
71	10—	20—	62—	8—	W5	2548	9145	9112	9132	1.06	0.4
72	5—	35—	62—	18—	W5	2878	11320	11310	11316	0.23	0.8
73	6—	36—	63—	12—	W5	3708	10710	10668	10709	5.20	7.6
74	5—	31—	65—	6—	W5	2615	8422	8350	8400–8418 Composite	0.31	2.0
75	9—	20—	65—	13—	W5	3644	10624	10612	10614	4.81	16.0
76	9—	20—	65—	13—	W5	3644	10624	10612	10624	1.29	4.6
77	16—	12—	66—	13—	W5	3830	10521	10507	10511	1.20	7.6
78	8—	11—	68—	10—	W5	3183	8988	8965	8983	7.55	36.7
79	3—	5—	68—	22—	W5	2297	10736	10707	10730	1.27	14.2
80	11—	18—	72—	17—	W5	2350	8558	8522	8552	4.85	15.8
81	11—	11—	73—	13—	W5	2229	7406	7403	7406	0.28	1.3
82	6—	6—	75—	5—	W5	2777	7397	7075	7372	2.18	8.1
83	12—	16—	75—	15—	W5	1914	7197	7180	7194	2.70	15.7
84	15—	16—	75—	19—	W5	2093	7857	7844	7852	4.74	25.5
85	14—	15—	75—	22—	W5	1885	8418	8400	8418	15.29	34.2
86	5—	1—	77—	20—	W5	2065	7838	7837	7837	9.60	1.0
87	12—	33—	77—	21—	W5	1915	7740	7730	7740	5.36	18.1
88	15—	21—	78—	20—	W5	2064	7644	7625	7644	1.93	10.1
89	12—	11—	78—	22—	W5	1900	7827	7818	7820	6.35	48.1
90	16—	9—	79—	22—	W5	1905	7627	7619	7625	4.46	11.4
91	1—	12—	79—	22—	W5	1929	7847	7840	7847	1.52	8.1
92	1—	16—	79—	22—	W5	1906	7424	7420	7424	9.48	12.9
93	10—	20—	79—	22—	W5	1880	7658	7630	7652	2.64	6.2
94	2—	25—	80—	17—	W5	2442	6808	6782	6808	3.13	19.8
95	16—	25—	80—	17—	W5	2391	6790	6754	6769	5.11	29.9
96	14—	34—	80—	17—	W5	2476	6877	6864	6875	6.46	43.0
97	8—	17—	80—	21—	W5	2089	7770	7738	7770	6.34	22.7
98	13—	18—	80—	23—	W5	1936	7598	7580	7598	6.48	0.2
99	5—	3—	81—	17—	W5	2446	6729	6684	6727	7.47	37.9
100	10—	6—	82—	1—	W5	1908	5009	5004	5007	1.12	0.1
101	7—	5—	82—	18—	W5	2314	7296	7271	7290	3.12	11.6
102	16—	13—	83—	24—	W5	2111	7116	7105	7114	10.05	10.9
103	13—	24—	84—	2—	W5	2077	5010	5001	5009	4.87	19.6
104	6—	11—	84—	5—	W5	2118	5357	5340	5348	2.59	20.3
105	6—	31—	84—	7—	W5	1987	5293	5283	5288	0.73	9.9
106	2—	15—	84—	16—	W5	2384	5912	5895	5912	13.59	45.2
107	1—	22—	84—	17—	W5	2227	6096	6090	6095	1.45	1.8
108	11—	3—	85—	12—	W5	1858	5156	5109	5152	1.32	25.7

TABLE 3 (*Continued*)

Index No.	Location					Elevation (feet asl)	Total depth (ft)	P€ depth (ft)	Sample depth (ft)	U (ppm)	Th (ppm)
	Lsd.	Sec.	Twp.	Rge.	Mer.						
109	16—	23—	85—	19—	W5	2012	6106	6090	6106	1.35	6.5
110	8—	22—	86—	9—	W5	1820	4981	4980	4981	4.88	12.6
111	6—	27—	86—	9—	W5	1770	4860	4849	4853	0.60	16.7
112	12—	32—	86—	9—	W5	1732	4791	4764	4780	0.85	39.8
113	16—	25—	86—	20—	W5	1707	6077	6010	6076	1.29	5.8
114	5—	21—	86—	22—	W5	2039	6589	6589	6589	0.53	1.0
115	2—	25—	86—	26—	W5	2278	6698	6685	6696	2.34	16.0
116	12—	30—	87—	7—	W5	2031	5030	5023	5028	5.73	70.0
117	8—	11—	87—	8—	W5	1974	4663	4658	4660	2.38	23.4
118	16—	11—	87—	8—	W5	1986	4647	4628	4646	3.37	33.6
119	12—	14—	87—	8—	W5	1935	5050	4993	5050	1.18	19.6
120	4—	16—	87—	8—	W5	1893	4838	4742	4799	5.01	89.8
121	12—	16—	87—	8—	W5	1879	4875	4836	4870	6.10	69.3
122	12—	17—	87—	8—	W5	1811	4797	4778	4797	5.85	66.9
123	2—	19—	87—	8—	W5	1796	4837	4825	4828	11.62	58.7
124	11—	21—	87—	8—	W5	1868	4800	4798	4800	6.27	66.9
125	10—	3—	87—	10—	W5	1733	4771	4749.5	4751	0.40	2.4
126	14—	17—	88—	6—	W5	2229	5059	5037	5059	3.56	49.2
127	4—	20—	88—	7—	W5	2061	5044	5020	5030	2.47	2.6
128	2—	4—	88—	8—	W5	1839	4835	4814	4817	11.95	39.4
129	10—	19—	87—	8—	W5	1786	4810	4768	4780	2.44	26.5
130	2—	22—	88—	8—	W5	1855	4926	4910	4910	1.52	1.4
131	2—	23—	88—	8—	W5	1918	4877	4860	4866	1.28	11.7
132	4—	29—	88—	8—	W5	1726	4653	4644	4651	32.11	30.2
133	2—	17—	89—	7—	W5	1912	4772	4742	4751	5.43	54.4
134	6—	20—	89—	19—	W5	1830	5905	5890	5905	2.07	11.2
135	15—	24—	90—	15—	W5	2431	5819	5807	5810	2.10	23.7
136	15—	24—	90—	15—	W5	2431	5819	5807	5819	0.49	8.6
137	9—	35—	91—	6—	W5	1981	4705	4686	4703	1.66	16.3
138	9—	24—	93—	18—	W5	1871	5705	5670	5705	14.90	14.5
139	10—	8—	99—	13—	W5	2256	5636	5627	5635	0.61	21.6
140	15—	24—	109—	17—	W5	1015	4467	4465	4467	5.28	11.9
141	15—	32—	109—	19—	W5	1092	4871	4868	4871	4.72	25.6
142	6—	24—	111—	22—	W5	2391	6391	6383	6385	1.17	11.5
143	7—	22—	116—	22—	W5	1114	5077	4968	5072	1.01	7.8
144	7—	10—	119—	20—	W5	1067	4528	4525	4528	7.47	8.4
145	9—	7—	124—	18—	W5	1003	3731	3725	3731	5.42	12.5
146	16—	18—	126—	14—	W5	1022	3148	3145	3148	0.54	5.7
147	16—	25—	72—	5—	W6	2446	11710	11695	11700	1.35	8.6
148	2—	2—	73—	1—	W6	2223	10195	10132	10195	5.29	61.4
149	13—	20—	75—	2—	W6	2117	9612	9593	9612	4.00	19.4
150	12—	20—	77—	3—	W6	2419	9347	9337	9347	6.69	20.1
151	7—	36—	77—	9—	W6	3031	11705	11645	11700	7.75	29.6
152	4—	20—	78—	1—	W6	1896	8264	8256	8264	5.88	27.8
153	12—	20—	78—	6—	W6	2287	9847	9775	9818	10.92	22.1
154	4—	29—	81—	1—	W6	2090	7255	7243	7255	4.32	10.1
155	2—	14—	82—	2—	W6	2188	7492	7480	7492	14.63	67.2
156	2—	5—	83—	2—	W6	2334	7977	7930	7977	4.45	11.6
157	14—	31—	84—	2—	W6	2325	8227	7840	8225	0.52	1.4
158	16—	12—	84—	8—	W6	2116	8014	8010	8014	2.99	20.7
159	4—	27—	85—	2—	W6	2569	8758	8750	8750	0.86	9.9
160	14—	10—	88—	2—	W6	2355	6962	6958	6962	4.38	20.1
161	8—	16—	88—	2—	W6	2401	6915	6882	6910	4.33	27.4
162	6—	11—	101—	4—	W6	1963	7320	7300	7320	6.49	20.0
163	11—	17—	102—	2—	W6	1562	6838	6835	6838	3.14	14.2
164	2—	16—	107—	6—	W6	1755	6960	6920	6957	4.70	24.1
165	16—	18—	107—	6—	W6	1774	7365	7315	7360	3.42	11.9
166	10—	27—	109—	9—	W6	1769	7329	7308	7329	3.04	11.2
167	15—	22—	115—	10—	W6	1350	6512	6362	6470	2.50	11.2
168	9—	26—	120—	11—	W6	2062	7005	6980	7005	6.37	14.4
169	9—	26—	120—	11—	W6	2062	7005	6980	7005	4.21	31.2
170	2—	7—	124—	2—	W6	2382	6121	6115	6121	1.53	3.2
171	12—	30—	125—	2—	W6	2447	5992	5965	5992	2.30	14.7
172	12—	31—	78—	14—	W6	2433	12040	11892	12038	5.13	27.2
173	6—	29—	81—	15—	W6	2382	11619	11614	11618	2.34	11.2
174	1—	26—	86—	16—	W6	2415	10913	10906	10909	0.15	0.8

Index No.	Location		
	Lsd.	Sec.	Twp.
175	57°47′ N		120°14′ W
176	58°05′ N		121°54′ W
177	58°16′ N		120°51′ W
178	60°09′ N		121°08′ W
179	60°51′ N		114°24′ W
180	60°55′ N		118°50′ W
181	61°19′ N		118°40′ W
182	61°20′ N		122°30′ W
183	62°20′ N		119°00′ W
North Dakota localities			
184		2—	155N—
185		28—	159N—
186		1—	159N—

Where two samples are listed for one w
P€—Depth to Paleozoic/Precambrian

BURWASH, R. A. and CULBERT, R geochemical and mineral patter basement of western Canada. Ca 1–18.

BURWASH, R. A. and CUMMING, source-rock in southwestern Sas Petrol. Geol. 22, pp. 405–412.

BURWASH, R. A. and KRUPIČKA, J vation in the Precambrian basem I. Deformation and chemistry. C 1381–1396.

—— 1970. Cratonic reactivatio basement of western Canada. isostasy. Can. J. Earth Sci. 7, pp

BURWASH, R. A., KRUPIČKA, J.. 1973. Cratonic reactivation in the of western Canada, III. Crustal e Sci. 10, pp. 283–291.

CLARK, S. P. JR., PETERMAN, Z. 1966. Abundances of uranium, t *In*: Handbook of Physical Cons Mem. 97, pp. 521–541.

CUMMING, G. L. 1974. Determi thorium in meteorites by the de Chem. Geol. 13, pp. 257–267.

TABLE 3 (*Concluded*)

Index No.	Location Lsd.	Sec.	Twp.	Rge.	Mer.	Elevation (feet asl)	Total depth (ft)	PC depth (ft)	Sample depth (ft)	U (ppm)	Th (ppm)
175	57°47′ N		120°14′ W			2371	10034	9800	10029	10.33	42.8
176	58°05′ N		121°54′ W			1920	9930	9925	9925	3.17	10.8
177	58°16′ N		120°51′ W			1434	8439	8439	8437	0.68	6.0
178	60°09′ N		121°08′ W			2288	8233	8220	8230	6.06	116.6
179	60°51′ N		114°24′ W			724	1181	1171	1173	0.83	5.8
180	60°55′ N		118°50′ W			1083	2910	2898	2900	0.55	3.5
181	61°19′ N		118°40′ W			497	2230	2192	2230	11.30	21.0
182	61°20′ N		122°30′ W			622	2237	1310	2085	0.97	3.4
183	62°20′ N		119°00′ W			2438	3229	3147	3225	1.53	2.2
North Dakota localities											
184		2—	155N—	96W		2316	13615	13592	13603	2.35	10.6
185		28—	159N—	63W		1562	3408	3404	3408	0.31	2.2
186		1—	159N—	95W		—	—	—	15128	1.07	4.4

Where two samples are listed for one well, two distinctly different lithologies were encountered in the core.
PC—Depth to Paleozoic/Precambrian unconformity, in feet.

BURWASH, R. A. and CULBERT, R. R. 1976. Multivariate geochemical and mineral patterns in the Precambrian basement of western Canada. Can. J. Earth Sci. 13, pp. 1–18.

BURWASH, R. A. and CUMMING, G. L. 1974. Helium source-rock in southwestern Saskatchewan. Bull. Can. Petrol. Geol. 22, pp. 405–412.

BURWASH, R. A. and KRUPIČKA, J. 1969. Cratonic reactivation in the Precambrian basement of western Canada, I. Deformation and chemistry. Can. J. Earth Sci. 6, pp. 1381–1396.

——— 1970. Cratonic reactivation in the Precambrian basement of western Canada, II. Metasomatism and isostasy. Can. J. Earth Sci. 7, pp. 1275–1294.

BURWASH, R. A., KRUPIČKA, J., and CULBERT, R. R. 1973. Cratonic reactivation in the Precambrian basement of western Canada, III. Crustal evolution. Can. J. Earth Sci. 10, pp. 283–291.

CLARK, S. P. JR., PETERMAN, Z. E., and HEIER, K. S. 1966. Abundances of uranium, thorium and potassium. *In*: Handbook of Physical Constants. Geol. Soc. Am. Mem. 97, pp. 521–541.

CUMMING, G. L. 1974. Determination of uranium and thorium in meteorites by the delayed neutron method. Chem. Geol. 13, pp. 257–267.

DARNLEY, A. G., GRASTY, R. L., and CHARBONNEAU, B. W. 1971. A radiometric profile across part of the Canadian Shield. Geol. Surv. Can. Pap. 70-46, 42 p.

EADE, K. E. and FAHRIG, W. F. 1971. Geochemical evolutionary trends of continental plates—a preliminary study of the Canadian Shield. Geol. Surv. Can. Bull. 179, 51 p.

GALE, N. H. 1967. Development of delayed neutron technique as rapid and precise method for determination of uranium and thorium at trace levels in rocks and minerals, with application to isotope geochronology. *In*: Radioactive dating and methods of low-level counting. Vienna, Int. Atomic Energy Agency, pp. 431–452.

ROSHOLT, J. N., PETERMAN, Z. E., and BARTEL, A. J. 1970. U–Th–Pb and Rb–Sr ages in granite reference sample from southwestern Saskatchewan. Can. J. Earth Sci. 7, pp. 184–187.

SHAW, D. M. 1967. U, Th and K in the Canadian Precambrian Shield and possible mantle compositions. Geochim. Cosmochim. Acta, 31, pp. 1111–1113.

WALLIS, R. H. 1970. A geological interpretation of gravity and magnetic data, northwest Saskatchewan. Can. J. Earth Sci. 7, pp. 858–868.

Uranium and thorium in the Precambrian basement of western Canada. I. Abundance and distribution

R. A. BURWASH
Department of Geology, University of Alberta, Edmonton, Alberta T6G 2E1
AND
G. L. CUMMING
Department of Physics, University of Alberta, Edmonton, Alberta T6G 2E1

Received 29 July 1975
Revision accepted for publication 23 October 1975

Delayed neutron activation analyses of 182 core samples from the basement of the western Canada sedimentary basin give mean values of 4.13 ppm U and 21.1 ppm Th. These values are almost twice the published values for the Shield as a whole. Replicate analyses of a composite sample of all cores indicates an analytical precision of ±1% for uranium and ±7% for thorium.

Histograms of number of samples *vs*. U and Th values indicate a negatively skewed frequency distribution. Analysis of composite samples prepared from a large number of hand specimens may tend to conceal this skewed nature. Mean abundance values will also be influenced by the form of the U and Th frequency distributions.

Trend surface analysis, with smoothing to reduce the effect of high or low single sample values, indicates two 'highs' common to both U and Th. The helium-producing area around Swift Current, Saskatchewan is associated with a high U–Th plutonic complex. A linear belt trending northeast from Edmonton appears to be a Hudsonian metamorphic belt in which U and Th have been concentrated. Several local concentrations of U or Th are found in the Peace River Arch of northern Alberta.

Des analyses par activation neutronique retardée de 182 échantillons de forage provenant du socle du bassin sédimentaire de l'Ouest Canadien, donnent des valeurs moyennes de 4.13 ppm pour l'uranium et de 21.1 ppm pour le thorium. Ces valeurs sont presque le double des valeurs publiées pour l'ensemble du Bouclier. Des analyses répétées d'un échantillon composite de tous les forages indiquent que la précision analytique est de ± 1% pour l'uranium et de ± 7% pour le thorium.

Dans des histogrammes où nous avons représenté le nombre d'échantillons en fonction des teneurs en U et Th, on obtient une courbe de fréquence asymétrique négative.

L'analyse d'échantillons composites préparés à partir de plusieurs échantillons macroscopiques tend à masquer cette asymétrie. Les teneurs moyennes seront aussi influencées par la forme des distributions de fréquence.

L'analyse de la surface de courbure adoucie pour réduire l'effet causé par des échantillons ayant des valeurs extrêmes, montre deux maximums communs à l'U et au Th. La région productrice d'hélium aux environs de Swift Current, en Saskatchewan, est associée à un complexe plutonique à haute teneur en U et Th. Une ceinture linéaire de direction nord-est à partir d'Edmonton semble être une ceinture métamorphique Hudsonienne dans laquelle l'U et le Th ont été concentrés. Plusieurs concentrations locales de U et Th sont situées dans l'arche de Peace River dans le Nord de l'Alberta.

[Traduit par le journal]

Introduction

The search for areas of uranium mineralization in the Canadian Shield has been greatly expedited by the development during the past ten years of readily portable, highly sensitive gamma-ray detectors for use in prospecting and ground surveys. In the last 6 years, airborne gamma spectrometers have been used to define areas a few miles to a few tens of miles wide and up to several hundred miles long with above average uranium and thorium contents (Darnley *et al.* 1971). The geometry of these belts suggests that they are related to regional zones of folding, shearing, and metamorphism. If such belts are widespread in the Canadian Shield, it is possible that they may also be recognized in the Precambrian basement underlying the western Canada sedimentary basin. Neither ground nor airborne gamma-

...ectors have proved useful for crystalline rock ...ed below a sedimentary cover. For basement ...anium and thorium values, we must thus rely ...cores from deep drill holes.

A collection of drill cores of unweathered rock ...m below the Precambrian–Paleozoic uncon...mity, covering an area of approximately ...000 sq. mi (1 000 000 sq. km) has already ...en the subject of detailed petrologic and geo...emical studies (Burwash and Krupička 1969, ...0; Burwash *et al.* 1973). In view of the fact ...at less than 200 samples are available to repre...nt this large area of Precambrian crust, it ...emed desirable to use a method of analysis for ...anium and thorium that would give the highest ...gree of analytical precision and accuracy con...ent with reasonable cost. The method chosen ...as delayed neutron activation analysis.

From the analyses carried out in this program ...as hoped to determine: (1) the average ura...m and thorium content of this area of the ...st; (2) the nature of the frequency distribution ...hin the sample population; and (3) the loca...n and extent of areas of anomalously high and ... uranium and thorium values, as defined by ...ad surface analysis of our data. The more ...ult question of the relationship of uranium ... thorium concentrations to other chemical ... petrologic variables in this suite of samples ...be considered in a subsequent paper.

Method

The method of delayed neutron activation anal... described by Gale (1967) was adapted by ...ming (1974) for use with the facilities of the ...Master Nuclear Reactor. The theory under...g the method is given in these two papers. In ...work, 5.000 g aliquots of powdered samples ...basement cores, previously analyzed for all ...er elements by X-ray fluorescence analysis, ...sealed in polythene vials. Each vial was ...ated for two 30 s intervals, once without ...um shielding and once with shielding. ...ty-five seconds after ejection from the re... the neutrons emitted during a 64 s counting ...d were recorded.

...uranium and thorium contents were cal...ed by comparison with standard samples ...ared by addition of known weights of pure ...um or thorium salts to an inert matrix. The ...um salt was checked for normal isotopic ...sition by H. Baadsgaard. The standard samples were usually run several times each day to detect changes in neutron flux within the reactor as control rods were inserted or withdrawn. For most of the determinations, the reactor was operating at a power of 5.0 MW. However, during one work session in August 1973, excessive atmospheric temperature and humidity caused daily changes between 5.0 and 4.75 MW, requiring calibration of standards at both power levels. The content of uranium and thorium in each rock sample was calculated using the formulas given by Cumming (1974). A single standard uranium sample prepared in 1970 was used in this program until June 1974, when it was found, by comparison with a new set of replicate standards, to give results systematically high by 3%. All values quoted in this paper have been recalculated to conform to the 1974 standards.

The precision and accuracy of our method was tested by making replicate analyses of two aliquots of a powder prepared from core from Mobil Oil Woodley Sinclair Cantuar 2-21. The aliquots were taken from a 25 g split of material, analyzed 5 times by Rosholt *et al.* (1970), using the isotope dilution technique. Since delayed neutron activation analysis is nondestructive, the same two samples were run a total of 15 times during the course of 3 working sessions at the reactor (over a period of 18 months). The results of these replicate analyses are given in Table 1. The 95% confidence intervals for U and Th as determined for the two methods of analysis overlap and hence, the mean values are not significantly different at the 95% confidence level.

Results

The results of the individual analyses of 182 cores from the Precambrian basement of the western Canada sedimentary basin are given in Table 3 (Addendum). Means are 4.13 ppm uranium and 21.1 ppm thorium. Replicate analyses ($n = 13$) of the composite sample of all basement cores (Burwash and Krupička 1969, p. 1382) gave 4.16 ± 0.04 ppm uranium (95% confidence interval) and 20.91 ± 1.50 ppm thorium (95% confidence interval), in excellent agreement with the means of the individual analyses. These values are compared with those of Shaw (1967) and Eade and Fahrig (1971) in Table 2. Our data suggests that the mean uranium and thorium content of the western Canadian basement is approximately twice the average of the Canadian

TABLE 1. Ninety-five percent confidence intervals for delayed neutron activation analyses and isotope dilution analyses of standard sample 3633[a]

	Uranium (ppm)	Thorium (ppm)
Delayed neutron activation analysis Burwash and Cumming (this work) (N = 15)	23.46±0.20	81.55±5.51
Isotope dilution Rosholt *et al.* (1970) (N = 5)	23.36±0.48	81.97±2.29

[a]U of A Sample No. 3633; Mobil Oil Woodley Sinclair Cantuar 2-21, Lsd. 2-Sec. 21- Twp. 16- Rge. 17- W. 3; Depth 7305 ft (2226.6 m).

TABLE 2. Uraniam and thorium content of Canadian Shield areas

	U ppm	Th ppm
Western Canada Basement (mean of 182 determinations, this paper)	4.13	21.1
Canadian Shield, mean (Shaw 1967)	2.45	10.3
Canadian Shield, average weighted according to size of structural province	2.1	13.0
Bear Province	8.1	35.7
Slave Province	1.7	8.4
Churchill Province	2.6	15.5
Superior Province (Eade and Fahrig 1971)	1.2	9 7

Shield as a whole. In terms of the regional averages given by Eade and Fahrig (1971), our values are intermediate between those of the Churchill and Bear provinces. As will be shown later, our maximum concentrations can be spatially related to features lying within the southwestward extension of the Churchill province.

Rigorous statistical comparisons of our data with previously published averages are probably unwarranted, due to: (1) different criteria for collection of samples, (2) different criteria for selection of samples to be analyzed, and (3) single rock as opposed to composite sample analysis.

An important difference between our work and that of Shaw (1967) and Eade and Fahrig (1971) is that our 182 analyses are on individual rock samples. Only one composite of all core samples was prepared for replicate analysis to assess precision of our methods. Shaw (1967) used 32 composites prepared from 330 individual rock specimens. Eade and Fahrig (1971), in an attempt to extend coverage of the Shield as widely as possible, used several thousand hand specimens from 26 areas to yield 78 composites. The preparation of composites has the disadvantage that high and low values from individual specimens are suppressed, and the analytical values reported tend to cluster toward the mean.

A histogram of number of samples *vs.* uran[ium] content in parts per million (Fig. 1) show[s] skewed frequency distribution, with a bia[s] ward values less than 1 ppm. The histogram number of samples *vs.* thorium content (Fi[g.] has the same shape as that for uranium. [The] slightly irregular profile of the histogram [for] thorium values < 12 ppm may reflect in part [the] lower accuracy of the method of delayed neut[ron] activation analysis for low thorium conte[nts] probably no better than ±10% for concentra[tions] less than 10 ppm on a single determination.

Comparison of Figs. 1 and 2 with the h[is]grams of uranium and thorium content of s[ome] igneous rocks published by Clark *et al.* (1[966] figs. 24-8 and 24-9) indicate that a con[ti]metamorphic terrain has both a greater r[ange] and a more highly skewed distribution th[an] entirely igneous population. This result s[hould] be anticipated in view of the diverse sedimen[tary] as well as metamorphic processes acting on s[ome] of the rock units sampled in our study.

Uranium Distribution

The results of applying a surface-smoo[thing] procedure to the areal distribution pattern[s] are shown in Fig. 3. The procedure involve[s] taining grid values for contouring by inter[active]

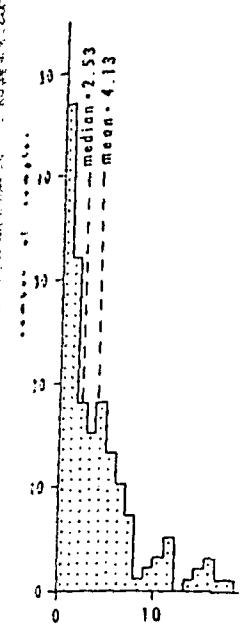

. 1. Histogram of ura[nium]
ment core samples fro[m]
182).

from samples in
are. This technique
al high values in
erage of sample loca
was used to assure
Valleys in the conto
methods used is gi[ven]
(1976). In areas of
than one well per
tude), a single hig[h]
ace a recognizabl[e]
ce. The overall
ment core samples
14.

ace the purpose of
to locate uranium
al igneous and
erate depths, rath
lations, we delet
entary and low
volcanic rocks, a
se). To the Cana
wells from North
tional Boundary
84, 185, and 186
in Table 3 would
shown in Fig. 3.

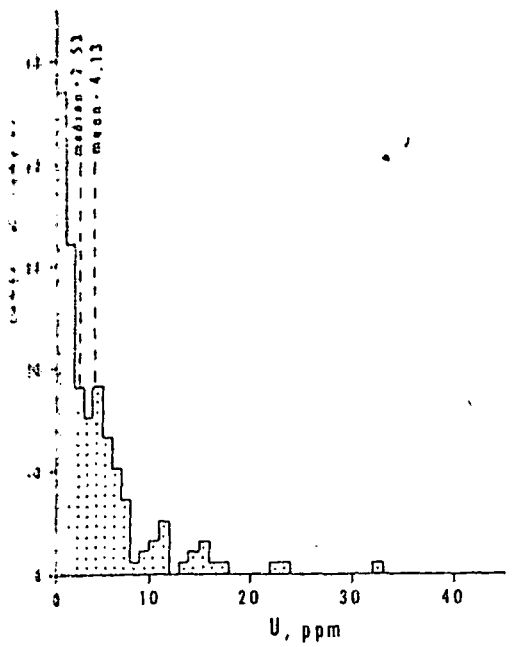

1. Histogram of uranium content of Precambrian ... core samples from the Western Canada Basin ... 182).

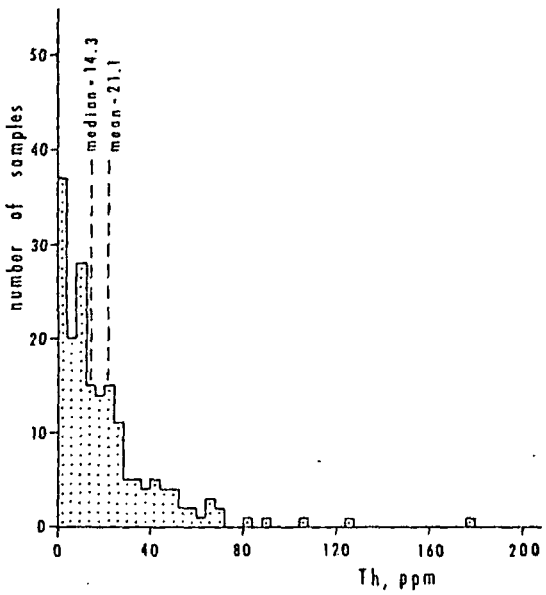

FIG. 2. Histogram of thorium content of Precambrian Basement core samples from the Western Canada Basin (n = 182).

... from samples in the vicinity of each grid ... This technique reduces influence of indi... high values in areas with a reasonable ... of sample locations. An additional rou... was used to assure the continuity of ridges ... leys in the contours. Further discussion of ... ethods used is given in Burwash and Cul... 1976). In areas of sparse well control (*i.e.*, ... than one well per degree of latitude and ... ade), a single high uranium value will still ... a recognizable anomaly on the trend ... . The overall distribution of analyzed ... ent core samples is shown by dots on Figs. ... 4.

... the purpose of the trend surface mapping ... locate uranium concentrations related to ... al igneous and metamorphic processes at ... ate depths, rather than supracrustal ac... ations, we deleted from the data base ... entary and low-grade metasedimentary ... volcanic rocks, and hypabyssal dike rocks ... ch. To the Canadian locations we added ... wells from North Dakota close to the In... nal Boundary (Table 3 (Addendum), ... 4, 185, and 186). The use of all analyses ... Table 3 would probably modify the con... shown in Fig. 3.

The map of uranium distribution shows two main positive anomalies. In southwestern Saskatchewan, a roughly equidimensional anomaly includes an area of uranium-rich epizonal plutons belonging to the closing phases of the Hudsonian orogeny. Two core samples (20 and 22, Table 3) strongly influence the trend surface. The commercial accumulation of helium in Lower Paleozoic strata of this area has been linked to basement petrology and topography (Burwash and Cumming 1974).

A linear anomaly trending northeastward from Edmonton toward the western margin of the exposed Shield contains the highest values on the trend surface (>24 ppm U). Four core samples (nos. 42, 54, 56, and 60) in a linear array are primarily responsible for this anomaly. It is probably significant that the strike of the anomaly corresponds closely to the regional structural fabric of the Churchill geologic province in northern Saskatchewan. It also lies very close to the southern limit of strong post-crystalline deformation in the Athabasca mobile zone (Burwash and Krupička 1969). The Kasba Lake – Edmonton gravity low, chosen by Burwash and Culbert (1976) as one of the major structural boundaries in the western Canadian basement, is parallel to and slightly north of the uranium anomaly. If some of the major lithologic units

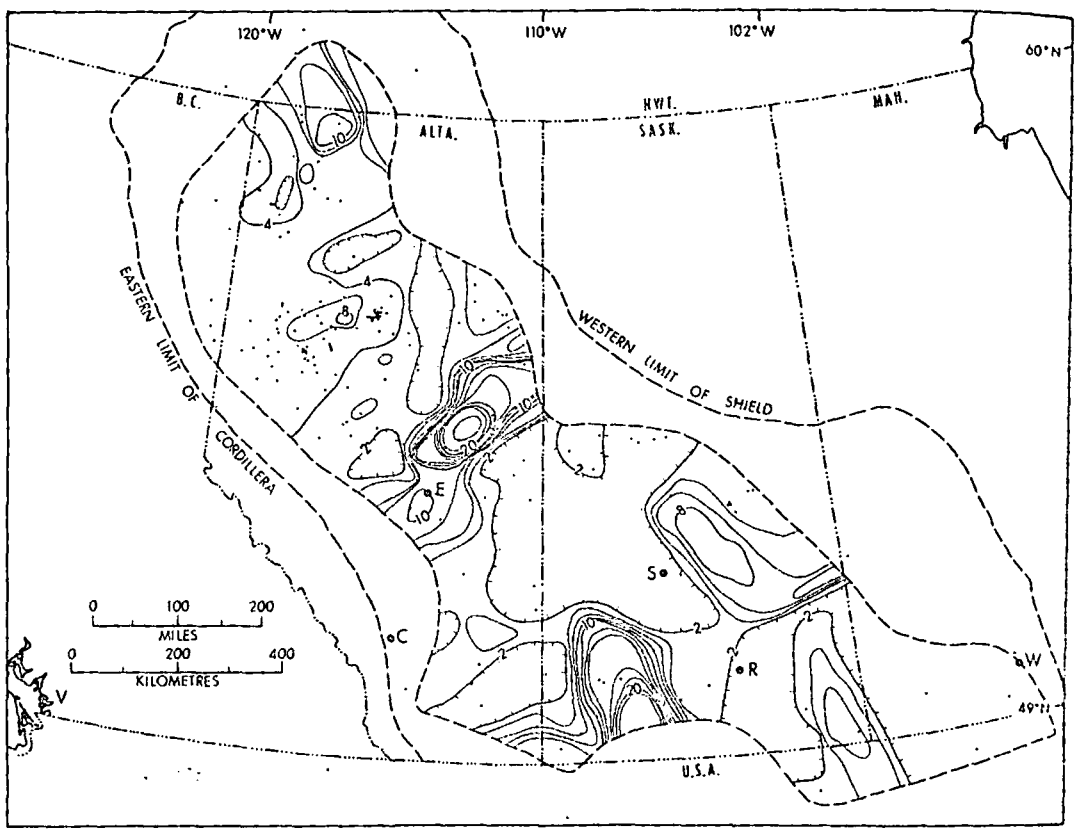

FIG. 3. Smoothed trend surface for uranium in the Precambrian Basement of the Western Canada Basin. Contour interval 2 ppm. Depressions shown by hachures. A few data points used by the computer lie outside the contoured area.

exposed in the Virgin River belt in northern Saskatchewan (Wallis 1970) extend southwestward into the subsurface, the uranium concentrations may be present in highly metamorphosed sedimentary rocks or in igneous rock bodies in which these were assimilated.

Four core samples from northern Alberta (nos. 85, 132, 138, and 155) with uranium contents >15 ppm lie within the major concentration of basement wells penetrating the Peace River Arch (Burwash and Krupička 1970, figs. 1 and 7). The smoothed trend surface shows only a broad positive uranium feature for this area, with values between 4 and 8 ppm U. In a very general fashion, the 4-ppm contour conforms to the shape of the Peace River Arch.

Near the northern and southern limits of the area of study, several contours have shapes suggesting regional trends. However, with the limited sample coverage in these areas, the confidence level of these contours is low and firm judgement can be made of their significan

Thorium Distribution

The trend surface map for thorium (Fig shows several of the same general trends as uranium map. In southwestern Saskatchew high uranium and thorium are associated wi late Hudsonian igneous event. The equidir sional anomaly on the thorium map is assoc with the same two drill cores as is the ura anomaly.

The well defined linear anomaly tren northeast from Edmonton, shown in Fig. present but less well defined on Fig. 4. It is p ably associated with three values in the ran to 60 ppm Th (samples 54, 56, and 64). A lated anomaly in north-central Alberta is d a single sample (no. 59) with 128 ppm Th. I vicinity of the Red Earth oil field, approxim

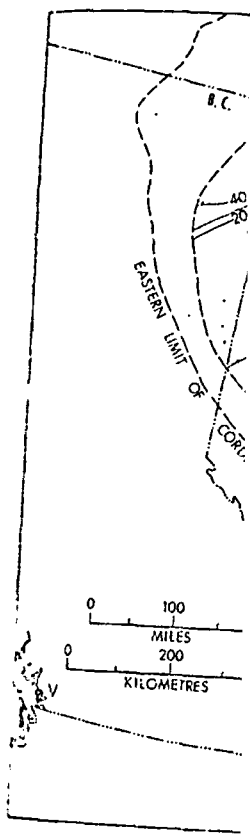

FIG. 4. Smoothed t
Basin. Contour interv

mi (350 km) north-n
ster of data points c
120, 121, 122, and 12
ter than 60 ppm. On
area is represented b
ontour.
areas on Fig. 4 wi
o areas of sparse sa
found in southeast
estern Manitoba c
subsurface extensi
nce. The low thorium
est half of central and
sent unexplained.

Conclusi

mean concentratio
m of the western Ca
ined from delayed ne
core samples from
than the average

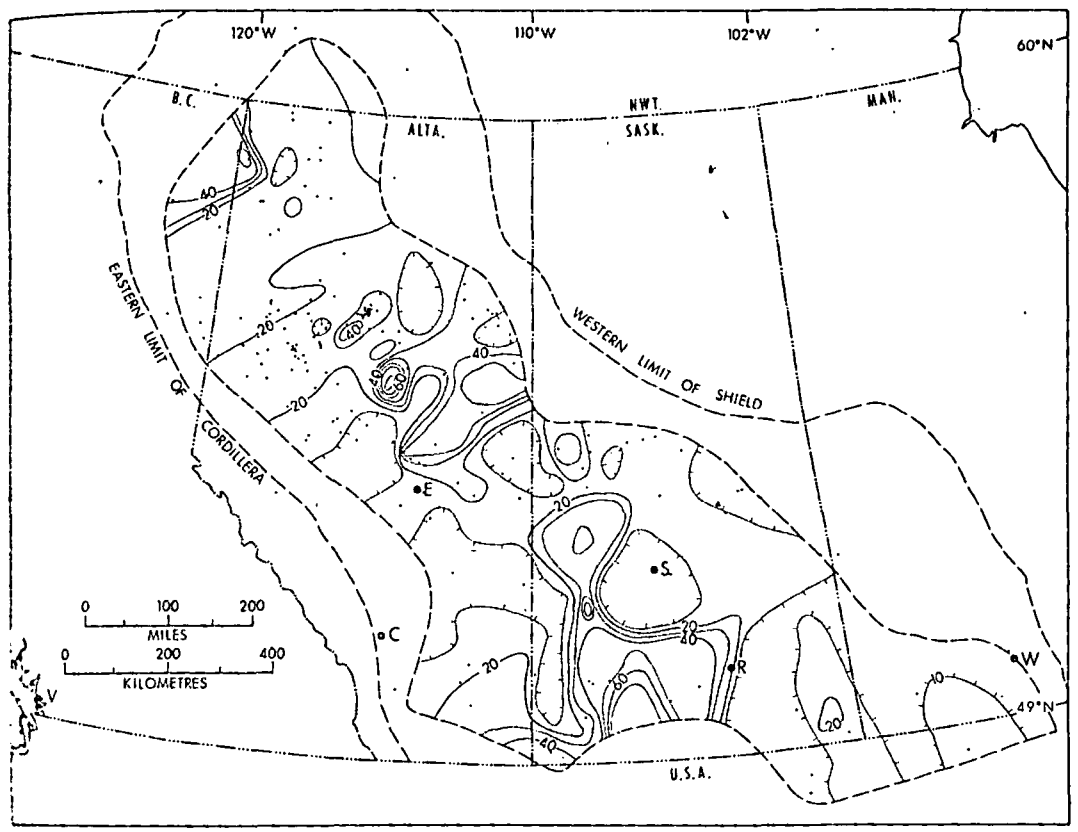

FIG. 4. Smoothed trend surface for thorium in the Precambrian Basement of the Western Canada Basin. Contour interval 10 ppm. Depressions shown by hachures.

...) mi (350 km) north-northwest of Edmonton, ...luster of data points contains 5 samples (nos. ..., 120, 121, 122, and 124) with thorium values ...ater than 60 ppm. On the trend surface map, ...s area is represented by an elliptical 40 ppm ...contour.

The areas on Fig. 4 with low thorium values ...e also areas of sparse sample control. The low ...es found in southeastern Saskatchewan and ...thwestern Manitoba correspond to the in...ed subsurface extension of the Superior ...nce. The low thorium values associated with ...west half of central and southern Alberta are ...resent unexplained.

Conclusion

...e mean concentrations of uranium and ...ium of the western Canadian basement, as ...mined from delayed neutron activation anal... of core samples from deep drill holes, are ...er than the average values for the whole Shield published by Shaw (1967) and Eade and Fahrig (1971). In terms of the regional averages given by Eade and Fahrig (1971), our area conforms most closely to the pattern of other areas of the Canadian Shield last affected by the Hudsonian orogeny (the Churchill and Bear Provinces).

The frequency distribution of both U and Th in our sample population is definitely not a distribution symmetrical about the mean, but is highly skewed toward lower values, as is shown by the separation of the mean and the median. In this circumstance, a few high values greatly alter the mean. In establishing a regional sampling program, a careful selection of a limited number of sampling sites for single rock analysis will provide a better clue to anomalous areas than composites from multiple rock specimens.

Trend surface analysis of uranium and thorium content, when combined with petrographic criteria for recognition of rocks of plutonic igneous

or metamorphic origin, can aid in the interpretation of regional crustal units. Anomalously high uranium and thorium values may identify discrete areas of plutonic activity (essentially equidimensional) or linear belts of probable metamorphic origin. Examples of uranium and thorium enrichment in both igneous and metamorphic settings are shown on our maps.

Acknowledgments

The authors wish to express their appreciation to the many oil companies who supplied the core samples on which this project depended. The cooperation of the staff of McMaster Nuclear Reactor made possible the delayed neutron activation analyses. Trend surface analysis was done by R. R. Culbert. D. A. Taylor assisted with the compilation of graphical material. Financial support for the project was given by grants from the National Research Council of Canada and the Department of Energy, Mines and Resources. The assistance of R. W. May as a critical reader is greatly appreciation. The manuscript was typed by V. Stephansson.

Addendum

TABLE 3. Precambrian Basement core sample locations, depths, and uranium–thorium analyses (ppm)

Index No.	Location					Elevation (feet asl)	Total depth (ft)	PC depth (ft)	Sample depth (ft)	U (ppm)	Th (ppm)
	Lsd.	Sec.	Twp.	Rge.	Mer.						
1	7—	29—	12—	2—	E1	800	1009	708	1009	0.93	
2	3—	1—	5—	2—	W1	787	1150	1042	1150	0.75	
3	3—	1—	8—	18—	W1	1364	3826	3816	3825	0.94	
4	9—	1—	37—	28—	W1	1186	2047	2035	2045	0.18	
5	16—	4—	3—	32—	W1	1617	8329	8315	8328	7.97	
6	3—	27—	8—	8—	W2	2058	8834	8680	8830	0.37	
7	2—	11—	15—	26—	W2	1937	7740	7682	7738	2.01	
8	1—	15—	48—	17—	W2	1425	2595	2543	2594	8.84	
9	11—	3—	50—	18—	W2	1370	3501	—	3056	0.28	
10	12—	3—	50—	18—	W2	1423	3269	—	2170	0.32	
11	12—	3—	50—	18—	W2	1423	3269	—	3170	0.29	
12	8—	9—	50—	18—	W2	1433	2437	2393	2378	1.77	
13	13—	18—	52—	13—	W2	1215	1619	1586	1615	3.91	
14	12—	15—	52—	14—	W2	1210	1790	1704	1785	3.19	
15	2—	5—	61—	24—	W2	1721	1825	1763	1820	1.01	
16	4—	31—	3—	26—	W3	3072	7339	7240	7335	0.47	
17	9—	32—	6—	22—	W3	3458	8858	8808	8820	11.76	
18	2—	4—	10—	19—	W3	3051	8777	8510	8774	3.31	
19	9—	20—	12—	2—	W3	2421	7785	7779	7785	4.60	
20	2—	21—	16—	17—	W3	2411	7312	7281	7305	23.46	
21	1—	9—	17—	14—	W3	2387	6755	6706	6755	4.80	
22	15—	3—	17—	18—	W3	2440	7260	7246	7260	15.25	
23	1—	31—	18—	28—	W3	2521	7440	7420	7440	0.12	
24	4—	16—	37—	1—	W3	1833	5415	5383	5410	1.28	
25	8—	15—	52—	2—	W3	1771	3297	3250	3290	0.54	
26	7—	14—	56—	17—	W3	2351	4333	4325	4332	0.33	
27	13—	21—	61—	15—	W3	1543	2773	2755	2767	0.28	
28	8—	11—	62—	22—	W3	1708	3461	3452	3460	3.38	
29	1—	36—	63—	5—	W3	1830	1923	1915	1921	0.44	
30	9—	21—	63—	8—	W3	1722	2061	2035	2061	1.43	
31	8—	8—	64—	2—	W3	2085	2028	2003	2009	0.41	
32	8—	8—	64—	2—	W3	2085	2028	2003	2026	1.97	
33	8—	30—	64—	15—	W3	1564	2435	2399	2435	1.45	
34	12—	14—	12—	12—	W4	2488	6981	6930	6975	4.58	
35	4—	12—	15—	27—	W4	3309	11836	11793	11815	0.50	
36	5—	1—	17—	14—	W4	2466	7281	7270	7276	0.15	
37	13—	22—	20—	12—	W4	2442	6155	6147	6147	n.d.	
38	6—	9—	31—	1—	W4	2409	7189	7168	7174	5.44	
39	13—	36—	35—	2—	W4	2667	7231	7229	7229	0.74	
40	1—	6—	38—	15—	W4	2746	8373	8345	8370	1.33	
41	16—	17—	48—	20—	W4	2479	8266	8105	8150	3.64	
42	8—	17—	50—	26—	W4	2373	8995	8984	8985	17.70	
43	8—	17—	50—	26—	W4	2373	8995	8984	8990	0.40	
44	14—	29—	52—	2—	W4	2089	5502	5468	5485	1.52	

TABLE 3 (*Continued*)

Location					Elevation	Total	-PC	Sample	U	Th
Lsd.	Sec.	Twp.	Rge.	Mer.	(feet asl)	depth (ft)	depth (ft)	depth (ft)	(ppm)	(ppm)
1—	11—	53—	12—	W4	2282	6437	6435	6437	7.57	7.1
8—	17—	53—	15—	W4	2380	7801	7790	7800	3.61	4.2
14—	14—	55—	15—	W4	2078	6534	6430	6533	1.03	3.3
7—	14—	57—	6—	W4	1984	5212	5207	5210	4.06	39.2
7—	14—	57—	6—	W4	1984	5212	5207	5210	0.96	9.9
6—	36—	58—	23—	W4	2074	7357	7162	7336	0.85	2.1
9—	29—	59—	24—	W4	2065	7527	7340	7527	0.07	0.7
10—	13—	60—	4—	W4	1973	4714	4700	4714	0.19	0.7
1—	27—	60—	26—	W4	2133	7519	7507	7518	7.59	7.9
16—	19—	62—	19—	W4	2323	6604	6590	6604	16.88	57.1
13—	17—	67—	23—	W4	2066	6406	6390	6405	2.74	5.1
4—	3—	69—	10—	W4	2515	5033	5019	5024	22.52	50.5
7—	24—	76—	18—	W4	2054	4641	4628	4633	0.67	15.6
7—	24—	76—	18—	W4	2054	4641	4628	4639	0.97	9.4
6—	10—	77—	25—	W4	2616	6120	6103	6120	3.15	127.7
12—	27—	78—	4—	W4	1857	2570	2557	2567	15.75	53.8
14—	9—	86—	7—	W4	1622	1793	1773	1792	1.27	22.3
7—	28—	87—	12—	W4	1540	2304	2299	2302	2.47	43.9
7—	11—	87—	17—	W4	1445	2863	2850	2860	0.55	15.9
5—	32—	88—	8—	W4	810	789	785	789	11.20	45.1
8—	36—	88—	8—	W4	831	936	906	929	0.68	21.4
8—	20—	89—	9—	W4	792	1142	1125	1141	1.75	41.9
10—	14—	91—	14—	W4	1560	2414	2408	2414	1.14	8.1
9—	34—	94—	14—	W4	1379	2000	1991	2000	2.55	179.5
12—	23—	98—	21—	W4	2259	3840	3836	3840	0.85	24.0
5—	29—	62—	1—	W5	2086	7575	7505	7575	0.63	2.1
10—	20—	62—	8—	W5	2548	9145	9112	9132	1.06	0.4
5—	35—	62—	18—	W5	2878	11320	11310	11316	0.23	0.8
6—	36—	63—	12—	W5	3708	10710	10668	10709	5.20	7.6
5—	31—	65—	6—	W5	2615	8422	8350	8400-8418 Composite	0.31	2.0
9—	20—	65—	13—	W5	3644	10624	10612	10614	4.81	16.0
9—	20—	65—	13—	W5	3644	10624	10612	10624	1.29	4.6
16—	12—	66—	13—	W5	3830	10521	10507	10511	1.20	7.6
8—	11—	68—	10—	W5	3183	8988	8965	8983	7.55	36.7
3—	5—	68—	22—	W5	2297	10736	10707	10730	1.27	14.2
11—	18—	72—	17—	W5	2350	8558	8522	8552	4.85	15.8
11—	11—	73—	13—	W5	2229	7406	7403	7406	0.28	1.3
6—	6—	75—	5—	W5	2777	7397	7075	7372	2.18	8.1
12—	16—	75—	15—	W5	1914	7197	7180	7194	2.70	15.7
15—	16—	75—	19—	W5	2093	7857	7844	7852	4.74	25.5
14—	15—	75—	22—	W5	1885	8418	8400	8418	15.29	34.2
5—	1—	77—	20—	W5	2065	7838	7837	7837	9.60	1.0
12—	33—	77—	21—	W5	1915	7740	7730	7740	5.36	18.1
15—	21—	78—	20—	W5	2064	7644	7625	7644	1.93	10.1
12—	11—	78—	22—	W5	1900	7827	7818	7820	6.35	48.1
16—	9—	79—	22—	W5	1905	7627	7619	7625	4.46	11.4
1—	12—	79—	22—	W5	1929	7847	7840	7847	1.52	8.1
1—	16—	79—	22—	W5	1906	7424	7420	7424	9.48	12.9
10—	20—	79—	22—	W5	1880	7658	7630	7652	2.64	6.2
2—	25—	80—	17—	W5	2442	6808	6782	6808	3.13	19.8
16—	25—	80—	17—	W5	2391	6790	6754	6769	5.11	29.9
14—	34—	80—	17—	W5	2476	6877	6864	6875	6.46	43.0
8—	17—	80—	21—	W5	2089	7770	7738	7770	6.34	22.7
13—	18—	80—	23—	W5	1936	7598	7580	7598	6.48	0.2
5—	3—	81—	17—	W5	2446	6729	6684	6727	7.47	37.9
10—	6—	82—	1—	W5	1908	5009	5004	5007	1.12	0.1
7—	5—	82—	18—	W5	2314	7296	7271	7290	3.12	11.6
16—	13—	83—	24—	W5	2111	7116	7105	7114	10.05	10.9
13—	24—	84—	2—	W5	2077	5010	5001	5009	4.87	19.6
6—	11—	84—	5—	W5	2118	5357	5340	5348	2.59	20.3
6—	31—	84—	7—	W5	1987	5293	5283	5288	0.73	9.9
2—	15—	84—	16—	W5	2384	5912	5895	5912	13.59	45.2
1—	22—	84—	17—	W5	2227	6096	6090	6095	1.45	1.8
11—	3—	85—	12—	W5	1858	5156	5109	5152	1.32	25.7

is project depended
taff of McMaster N
e the delayed neutron
d surface analysis was
A. Taylor assisted with
cal material. Financial
as given by grants from
Council of Canada and
gy, Mines and Resou
W. May as a critical re
ion. The manuscript
son.

thorium analyses (ppm)

Sample depth (ft)	U (ppm)
1009	0.93
1150	0.75
3825	0.94
2045	0.18
8328	7.97
8830	0.37
7738	2.01
2594	8.84
3056	0.28
2170	0.32
3170	0.29
2378	1.77
1615	3.91
1785	3.19
1820	1.01
7335	0.47
8820	11.76
8774	3.31
7785	4.60
7305	23.46
6755	4.80
7260	15.25
7440	0.12
5410	1.28
3290	0.54
4332	0.33
2767	0.28
3460	3.38
1921	0.44
2061	1.43
2009	0.41
2026	1.97
2435	1.45
6975	4.58
11815	0.50
7276	0.15
6147	n.d.
7174	5.44
7229	0.74
8370	1.33
8150	3.64
8985	17.70
8990	0.40
5485	1.52

TABLE 3 (*Continued*)

Index No.	Location					Elevation (feet asl)	Total depth (ft)	P€ depth (ft)	Sample depth (ft)	U (ppm)	Th (ppm)
	Lsd.	Sec.	Twp.	Rge.	Mer.						
109	16—	23—	85—	19—	W5	2012	6106	6090	6106	1.35	
110	8—	22—	86—	9—	W5	1820	4981	4980	4981	4.88	
111	6—	27—	86—	9—	W5	1770	4860	4849	4853	0.60	
112	12—	32—	86—	9—	W5	1732	4791	4764	4780	0.85	
113	16—	25—	86—	20—	W5	1707	6077	6010	6076	1.29	
114	5—	21—	86—	22—	W5	2039	6589	6589	6589	0.53	
115	2—	25—	86—	26—	W5	2278	6698	6685	6696	2.34	
116	12—	30—	87—	7—	W5	2031	5030	5023	5028	5.73	
117	8—	11—	87—	8—	W5	1974	4663	4658	4660	2.38	
118	16—	11—	87—	8—	W5	1986	4647	4628	4646	3.37	
119	12—	14—	87—	8—	W5	1935	5050	4993	5050	1.18	
120	4—	16—	87—	8—	W5	1893	4838	4742	4799	5.01	
121	12—	16—	87—	8—	W5	1879	4875	4836	4870	6.10	
122	12—	17—	87—	8—	W5	1811	4797	4778	4797	5.85	
123	2—	19—	87—	8—	W5	1796	4837	4825	4828	11.62	
124	11—	21—	87—	8—	W5	1868	4800	4798	4800	6.27	
125	10—	3—	87—	10—	W5	1733	4771	4749.5	4751	0.40	
126	14—	17—	88—	6—	W5	2229	5059	5037	5059	3.56	
127	4—	20—	88—	7—	W5	2061	5044	5020	5030	2.47	
128	2—	4—	88—	8—	W5	1839	4835	4814	4817	11.95	
129	10—	19—	87—	8—	W5	1786	4810	4768	4780	2.44	
130	2—	22—	88—	8—	W5	1855	4926	4910	4910	1.52	
131	2—	23—	88—	8—	W5	1918	4877	4860	4866	1.28	
132	4—	29—	88—	8—	W5	1726	4653	4644	4651	32.11	
133	2—	17—	89—	7—	W5	1912	4772	4742	4751	5.43	
134	6—	20—	89—	19—	W5	1830	5905	5890	5905	2.07	
135	15—	24—	90—	15—	W5	2431	5819	5807	5810	2.10	
136	15—	24—	90—	15—	W5	2431	5819	5807	5819	0.49	
137	9—	35—	91—	6—	W5	1981	4705	4686	4703	1.66	
138	9—	24—	93—	18—	W5	1871	5705	5670	5705	14.90	
139	10—	8—	99—	13—	W5	2256	5636	5627	5635	0.61	
140	15—	24—	109—	17—	W5	1015	4467	4465	4467	5.28	
141	15—	32—	109—	19—	W5	1092	4871	4868	4871	4.72	
142	6—	24—	111—	22—	W5	2391	6391	6383	6385	1.17	
143	7—	22—	116—	22—	W5	1114	5077	4968	5072	1.01	
144	7—	10—	119—	20—	W5	1067	4528	4525	4528	7.47	
145	9—	7—	124—	18—	W5	1003	3731	3725	3731	5.42	
146	16—	18—	126—	14—	W5	1022	3148	3145	3148	0.54	
147	16—	25—	72—	5—	W6	2446	11710	11695	11700	1.35	
148	2—	2—	73—	1—	W6	2223	10195	10132	10195	5.29	
149	13—	20—	75—	2—	W6	2117	9612	9593	9612	4.00	
150	12—	20—	77—	3—	W6	2419	9347	9337	9347	6.69	
151	7—	36—	77—	9—	W6	3031	11705	11645	11700	7.75	
152	4—	20—	78—	1—	W6	1896	8264	8256	8264	5.88	
153	12—	20—	78—	6—	W6	2287	9847	9775	9818	10.92	
154	4—	29—	81—	1—	W6	2090	7255	7243	7255	4.32	
155	2—	14—	82—	2—	W6	2188	7492	7480	7492	14.63	
156	2—	5—	83—	2—	W6	2334	7977	7930	7977	4.45	
157	14—	31—	84—	2—	W6	2325	8227	7840	8225	0.52	
158	16—	12—	84—	8—	W6	2116	8014	8010	8014	2.99	
159	4—	27—	85—	2—	W6	2569	8758	8750	8750	0.86	
160	14—	10—	88—	2—	W6	2355	6962	6958	6962	4.38	
161	8—	16—	88—	2—	W6	2401	6915	6882	6910	4.33	
162	6—	11—	101—	4—	W6	1963	7320	7300	7320	6.49	
163	11—	17—	102—	2—	W6	1562	6838	6835	6838	3.14	
164	2—	16—	107—	6—	W6	1755	6960	6920	6957	4.70	
165	16—	18—	107—	6—	W6	1774	7365	7315	7360	3.42	
166	10—	27—	109—	9—	W6	1769	7329	7308	7329	3.04	
167	15—	22—	115—	10—	W6	1350	6512	6362	6470	2.50	
168	9—	26—	120—	11—	W6	2062	7005	6980	7005	6.37	
169	9—	26—	120—	11—	W6	2062	7005	6980	7005	4.21	
170	2—	7—	124—	2—	W6	2382	6121	6115	6121	1.53	
171	12—	30—	125—	2—	W6	2447	5992	5965	5992	2.30	
172	12—	31—	78—	14—	W6	2433	12040	11892	12038	5.13	
173	6—	29—	81—	15—	W6	2382	11619	11614	11618	2.34	
174	1—	26—	86—	16—	W6	2415	10913	10906	10909	0.15	

TABLE 3 (*Concluded*)

Location					Elevation (feet asl)	Total depth (ft)	PC depth (ft)	Sample depth (ft)	U (ppm)	Th (ppm)
Lsd.	Sec.	Twp.	Rge.	Mer.						
57°47′ N		120°14′ W			2371	10034	9800	10029	10.33	42.8
58°05′ N		121°54′ W			1920	9930	9925	9925	3.17	10.8
58°16′ N		120°51′ W			1434	8439	8439	8437	0.68	6.0
60°09′ N		121°08′ W			2288	8233	8220	8230	6.06	116.6
60°51′ N		114°24′ W			724	1181	1171	1173	0.83	5.8
60°55′ N		118°50′ W			1083	2910	2898	2900	0.55	3.5
61°19′ N		118°40′ W			497	2230	2192	2230	11.30	21.0
61°20′ N		122°30′ W			622	2237	1310	2085	0.97	3.4
62°20′ N		119°00′ W			2438	3229	3147	3225	1.53	2.2
Dakota localities										
2—		155N—	96W		2316	13615	13592	13603	2.35	10.6
28—		159N—	63W		1562	3408	3404	3408	0.31	2.2
1—		159N—	95W		—	—	—	15128	1.07	4.4

[illegible] two samples are listed for one well, two distinctly different lithologies were encountered in the core.
[illegible]. Depth to Paleozoic/Precambrian unconformity, in feet.

[illegible] BURWASH, R. A. and CULBERT, R. R. 1976. Multivariate geochemical and mineral patterns in the Precambrian basement of western Canada. Can. J. Earth Sci. 13, pp. [illegible]-18.

[illegible] BURWASH, R. A. and CUMMING, G. L. 1974. Helium source-rock in southwestern Saskatchewan. Bull. Can. Petrol. Geol. 22, pp. 405–412.

[illegible] BURWASH, R. A. and KRUPIČKA, J. 1969. Cratonic reactivation in the Precambrian basement of western Canada, I. Deformation and chemistry. Can. J. Earth Sci. 6, pp. [illegible]-1396.

– 1970. Cratonic reactivation in the Precambrian basement of western Canada, II. Metasomatism and metastasy. Can. J. Earth Sci. 7, pp. 1275–1294.

[illegible] BURWASH, R. A., KRUPIČKA, J., and CULBERT, R. R. [illegible] Cratonic reactivation in the Precambrian basement of western Canada; III. Crustal evolution. Can. J. Earth [illegible] 10, pp. 283–291.

[illegible], S. P. JR., PETERMAN, Z. E., and HEIER, K. S. [illegible] Abundances of uranium, thorium and potassium. In Handbook of Physical Constants. Geol. Soc. Am. Mem. 97, pp. 521–541.

[illegible]WING, G. L. 1974. Determination of uranium and thorium in meteorites by the delayed neutron method. Geochem. Geol. 13, pp. 257–267.

DARNLEY, A. G., GRASTY, R. L., and CHARBONNEAU, B. W. 1971. A radiometric profile across part of the Canadian Shield. Geol. Surv. Can. Pap. 70-46, 42 p.

EADE, K. E. and FAHRIG, W. F. 1971. Geochemical evolutionary trends of continental plates—a preliminary study of the Canadian Shield. Geol. Surv. Can. Bull. 179, 51 p.

GALE, N. H. 1967. Development of delayed neutron technique as rapid and precise method for determination of uranium and thorium at trace levels in rocks and minerals, with application to isotope geochronology. *In*: Radioactive dating and methods of low-level counting. Vienna, Int. Atomic Energy Agency, pp. 431–452.

ROSHOLT, J. N., PETERMAN, Z. E., and BARTEL, A. J. 1970. U–Th–Pb and Rb–Sr ages in granite reference sample from southwestern Saskatchewan. Can. J. Earth Sci. 7, pp. 184–187.

SHAW, D. M. 1967. U, Th and K in the Canadian Precambrian Shield and possible mantle compositions. Geochim. Cosmochim. Acta, 31, pp. 1111–1113.

WALLIS, R. H. 1970. A geological interpretation of gravity and magnetic data, northwest Saskatchewan. Can. J. Earth Sci. 7, pp. 858–868.

Reprinted from

Canadian Journal of Earth Sciences

Réimpression du

Journal canadien des sciences de la terre

The geochemistry of possible metavolcanic rocks and their relationship to mineralization at Montauban-Les-Mines, Quebec

Karen Stamatelopoulou-Seymour
and Wallace H. MacLean

Volume 14 • Number 11 • 1977

Pages 2440–2452

National Research Council Canada
Conseil national de recherches Canada

The geochemistry of possible metavolcanic rocks and their relationship to mineralization at Montauban-Les-Mines, Quebec

KAREN STAMATELOPOULOU-SEYMOUR AND WALLACE H. MACLEAN

Department of Geological Sciences, McGill University, 3450 University Street, Montreal, P.Q., Canada H3A 2A7

Received March 21, 1977

Revision accepted for publication June 13, 1977

Base metal and gold ores in thin calc-silicate and cordierite gneiss units at Montauban-Les-Mines have historically been described as pyrometasomatic deposits related to granitic intrusions. They are stratigraphically overlain by quartzo–feldspathic gneiss and amphibolite, the uppermost amphibolite unit being a pillowed metabasalt.

Chemical analysis shows all the amphibolites to be derived from basic igneous rocks, probably basaltic flows or shallow intrusives. Some analyses of quartzo–feldspathic gneisses follow igneous trends on variation diagrams and plot closely with those of indisputable volcanic rocks associated with massive sulfide deposits from the Kuroko District, Japan, and Noranda, Quebec. They appear to be metamorphosed intermediate to acidic volcanic tuffs and associated sediments, and are thus termed 'leptites'.

The volcanic environment of the ore deposits, their general conformability to stratification, and other distinguishing features, strongly suggest they may be exhalite deposits formed in the overlapping carbonate–sulfide facies.

On a auparavant décrit les minerais de métaux de base et d'or dans de minces unités de gneiss à silicates calciques et à cordiérite à Montauban-les-Mines comme des dépôts pyrométasomatiques reliés à des intrusions granitiques. Ils sont recouverts stratigraphiquement par des gneiss quartzo–feldspathiques et des amphibolites, l'unité supérieure d'amphibolite étant constituée d'un métabasalte en coussins.

L'analyse chimique démontre que toutes les amphibolites dérivent de roches ignées basiques, probablement de coulées basaltiques ou d'intrusions à faible profondeur. Quelques analyses de gneiss quartzo–feldspathiques suivent la tendance des roches ignées sur les diagrammes de variation et se groupent près des roches d'origine indisputablement volcanique associées aux dépôts de sulfures massifs des districts de Kuroko, au Japon, et de Noranda, au Québec. Ces roches semblent être des tufs volcaniques métamorphisés de composition intermédiaire à acide et leurs sédiments associés, et ainsi on les désigne sous le nom de 'leptites'.

Le milieu volcanique des dépôts de minerai, leur concordance générale avec la stratification, et d'autres caractéristiques distinctives suggèrent fortement que ce sont des dépôts d'exhalites formés par le recouvrement des faciès carbonate–sulfure.

[Traduit par le journal]

Can. J. Earth Sci., 14, 2440–2452 (1977)

Introduction

Lead–zinc, copper, and gold deposits occur at Montauban-Les-Mines, Portneuf County, Quebec, 84 km west of Quebec City and 200 km north of Montreal (Fig. 1). They lie within a calc-silicate and gneiss formation in a series of quartzo–feldspathic gneisses and amphibolites in the Grenville Province of the Canadian Shield.

The sulfide bodies, composed mainly of coarse-grained sphalerite and galena, and lesser pyrite, pyrrhotite, and chalcopyrite, form irregular lenses and pods surrounded by equally coarse-grained calc-silicate and silicate host rocks. Small lode gold deposits are spatially associated with sulfide lenses. Mining began in 1913 and continued intermittently until 1955. The area is presently being explored for base metals and gold (Flanagan and McAdam 1976).

The ores have historically been described as pyrometasomatic replacement deposits related to nearby intrusions of granitic and dioritic rocks (Alcock 1930; Osborne 1939; Wilson 1939; Smith 1956). As the ores are generally conformable with their host rocks and have many characteristics of volcanogenic sulfide deposits, as described by Sangster (1972), Ridler (1971), Ridler and Shilts (1974), Rickard and Zweifel (1975), and others, an investigation was made to see if the deposits at Montauban were compatible with such an origin. In this first report, the petrography and chemistry of the wall-rocks are studied to determine whether the amphibolites and some of the gneisses could be

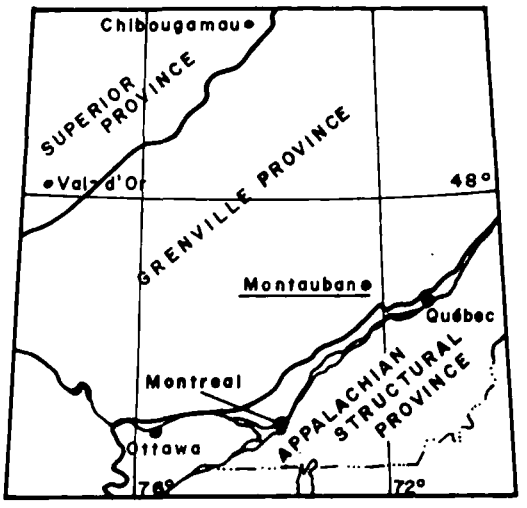

FIG. 1. Location map.

derived from volcanic rocks. In another paper, we will report on the ores and their relation to the wall rocks. Field work was carried out in September 1972, in the process of collecting data for an M.Sc. thesis. One of the main traverses with sampling points is shown in Fig. 3.

The immediate host rocks to the ore are coarse-grained calc-silicate composed of diopside, tremolite, calcite, and dolomite, and cordiorite – anthophyllite gneiss with garnet, quartz, and sillimanite. These are, in turn, surrounded by hornblende-bearing gneiss, quartzo–feldspathic gneiss and amphibolite, all of which belong to the Grenville Series. Complex folding and amphibolite facies metamorphism have obliterated most primary features. Rocks of the Grenville Series in this part of the Grenville Province were generally considered to be of sedimentary origin (Alcock 1930; Osborn 1939; Pyke 1966), although some amphibolite was shown by Pyke (1966) to be metabasalt.

Evans and Leake (1960) and Leake (1964) have designed chemical discrimination techniques to distinguish para- and ortho-amphibolites, and we have applied these to the Montauban amphibolites. These discrimination techniques have been extended by Van de Kamp (1968) to more siliceous gneisses where the original rock may have been sediment or volcanogenic material of acidic composition. The chemical differences here are not as obvious. Acidic and intermediate volcanic rocks, particularly those close to volcanogenic ore deposits, are frequently altered by processes involving the mobility and loss of alkalis and calcium, silicification and chloritization (Franklin *et al.* 1975; Spitz and Darling 1975; Descarreaux 1973; Tatsumi and Clark 1972). Superimposed on this are possible chemical changes due to metamorphism. But even with these changes the igneous nature of the rocks may possibly be established. Thus, we have used these chemical discrimination techniques on Montauban gneisses to show that at least some of them could be derived from acidic volcanogenic material.

Regional Geology

Pyke (1966) mapped the area at a scale 1 in. = 1 mi (Fig. 2), and assigned all the rocks, except the intrusive rocks, to his 'Grenville Series' (Table 1). The bulk of the Series in the area is represented by northerly trending quartz–plagioclase–biotite–(hornblende) gneisses containing sillimanite, cordierite, or garnet bearing members. These gneisses, referred to here generally as quartzo–feldspathic gneisses, are intercalated with amphibolites, minor quartzite, and calc-silicate units, one of the latter being the host to the Pb–Zn mineralization. The quartzo–feldspathic gneisses have not been extensively migmatized and, in the past, were interpreted as being mainly paragneiss. They are cut by large intrusive bodies ranging in composition from granite to gabbro (Table 1). Regional metamorphism is in the amphibolite facies.

The lithologies in the vicinity of the mine can be divided into four rock groups (Fig. 3). (a) Calc-silicate, carbonate, and cordierite gneiss. These gneisses range from 30–60 m in thickness and enclose and host the mineralized zones. (b) Hornblende and biotite bearing gneiss. These are dark grey monotonous gneisses that lie east of the mineralized zone, and were called 'composite gneiss' by Smith (1956). Garnet bearing pegmatite dykes are typically abundant in this unit. (c) Quartzo–feldspathic gneiss. These well banded gneisses contain muscovite, biotite, and hornblende bearing members, and a few thin layers of amphibolite. They extend westward from the mineralized zone for 1 km. (d) Amphibolite (pillowed metabasalt (Pyke 1966)). This rock type forms a ridge 1 km west of the deposits.

The structure of the rocks in this area, as in most of the Grenville Province, is complex and

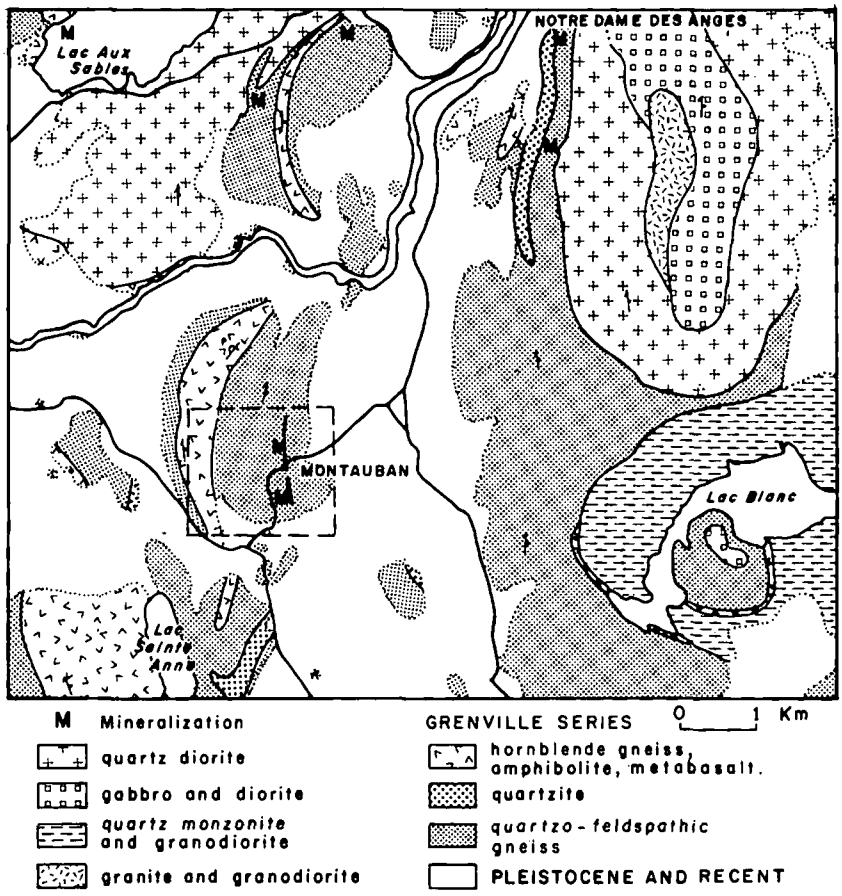

FIG. 2. Geological map of the Montauban district (after Pyke 1966). The rectangle at Montauban outlines the area for Fig. 3.

TABLE I. Table of Precambrian formations (after Pyke 1966)

Granitic dykes and sills
—Intrusive contact—
Late Tectonic(?) Granite, quartz monzonite, granodiorite, syenodiorite; lesser diorite, gabbro, and related basic rocks; minor pegmatite, aplite, diabase (?)
—Intrusive contact—
Syntectonic Quartz monzonite, granodiorite; minor pegmatite and aplite. Quartz diorite
—Intrusive contact—
Augen and porphyroblastic hornblende and biotite gneiss
— —
'Grenville Series' Biotite gneiss, hornblende gneiss; lesser quartzite, basic volcanics; minor limestone, calc-silicate

not well understood. Locally the rocks strike northerly and dip about 40° to the east. The local structure at the ore zone has been interpreted as being: (1) the east limb of an overturned syncline (Smith 1956; Pyke 1966), and (2) the axial trace of a syncline overturned to the west (O'Neil and Osborne 1939; Wilson 1939). Pillow structures in the metabasalt face west indicating the unit is overturned (Pyke 1966). There is no evidence of a fold closure or major fault in the rocks between the pillowed metabasalt and the mine, hence we assume that all the rocks are overturned and belong to a continuous stratigraphic sequence.

Petrography and Chemistry

The calc-silicate, quartzo–feldspathic and other gneisses and various amphibolites were sampled for petrographic and chemical analyses. The chemical analyses were used in an attempt

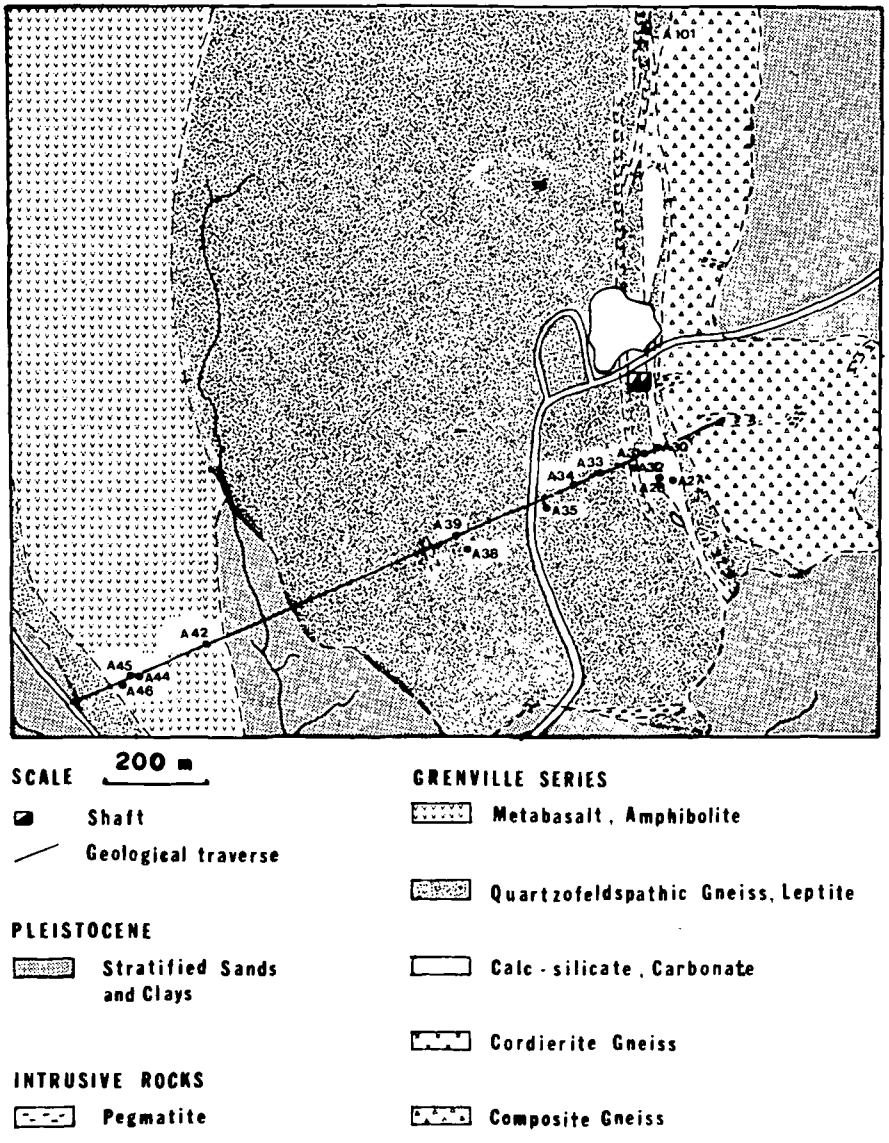

FIG. 3. Geological map at the Montauban mine area (after Wilson 1939), showing lithologies and location of one of the sampling traverses.

to distinguish between a sedimentary, volcanic, or metasomatic derivation of the rocks using the discrimination techniques outlined by Bastin (1909), Evans and Leake (1960), Leake (1964), and Van de Kamp (1968).

Major elements were analyzed by X-ray fluorescence against rock standards BCR-1, AGV-1, and GA. The data were corrected by computer for matrix effects and normalized on a volatile-free basis (Gunn 1967). Precision of analysis for Na and Mg is $\pm 5\%$, and that for other elements is better than 2%. Cr, Co, Ni, and Cu were analyzed by atomic absorption spectrometry; the precision of analysis is within $\pm 5\%$ of the element in the sample.

Amphibolites

Amphibolite rocks are common in the Montauban area. Osborne (1939) first suggested that they could be of volcanic origin, and later Pyke (1966) found pillow structures in the large mass of amphibolite 1 km west of the mine (Figs. 2, 3).

TABLE 2. Chemical analyses of Montauban amphibolites: on a volatile-free basis and recalculated to 100%. A-42, A-44, A-45, and A-46 are from the ridge west of the mine (Fig. 3). Pyke's (1966) analysis of pillowed metabasalt from this ridge is in the last column

	A-32	A-42	A-44	A-45	A-46	A-48	A-63	A-75	A-105	Pyke (1966)
SiO_2	51.38	48.86	49.81	49.13	48.01	50.13	49.57	47.30	51.46	48.98
TiO_2	1.03	1.02	1.28	1.18	1.23	0.75	1.37	0.82	0.86	0.99
Al_2O_3	18.49	17.50	16.71	16.13	16.86	16.90	14.88	15.87	19.71	15.60
Fe_2O_3	10.62*	2.19	0.88	1.70	1.44	1.32	12.85*	0.87	1.48	1.94
FeO	—	7.51	9.86	9.35	9.51	8.07	—	11.12	7.44	9.39
MnO	—	0.20	0.19	0.19	0.30	0.17	—	0.21	0.16	0.19
MgO	5.07	4.82	7.63	8.65	6.93	7.67	8.55	8.77	4.90	7.51
CaO	10.16	14.33	11.80	11.14	12.52	10.60	9.33	12.27	9.39	12.52
Na_2O	2.25	3.02	1.23	2.08	2.42	3.54	2.87	2.23	3.27	2.51
K_2O	0.82	0.29	0.39	0.23	0.51	0.62	0.25	0.31	1.15	0.20
P_2O_5	0.18	0.26	0.22	0.21	0.26	0.24	0.32	0.22	0.18	0.16
ppm										
Cr	—	245	144	166	198	310		269	32	
Co	—	54	52	53	49	53		54	39	
Cu	—	120	68	49	16	102		92	16	
Ni	—	151	81	96	79	137		148	44	

*Total iron as Fe_2O_3.

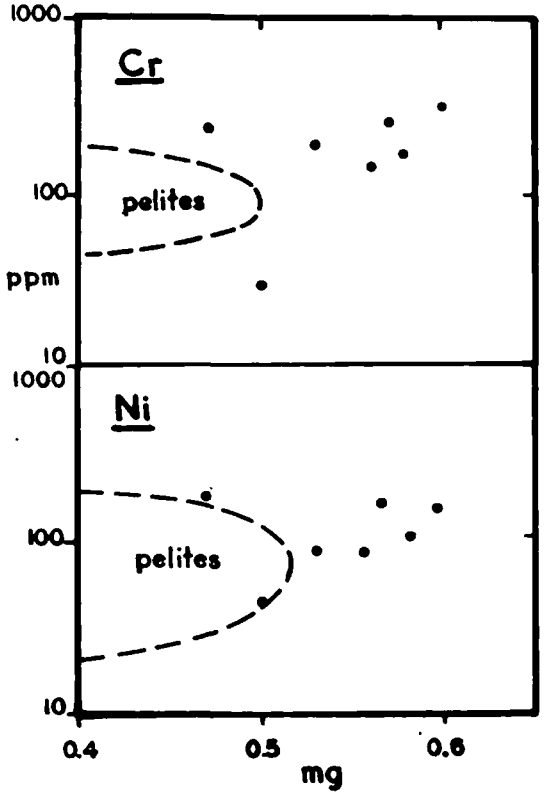

FIG. 4. Ni and Cr vs. Niggli *mg* for Montauban amphibolites. The field for pelites in this and other diagrams is after Leake (1964). The increase in Ni and Cr with *mg* indicates igneous rocks.

Minor amphibolite units without these primary features, too thin to be noted on Pyke's map, are intercalated with quartzo–feldspathic gneisses between the mine and the metabasaltic ridge.

In thin section the amphibolites are composed of medium-grained green–brown hornblende, plagioclase (An_{51-63}), biotite, quartz and, in some samples, clinopyroxene, garnet, and opaque oxides.

Chemical analyses of the amphibolites are listed in Table 2 along with Pyke's (1966) analysis of the pillowed metabasalt. It is readily evident that they are very similar and that the rocks are probably closely related. The possibility of a common parentage for the amphibolites can be tested by other means.

Leake (1964) emphasized the difference between sedimentary and igneous rocks by using the variation in the relative amounts of elements rather than their absolute concentration. For this purpose Ni and Cr are useful since they show positive correlation with Niggli *mg* in rocks of igneous parentage, "whereas mixtures of pelite and dolomite or limestone become richer in Cr and Ni with decrease in *mg*" (Leake 1964). Cr and Ni show a positive correlation with *mg* for all the Montauban amphibolites (Fig. 4) and, thus, may be considered to be derived from igneous rocks.

The average contents of Cu, Cr, Co, and Ni in the amphibolites (Table 2) also fall within the

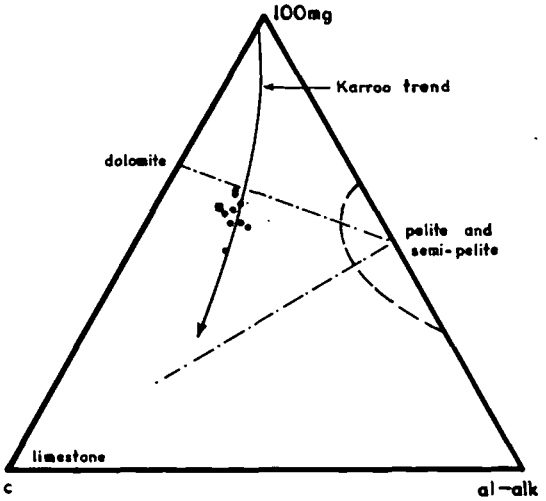

FIG. 5. Plot of Niggli values for the thin intercalated amphibolites (circles) and thick pillowed metabasalt (square) from Pyke (1966). The plots cluster in a small area on the differentiation trend line of Karroo dolerites (Leake 1964).

range for average basalts as compiled by Prinz (1967). Turekian (1963) noted the marked covariance of Cr and Ni and the narrow ranges of Cr/Ni values within a basaltic area and within the same region, 1.3–1.6 (Turekian 1963), 0.6–3.9 (Prinz 1967). The average Cr/Ni value of 1.7 and the range of 0.7–2.5 for the amphibolites at Montauban indicate that they may all be of the same parentage.

The analyses of the Montauban amphibolites also exhibit a close grouping in the Niggli 100 *mg–c–(al–alk)* and *c–mg* plots, used by Leake (1964), where they coincide with the middle stage differentiates on the igneous trend of the Karroo dolerites (Figs. 5, 6). The case for an igneous parentage is further substantiated in the *(al–alk)–c* diagram (Fig. 7), where the Montauban amphibolites plot closely with the Karroo dolerites within the igneous field.

On an AFM diagram (Fig. 8) the Montauban amphibolites plot closely together and mostly within the tholeiitic field.

From these tests we conclude that the small amphibolite units are metamorphosed tholeiitic basalt, probably belonging to the same magma series as the pillowed metabasalt.

Quartzo–Feldspathic Gneisses

Quartzo–feldspathic gneisses are the most abundant rocks of the Grenville Series at Montauban. A number of the gneisses sampled here lie between the metavolcanic ridge and the mine (Fig. 3). They are dark to light grey, fine to medium grained, finely banded, and have a general northerly strike with a strong foliation commonly parallel to the compositional layering.

Three main varieties of gneiss have been recognized based on mineralogical criteria: (1) quartz–biotite–feldspar, (2) quartz–biotite–hornblende–feldspar, and (3) quartz–biotite–muscovite–sillimanite–(garnet). Their prograde mineral assemblages are all compatible with the almandine-amphibolite facies of metamorphism, sillimanite subfacies.

'Grenville paragneiss' was the name used by previous investigators for these quartz-rich, biotite bearing gneisses in the Montauban area, which were considered to be exclusively of sedimentary origin (Bancroft 1915; Smith 1956). In the present text the general term quartzo–feldspathic gneiss is used instead, as it may include rocks of volcanic as well as sedimentary origin. The term 'leptite' is used for some of these gneisses as it denotes rocks of possible acidic volcanic origin (Sederholm 1935).

Twenty-four samples of quartzo–feldspathic gneiss at Montauban have been screened for excess alumina (more than 5% corundum in the norm), which would indicate a sedimentary rock (Bastin 1909), or an extremely altered rock. Sixteen of the samples had less than 5% normative corundum and were thus selected as possible nonsediments and have been assigned the term 'leptites'. Chemical analyses of these rocks are given in Table 3 and are plotted on variation diagrams (Leake 1964; Van de Kamp 1968) together with acidic volcanic rocks from Kuroko deposits of Japan, the Millenbach Mine, Noranda, Quebec, and the Hermon Group leptites (Jennings 1969). On *mg–c* (Fig. 9), *(al–alk)–c* (Fig. 10), and *(al–alk)–c–100 mg* (Fig. 11) diagrams the Montauban leptites generally plot with known acidic volcanic rocks, and on Figs. 10 and 11 they systematically follow igneous differentiation trends. In this way it can be inferred that these quartzo–feldspathic gneisses at Montauban may comprise highly metamorphosed equivalents of intercalated acidic volcanic tuffs, silicified tuffs, and associated sediments.

Calc-silicate

The main host rock for the massive Pb–Zn

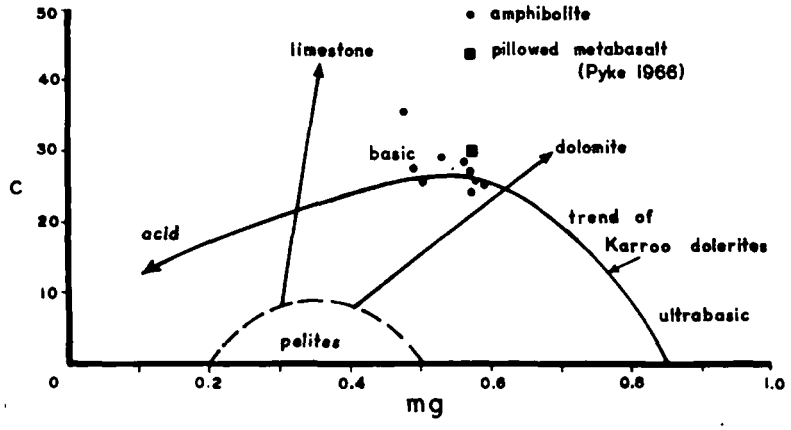

FIG. 6. Plot of Niggli *c* vs. *mg* values showing distribution of Montauban amphibolites along basic part of trend of Karroo dolerites (Leake 1964).

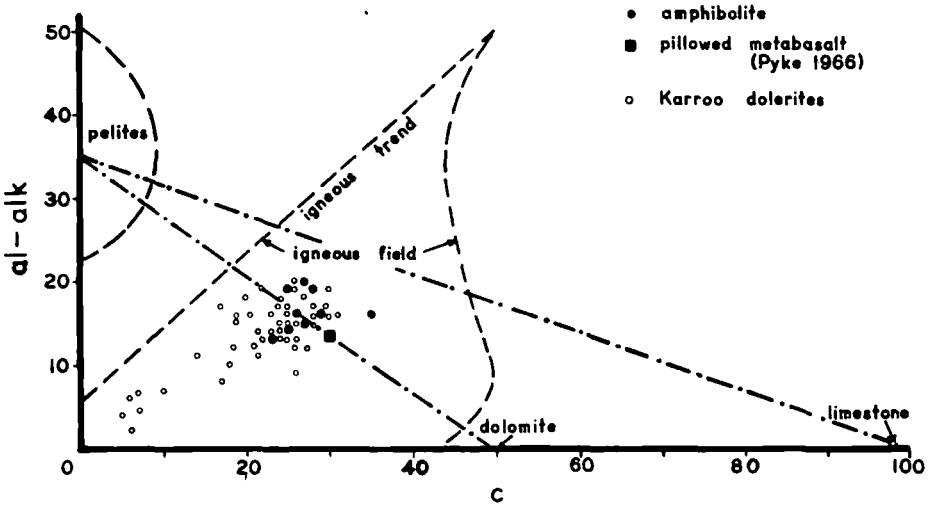

FIG. 7. Niggli (*al–alk*) vs. *c* diagram for Montauban amphibolites and Karroo dolerites.

ores is a calc-silicate unit which has an outcrop length of approximately 1000 m and varies in width from 1 to 60 m (Fig. 3). The rock consists mainly of medium-grained tremolite, and lesser pale green diopside which either has a granular texture or occurs as large euhedral crystals up to 10 cm × 30 cm in size. Quartz, calcite, and dolomite are associated with the silicate minerals. Analyses of this unit are given in Table 5.

Other minerals identified are: gahnite, wilsonite, white to brown phlogopite, epidote, garnet, apatite, sphene, brucite, graphite, anorthite, and hisingerite. Leuchtenbergite, penninite, antigorite, tourmaline, and breunnerite have been reported by Wilson (1939). Barite was detected during the milling of the ore. Ore minerals are mainly sphalerite and galena with lesser pyrite, pyrrhotite, chalcopyrite, cubanite, and tetrahedrite.

Other calc-silicate and carbonate zones with associated sulfide or iron oxide mineralization are present in the Montauban district (Stamatelopoulou-Seymour 1975; Pyke 1966).

Cordierite Gneiss

Cordierite gneiss is of restricted occurrence in the Montauban area (Fig. 3), where it is mineralized with vienlets and disseminations of

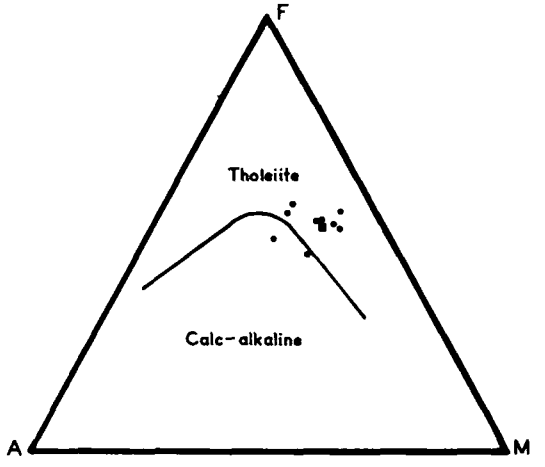

FIG. 8. AFM diagram for thin intercalated amphibolites (circles) and pillowed metabasalt (square).

chalcopyrite, pyrrhotite, sphalerite, gold, and minor galena and pyrite, sometimes sufficiently concentrated to be mined. Overall, this unit is characterized by its close association with the calc-silicate unit, its peculiar mineralogy, and its role as host to sulfide and gold mineralization. It is grey in colour, generally quartz-rich, and lies to the north, and partly envelops the northern part of the calc-silicate unit. It is rich in small red garnets and phlogopite and is conformable with the quartzo–feldspathic gneisses. The mineral assemblage is quartz–cordierite–biotite (phologopite) – muscovite – garnet–anthophyllite –plagioclase–(sillimanite). Sillimanite is subordinte and not present with plagioclase. Bands of anthophyllite in a groundmass of cordierite are intercalated in the gneiss (Wilson 1939). Chemical analyses of the gneiss are listed in Table 4.

Composite Gneiss

This grey, fine to coarsely grained and banded, hornblende–biotite gneiss, probably over 1 km thick, lies directly beneath the calc-silicate and the cordierite gneiss. Pegmatite dykes, up to 30 m thick, are much more numerous in this gneiss than in other rocks in the vicinity of the mine. Only one sample of the gneiss has been analyzed (Table 4), giving little more than an indication of its composition. This one analysis falls within the range of basalts and is unlike most sedimentary rocks.

TABLE 3. Chemical analyses of leptites: on a volatile-free basis and recalculated to 100%

	A-31	A-38	A-39	A-69	A-70	A-77	A-80	A-84	A-88	A-89	A-90	A-121	A-33	A-34	A-35	A-123
SiO_2	75.33	67.35	65.01	76.91	71.69	74.71	69.65	75.26	76.93	68.74	64.56	75.14	86.44	80.27	85.66	89.34
TiO_2	0.47	0.61	0.43	0.39	0.45	0.30	0.40	0.62	0.16	0.37	0.65	0.30	0.17	0.21	0.24	0.07
Al_2O_3	11.35	14.91	16.71	10.31	13.89	12.55	15.22	13.21	12.34	15.57	16.48	13.09	7.53	10.93	8.74	6.55
Fe_2O_3*	4.30	6.72	6.31	3.37	4.09	3.08	4.48	3.69	2.10	3.89	6.43	3.70	1.41	1.74	1.95	0.42
MgO	1.97	1.38	0.99	2.23	1.53	0.73	1.74	0.98	1.19	2.30	3.75	0.60	0.44	0.54	0.51	0.26
CaO	4.61	3.83	2.81	5.54	4.97	1.11	2.52	1.74	2.02	1.59	1.80	1.32	0.78	0.65	1.04	1.64
Na_2O	0.81	3.29	2.93	0.44	0.74	2.97	3.84	2.14	2.04	4.90	2.04	4.12	2.48	4.41	0.85	1.31
K_2O	1.03	1.66	4.81	0.61	2.46	4.45	2.02	2.32	3.16	2.49	4.28	1.66	0.69	1.23	1.01	0.36
P_2O_5	0.14	0.25	0.00	0.20	0.18	0.08	0.11	0.03	0.06	0.14	0.00	0.07	0.06	0.00	0.00	0.04

*Total iron as Fe_2O_3.

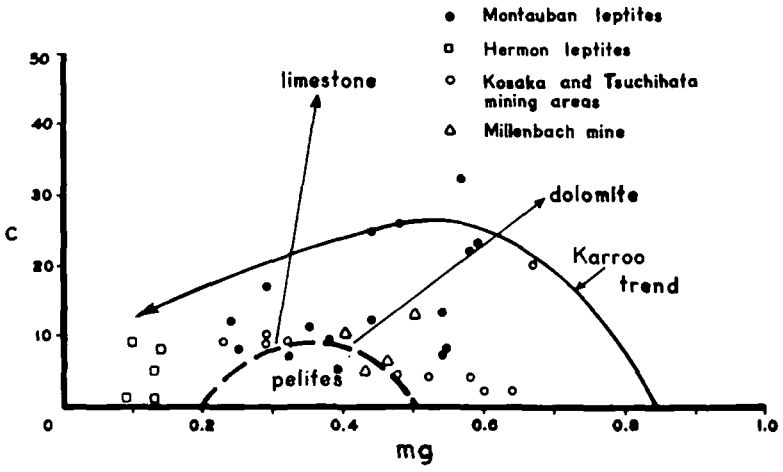

FIG. 9. Niggli *c* vs. *mg* diagram for Montauban leptites, plotted with the Hermon leptites (Jennings 1969), and volcanic rocks from the Kosaka and Tsuchihata Kuroko areas in Japan (Tatsumi and Clark 1972), and the Millenbach mine, Noranda, Quebec (Simmons *et al.* 1973). The scatter in analyses may be due to widespread hydrothermal alteration.

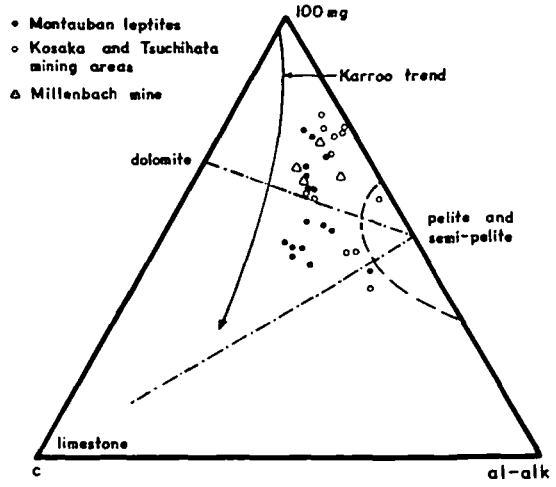

FIG. 10. Niggli 100 *mg*–*c*–(*al*–*alk*) diagram for the Montauban leptites and other rocks.

Discussion

A knowledge of the types of rock that existed at Montauban prior to metamorphism is needed to understand and interpret the possible environment of deposition of the ores. With severe structural deformation and amphibolite-grade metamorphism, decipherable primary sedimentary or volcanic textural features, except those in a massive metabasalt unit, appear to have been obliterated. The chemical nature of rocks, however, provides some basis for distinguishing between a sedimentary and igneous (volcanic) origin for the amphibolites and for some of the gneisses.

The problem of the amphibolites at Montauban was simplified by the presence of well-preserved pillow structures in one thick unit that chemical analyses show to be a basalt (Table 2). Other thin and fairly sparse amphibolite units between the thick metabasalt and the mine have no such physical volcanic features, but the close similarity of their chemical analyses to the pillowed metabasalt (Table 2), and their close grouping on discrimination diagrams (Figs. 4–8), indicate that they are all basalts and probably have a common volcanic heritage. The thin units were probably flows, tuffs, or sills.

The parent rocks for the quartzo–feldspathic gneisses are more difficult to identify. On the basis of a simple comparison of the major element contents they cannot be distinguished from some graywackes and arkoses. In our study we have mainly followed the chemical discrimination procedures used by Van de Kamp (1968) to distinguish between sedimentary and volcanic progenitors in the Haliburton–Madoc area of Ontario. The scatter of data points on discrimination diagrams (Figs. 9–11) is greater than for the amphibolites. Nevertheless, on the (*al*–*alk*)–*c* (Fig. 11), and other diagrams, they define an igneous trend and do not appear to be formed from mixtures of pelite–limestone rocks. They plot closely with known intermediate and acidic

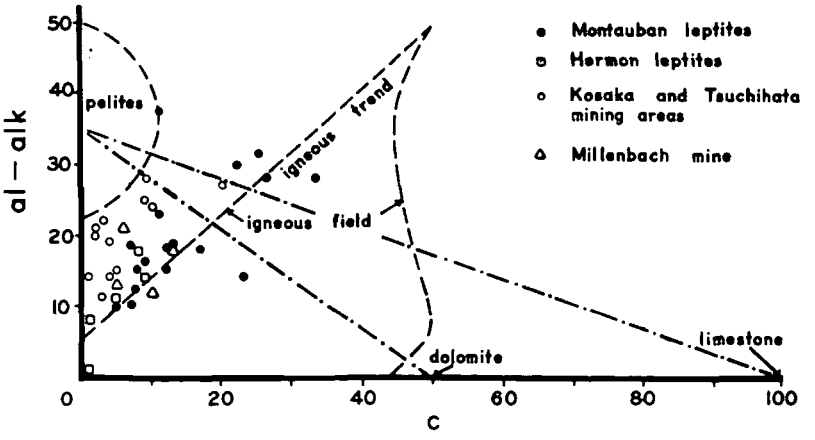

FIG. 11. Niggli (*al–alk*) vs. *c* plot. Note the igneous trend of the Montauban leptites.

TABLE 4. Chemical analyses of cordierite and composite gneisses: on a volatile-free basis and recalculated to 100%

	Cordierite gneiss		Composite gneiss
	A-101	A-133	A-10
SiO_2	82.76	70.43	50.23
TiO_2	0.17	0.54	0.69
Al_2O_3	7.18	12.54	17.08
Fe_2O_3	5.51*	0.70	10.52*
FeO	—	4.89	—
MnO	—	0.21	—
MgO	3.16	5.68	7.70
CaO	0.29	1.25	9.43
Na_2O	0.02	0.32	3.56
K_2O	0.87	3.59	0.57
P_2O_5	0.03	0.25	0.22

*Total iron as Fe_2O_3.

TABLE 5. Chemical analyses of calc-silicates: on a volatile-free basis and recalculated to 100%

	A-27	A-28	A-30
SiO_2	29.94	51.44	55.14
TiO_2	0.03	0.09	0.03
Al_2O_3	3.15	5.01	9.41
Fe_2O_3*	0.98	3.57	1.56
MgO	20.99	21.63	13.87
CaO	19.14	12.44	16.20
Na_2O	0.17	1.08	0.24
K_2O	0.06	0.08	0.58
P_2O_5	0.41	0.14	0.27
CO_2	25.13	4.52	2.71

*Total iron as Fe_2O_3.

volcanic rocks from the Kuroko district of Japan (Tatsumi and Clark 1972), and with volcanic rocks at the Millenback mine, Noranda, Quebec (Simmons *et al.* 1973). For these reasons we have called them leptites, after the definition of Sederholm (1935).

Some of the Montauban leptites are very quartz-rich and may represent silicified volcanic rocks. On the other hand, there are quartzite units at Montauban (Pyke 1966) which may grade into or interfinger with these leptites.

Volcanic rocks near volcanogenic sulfide deposits are frequently altered and lose some of their 'igneous' chemical characteristics. Spitz and Darling (1975) noted a general peraluminous trend in the acidic volcanic rocks in the Upper Malartic Group at Val d'Or, Quebec, and related it to large-scale alkali and CaO depletion caused by hydrothermal alteration. Descarreaux (1973) had shown similar chemical features in this and other parts of the Abitibi greenstone belt in Quebec. In Japan, Tatsumi and Clark (1972) noted widespread alteration, including silification, in the rocks surrounding Kuroko deposits. These and other studies point out convincingly that intermediate and acidic volcanic rocks around volcanogenic sulfide deposits are frequently hydrothermally altered on a district scale, and that plots of their chemical analyses may diverge considerably from primary igneous trends. Such could be the case at Montauban where the leptites show igneous chemical trends with considerable scatter of analyses.

Chemical changes may also have been imposed by amphibolite facies metamorphism. It has not been possible to assess this for the Mon-

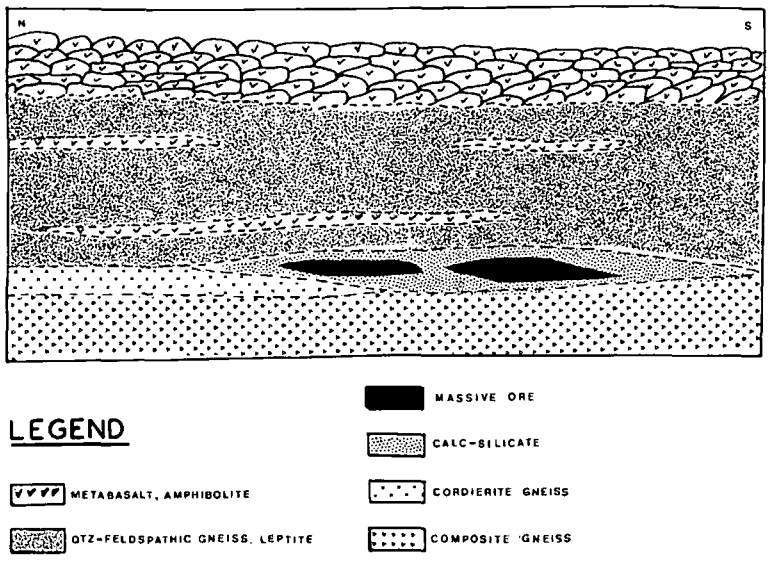

FIG. 12. Diagrammatic reconstruction of a north–south cross section through the Montauban ore zone.

tauban leptites, but it is probably minor as metamorphism has apparently had no major effect on the bulk chemistry of the intercalated basalts (amphibolites).

The cordierite gneiss, containing vienlet and disseminated copper and gold mineralization, lies at the western end of the calc-silicate zone. Cordierite rocks are known in many metamorphic terrains and examples can be cited from the Precambrian of Canada and Scandinavia where their origin has often been attributed to metasomatism, either by igneous or ultrametamorphic processes (Eskola 1932; MacRae 1973). Cordierite rocks are also frequently associated with metamorphosed base metal deposits, in particular massive sulfide deposits (Geijer 1921; Sangster 1972). The interpretation used here is that the cordierite bearing rocks at Montauban represent metamorphosed chloritic alteration rocks associated with the massive sulfide deposit. These rocks are quartz-rich, and their similarity to the leptites suggests they may have been derived from them by chloritization, during which Mg was added and alkalis and CaO were leached. During regional metamorphism chlorite may have reacted with quartz or muscovite to form cordierite–anthophyllite or cordierite–biotite assemblages, respectively (Tuominen and Mikkola 1950; Winkler 1974).

At this point it is worthwhile to unfold the rocks to their original position. According to Pyke (1966) and Smith (1956) the local structure is a syncline overturned to the west and plunging gently to the north, with overturned pillowed metabasalt occupying the axial part of the syncline. Thus, stratigraphic tops at the mine are to the west. The unfolded units are shown schematically in cross section in Fig. 12.

The lowest unit of the sequence (Fig. 12) is the 'composite' gneiss of Smith (1956) which our one chemical analysis indicates to have a basaltic composition. This gneiss is overlain by the ore zone unit consisting of calc-silicate and carbonate that host the massive Pb–Zn sulfide ore, and cordierite gneiss that contains the disseminated and stringer copper and gold ore. The next unit is comprised of leptites and associated metasediments which grade into, or interfinger with, quartzite; thin amphibolites, basaltic flows, or sills are interlayered with these felsic rocks. Pillowed metabasalt, indicating a subaqueous environment of deposition, forms the highest unit in this structure.

Sequences of volcanic rocks of this type, that is, interlayered felsic and basic volcanic rocks deposited in a marine environment, are typical hosts for volcanogenic sulfide deposits in the Precambrian of Canada (Sangster 1972), the Kuroko district of Japan (Matsukuma and Horikoshi 1970), and elsewhere. The Montauban

deposits have many of the characteristics of the "exhalite" deposits proposed by Ridler (1971) and Ridler and Shilts (1974) who define them as a class of chemical sediments of predominately volcanic origin. According to Ridler's geological and geochemical classification, the Montauban carbonate could be an exogenous proximal exhalite in the overlapping carbonate–sulfide facies, where the sulfide facies is represented by the ores. The disseminated chalcopyrite ore is in an extended and parallel zone of cordierite gneiss, interpreted to be a metamorphosed chloritic alteration rock. It may have formed by *in situ* Mg–metasomatism of sediment or tuff in a restricted marine basin (Roberts 1975), by mass slumping or density flow of chloritic material down a sumarine slope (MacLean and MacGeehan 1976), or by the structural transposition of an alteration pipe (Sangster 1972).

It is difficult to distinguish these rocks in high-grade metamorphic terrain such as in the Grenville Province, but nevertheless, it is highly important to do so when evaluating this part of the Canadian Shield for volcanogenic sulfide deposits so prevalent in it elsewhere.

Summary

Gneisses, amphibolites, and calc-silicate rocks in the vicinity of the base metal and gold ores at Montauban-Les-Mines have been chemically analyzed, and chemical discrimination techniques have been used to distinguish between sedimentary and igneous (volcanic) origins for these rocks.

Thin amphibolite units, intercalated with quartzo–feldspathic gneisses, are almost identical in chemical composition to a thick pillowed metabasalt (ortho-amphibolite) 1 km west of the mine. They also plot as ortho-amphibolites on variation diagrams and have trace element abundances and ratios characteristic of basic igneous rocks. They are probably derived from basaltic flows or shallow intrusions.

The parent rocks to the quartzo–feldspathic gneisses are not so easily identified. However, many of the gneisses have igneous trends on variation diagrams that discriminate between metavolcanic (leptites) and metasedimentary varieties. The Montauban leptites plot on these diagrams in the same fields as indisputable intermediate and acidic volcanic rocks associated with the Kuroko ores of Japan and the massive sulfides at Noranda, Quebec. They are probably derived from intermediate and acidic tuffs and associated sediments.

A thin calc-silicate unit at the base of the leptites is host to the massive Pb–Zn ore. It is underlain by an equally thin cordierite gneiss, which is host to disseminated and vienlet copper and gold ore. The calc-silicate may represent an impure carbonate rock analogous to an exhalite horizon where carbonate and sulfide facies overlap. The cordierite gneiss is probably a metamorphosed chloritic alteration rock associated with the ores.

Acknowledgements

We thank D. Francis and P. MacGeehan for their critical reviews of the manuscript, and R. G. Webber for the use of the XRF equipment. J. S. Stevenson kindly helped with petrographic and mineralogic problems. The study was supported by the National Research Council of Canada Grant A7719.

ALCOCK, F. J. 1930. Zinc and lead deposits of Canada. Geological Survey of Canada, Economic Geology Report, Series 8, pp. 79–90.

BANCROFT, J. A. 1915. The geology of parts of the townships of Montauban and Chavigny and the seigniory of Grondines. Quebec Department of Colonization, Mines and Fisheries, Mines Branch, pp. 103–143.

BASTIN, E. S. 1909. Chemical composition as a criterion in identifying metamorphosed sediments. Journal of Geology, **17**, pp. 445–472.

DESGARREAUX, J. 1973. A petrochemical study of the Abitibi volcanic belt and its bearing on the occurrences of massive sulfide ore. Canadian Institute of Mining and Metallurgy Bulletin, **66**, pp. 61–69.

ESKOLA, P. 1932. Conditions during the earliest geological times. Academia Scientarum Fennica, Ser. A, **V-XXXVI**, No. 4.

EVANS, B. W., and LEAKE, B. E. 1960. The composition and origin of the striped amphibolites of Connemara, Ireland. Journal of Petrology, **1**, pp. 337–363.

FLANNAGAN, J. T., and MCADAM, J. 1976. The Montauban gold deposits related to base metal mineralization in the Grenville Province. Paper presented at the annual meeting of the Canadian Institute of Mining and Metallurgy, Quebec City, P.Q.

FRANKLIN, J. M., KASARDA, J., and POULSEN, K. H. 1975. Petrology and chemistry of the alteration zone of the Mattabi massive sulfide deposit. Economic Geology, **70**, pp. 63–79.

GEIJER, P. 1921. Recent work on the Archean sulfide ores of Scandinavia. Economic Geology, **16**, pp. 279–288.

GUNN, B. M. 1967. Matrix correction for X-ray fluorescence spectrometry by digital computer. Canadian Spectroscopy, **12**(2), pp. 2–7.

HEITANEN, A. 1947. Archean geology of the Turku district

in S.W. Finland. Geological Society of America Bulletin, **58**, pp. 1019–1084.

JENNINGS, D. S. 1969. Origin and metamorphism of part of the Herman Group near Bancroft, Ontario. Ph.D. thesis, McMaster University, Hamilton, Ont.

LEAKE, B. E. 1964. The chemical distinction between ortho- and para-amphibolites. Journal of Petrology, **5**, pp. 238–254.

MACLEAN, W. H., and MACGEEHAN, P. J. 1976. Garon Lake Mine, Matagami, Quebec. Mineral exploration research institute case history 76-1, McGill University, Montreal, P.Q. 67 p.

MACRAE, N. D. 1973. Sulfurization of basalt under thermal metamorphic conditions to produce cordierite-bearing rocks. Canadian Journal of Earth Sciences, **11**, pp. 246–253.

MATSUKUMA, T., and HORIKOSHI, E. 1970. Kuroko deposits in Japan, a review. *In* Volcanism and ore genesis. *Edited by* T. Tatsumi. University of Tokyo Press, Tokyo, Japan, pp. 153–179.

O'NEIL, J. J., and OSBORNE, F. F. 1939. Tetrault Mine, Montauban-Les-Mines, Portneuf County. Quebec Bureau of Mines, Preliminary Report No. 136.

OSBORNE, F. F. 1939. The Montauban mineralized zone, Quebec. Economic Geology, **34**, pp. 712–726.

PRINZ, M. 1967. Geochemistry of basaltic rocks: trace elements. *In* Basalts, Vol. 2. *Edited by* H. Hess and A. Poldervaart. Interscience, New York, NY, pp. 271–323.

PYKE, D. R. 1966. The Precambrian geology of the Montauban area, Quebec. Ph.D. thesis, McGill University, Montreal, P.Q., 181 p.

RICKARD, D. T., and ZWEIFEL, H. 1975. Genesis of Precambrian sulfide ores, Skellefte District, Sweden. Economic Geology, **70**, pp. 255–274.

RIDLER, R. H. 1971. Analysis of Archean volcanic basins *in* the Canadian Shield using the exhalite concept (Abstract). Canadian Institute of Mining and Metallurgy Bulletin, **64**, No. 714, p. 20.

RIDLER, R. H., and SHILTS, W. W. 1974. Exploration for Archean polymetallic sulfide deposits in permafrost terrains. Geological Survey of Canada, Paper 73-74, 33 p.

ROBERTS, R. G. 1975. The geological setting of the Mattagami Lake Mine, Quebec: A volcanogenic massive sulfide deposit. Economic Geology, **70**, pp. 115–129.

SANGSTER, D. F. 1972. Precambrian volcanogenic massive sulfide deposits in Canada: a review. Geological Survey of Canada, Paper 72-22, 44 p.

SEDERHOLM, J. J. 1935. Selected works: granites and migmatites. John Wiley and Sons Inc., New York, NY. 608 p.

SIMMONS, B. D., and the GEOLOGICAL STAFF. 1973. Geology of the Millenbach massive sulfide deposit, Noranda, Quebec. Canadian Institute of Mining and Metallurgy Bulletin, **66**, No. 739, pp. 67–78.

SMITH, J. R. 1956. Montauban-Les-Mines area. Quebec (Province), Department of Mines, Geological Report, **65**, 39 p.

SPITZ, G., and DARLING, R. 1975. The petrochemistry of altered volcanic rocks surrounding the Louvem copper deposit, Val d'Or, Quebec. Canadian Journal of Earth Sciences, **12**, pp. 1820–1849.

STAMATELOPOULOU-SEYMOUR, K. 1975. Metamorphosed volcanogenic Pb–Zn deposits at Montauban, Québec. M.Sc. thesis, McGill University, Montreal, P.Q. 230 p.

TATSUMI, T., and CLARK, L. A. 1972. Chemical composition of acid volcanic rocks genetically related to formation of Kuroko deposits. Journal of Geological Society of Japan, **78**, pp. 191–201.

TUOMINEN, H. V., and MIKKOLA, T. 1950. Metamorphic Mg–Fe enrichment in the Orijarvi region as related to folding. Bulletin de la Commission Géologique de Finlande, **150**, pp. 67–92.

TUREKIAN, K. K. 1963. The chromium and nickel distribution in basaltic rocks and eclogites. Geochimica et Cosmochimica Acta, **27**, pp. 835–846.

VAN DE KAMP, P. C. 1968. Geochemistry and origin of metasediments in the Haliburton–Madoc area, southeastern Ontario. Canadian Journal of Earth Sciences, **5**, pp. 1337–1372.

WILSON, N. L. 1939. An investigation of the metamorphism of the Orijarvi type with special reference to the zinc–lead deposits at Montauban-Les-Mines, P.Q. Ph.D. thesis, McGill University, Montreal, P.Q., 163 p.

WINKLER, H. G. F. 1974. Petrogenesis of metamorphic rocks. Springer-Verlag New York Inc., New York, NY, 320 p.

Canadian Journal of Earth Sciences

Published by
THE NATIONAL RESEARCH COUNCIL OF CANADA

Journal canadien des sciences de la terre

Publié par
LE CONSEIL NATIONAL DE RECHERCHES DU CANADA

Volume 13 Number 2 February 1976

Volume 13 numéro 2 février 1976

Geochemical evolution of copper-bearing granitic rocks of Guichon Creek Batholith, British Columbia, Canada

M. A. OLADE
Department of Geology, University of Ibadan, Ibadan, Nigeria

Received 10 March 1975
Revision accepted for publication 2 September 1975

The Guichon Creek batholith, located in south-central British Columbia, is host to numerous porphyry copper deposits that are considered as being closely related to the pluton. Variations in major and trace element distribution are consistent with a model of crystallization-fractionation of a K-poor calc-alkaline magma of intermediate composition. Relatively low Rb and Rb/Sr values, and high K/Rb ratios are consistent with Sr isotopic ratios that suggest a subcrustal source region for the generation of the magma, probably by partial melting of subducted oceanic crust at relatively shallow depths.

Cu, like other femic elements, (Zn, Mn, V, Ni, Co, Ti) generally decreases with increasing fractionation, which reflects normal differentiation trends. The apparent lack of positive correlation between Cu contents of rocks and ore potential of intrusive units may be explicable if mineralization is regarded as an independent by-product of magma generation, rather than the result of differentiation processes. Close relationships between trace metal values and degree of fractionation emphasize the need for assigning different background values to each intrusive unit, during geochemical exploration.

Le batholite de Guichon Creek, situé dans le centre sud de la Colombie Britannique, est l'hôte de plusieurs gisements de cuivre de type 'porphyry copper' qui seraient apparentés au pluton. Les variations dans la distribution des éléments majeurs et des oligoéléments sont en accord avec un modèle de cristallisation-fractionnement d'un magma intermédiaire de la série calco-alcaline, pauvre en K. Des valeurs relativement peu élevées de Rb et Rb/Sr sont en accords avec des rapports isotopiques de Sr qui suggèrent que le magma fût généré dans une région-source sub-corticale, probablement par fusion partielle à des profondeurs relativement faibles d'une croûte océanique subsidente.

Le Cu, commes les autres éléments fémiques, (Zn, Mn, V, Ni, Co, Ti), diminue généralement avec l'augmentation du fractionnement qui montre des courbes normales de différentiation. L'absence apparente de corrélation positive entre la teneur en Cu des roches et le potentiel minéral des unités intrusives peut être explicable si on considère la minéralisation comme un sous-produit de la génération du magma plutôt que le produit de processes de différentiation. Les relations étroites entre les valeurs de métal traceur et le degré de fractionnement montrent l'importance de l'attribution de différentes valeurs de mouvement propre (background) à chaque unité intrusive, lors de l'exploration géochimique.

[Traduit par le journal]

Introduction

The Guichon Creek batholith, located in the Intermontane Structural Belt of Southern Canadian Cordillera (Fig. 1), is host to several large producing and undeveloped porphyry copper deposits. Aggregate tonnage of these deposits exceeds 1.8 billion tons of ore, grading approximately 0.4% Cu. Because of spatial and temporal relationships between the batholith and copper mineralization (Northcote 1969), considerable interest has been shown in the evolution and petrogenesis of the pluton. In response to this

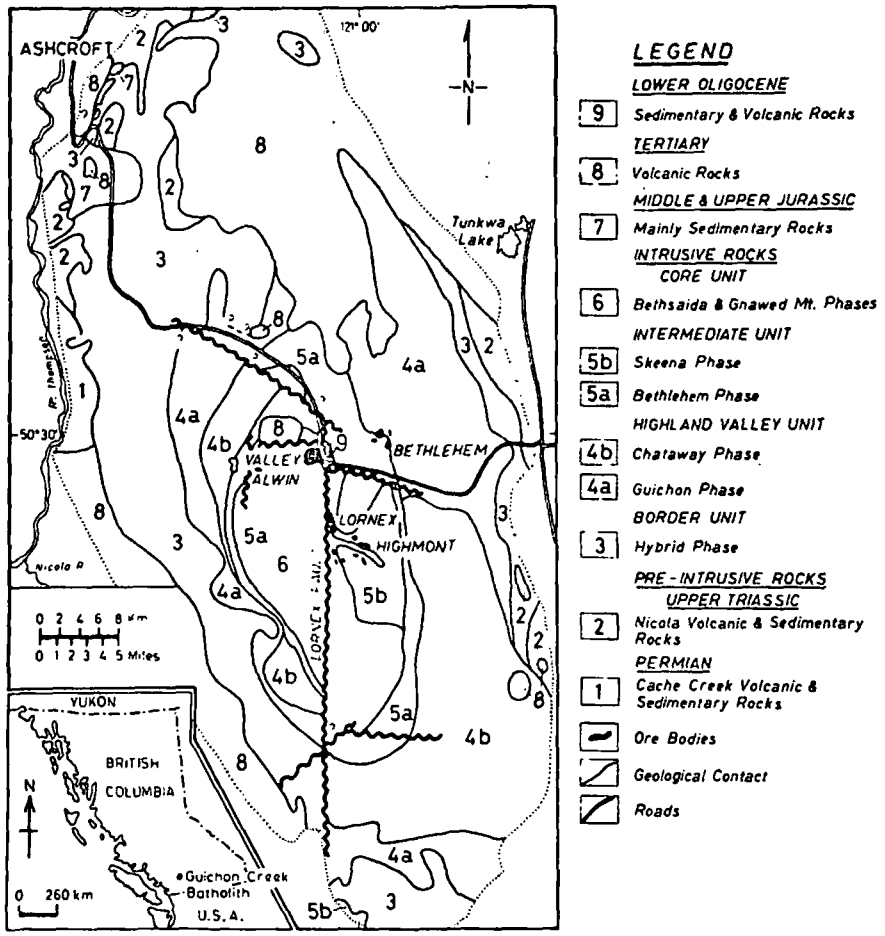

FIG. 1. Location and generalized geologic map of Guichon Creek Batholith (Modified after McMillan 1972).

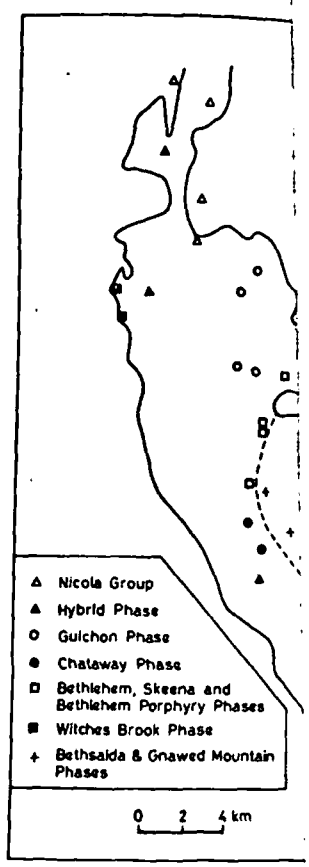

FIG. 2. Map of Guichon C location of analyzed samples.

interest, several geologic and geophysical investigations have been undertaken by numerous workers, notably Carr (1966), Northcote (1969), McMillan (1972, 1973), Hylands (1972), and Ager *et al.* (1973). With the exception of studies on the distribution of Cu and Zn in rocks of the Guichon Creek batholith (Brabec and White, 1971), and Sr isotope at Craigmont mine (Chrismas *et al.* 1969), relatively little published geochemical work of petrogenetic significance has been undertaken in the batholith.

To further the understanding of relationships between mineralization and major and trace element geochemistry, and to provide adequate background geochemical data for mineral exploration purposes, 61 fresh rock samples (Fig. 2) were analyzed for major elements, 52 of these for selected trace elements, and 34 for Rb, Sr, and S. In addition, results of 10 unpublished major element analyses compiled by Brabec (1970) are included in the plots of chemical variation diagrams.

This paper discusses the geochemical evolution and petrogenesis of the Guichon Creek batholith in the light of major and trace element geochemistry.

Geology of Guichon Creek Batholith

Regional Setting

The Triassic Guichon Creek batholith is a concentrically zoned granitoid pluton, elongated slightly west of north, and underlying an area of approximately 1300 sq. km. It intrudes sedimentary and volcanic rocks of the Permian Cache Creek and Upper Triassic Nicola Groups, within a tectonic setting that is considered either eugeosynclinal or as an oce (Dercourt 1972; Monger *et* lith is overlain unconforma sic to Tertiary volcanic and

Petrology

The petrology of Guichor been described by numero White *et al.* (1957), Carr (1969), McMillan (1972), a The batholith is composed o delineated by variations in t phases, which vary in comp to quartz monzonite, are gr modal similarities and conta cote 1969; Hylands 1972). N been presented by Northcot

The Border Unit forms th batholith, and is composed variable to uniformly fine-gr locally enriched in mafic mir

The Highland Valley Uni

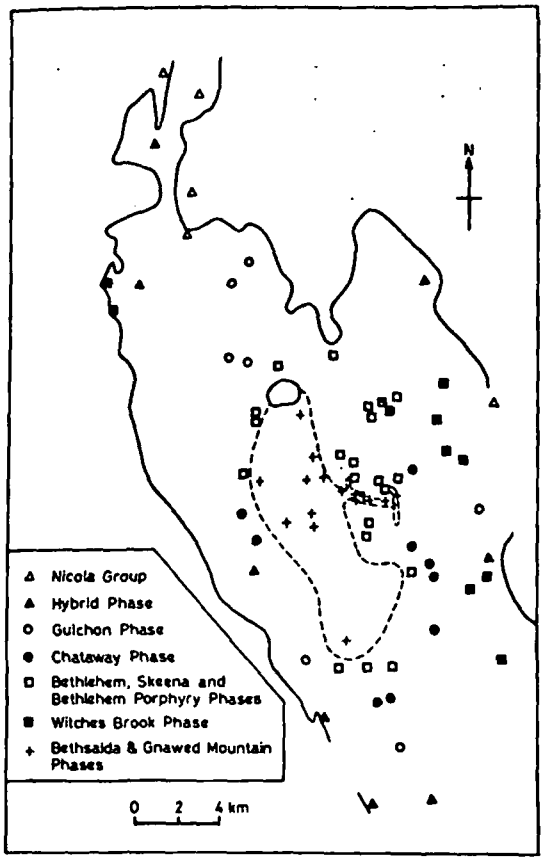

FIG. 2. Map of Guichon Creek batholith, showing location of analyzed samples.

eugeosynclinal or as an oceanic–island arc couple (Dercourt 1972; Monger *et al.* 1972). The batholith is overlain unconformably by Middle Jurassic to Tertiary volcanic and sedimentary rocks.

Petrology

The petrology of Guichon Creek batholith has been described by numerous workers; notably, White *et al.* (1957), Carr (1966), Northcote (1969), McMillan (1972), and Hylands (1972). The batholith is composed of nine igneous phases delineated by variations in texture (Fig. 1). These phases, which vary in composition from diorite to quartz monzonite, are grouped into units on modal similarities and contact relations (Northcote 1969; Hylands 1972). Modal analyses have been presented by Northcote (1969).

The Border Unit forms the outer zone of the batholith, and is composed of hybrid, highly variable to uniformly fine-grained diorite that is locally enriched in mafic minerals.

The Highland Valley Unit forms a complete ring within the Border Unit and comprises the Guichon and Chataway Phases (Fig. 1). Medium-grained Guichon quartz diorite is characterized by anhedral quartz grains and unevenly distributed mafic minerals, whereas the equigranular Chataway granodiorite is composed of evenly distributed, equant grains of hornblende and biotite, which constitute approximately 12% of the mode (McMillan 1972).

The Intermediate Unit lies between the Highland Valley Unit and the core of the batholith (Fig. 1). It is composed of the Bethlehem and Skeena granodiorites, and Witches Brook and Bethlehem Porphyry dikes. The Bethlehem and Skeena Phases are characterized by randomly distributed, coarse, poikilitic hornblende, set in a matrix of medium-grained felsic minerals. However, the Skeena differs from the Bethlehem granodiorite in possessing coarse-grained quartz phenocrysts and interstitial, ragged microperthite. Rocks of the Witches Brook Phase occur as fine to medium-grained dikes and stocks of granodiorite to granite composition. Dikes of the Bethlehem Porphyry Phase are closely associated with the Bethlehem Phase and range in composition from dacite to quartz latite porphyry.

The Core Unit comprises granodiorites to quartz monzonites of the Bethsaida Phase and related porphyry dikes of the Gnawed Mountain Phase. Rocks of the Bethsaida Phase are coarse grained, commonly porphyritic, and consist of subhedral phenocrysts of quartz, and plagioclase, interstitial microperthite, and coarse biotite 'books' (Northcote 1969). Porphyries of the Gnawed Mountain Phase contain quartz and less commonly plagioclase phenocrysts set in an aplitic matrix. Mafic minerals, mainly biotite, constitute less than 5% of the mode.

Variations in mineralogical composition within the batholith indicate that hornblende, accessory minerals, biotite, and anorthite content of plagioclase all decrease, whereas quartz content increases from the border to core of the pluton (Northcote 1969). Pyroxene (mostly augite) is not found in rocks younger than the Highland Valley Unit. K-feldspar shows no systematic variations throughout the batholith, although dike rocks of the Witches Brook Phase are noticeably enriched in K-feldspar. Textural change is manifested by increasing grain size toward the core. Specific gravity of rocks also decreases inward (Northcote 1969).

TABLE 1. Average composition of intrusive units of Guichon Creek batholith

	Hybrid	Guichon	Chataway	Bethlehem	Bethlehem Porphyry	Skeena	Witches Brook	Bethsaida	Gnawed Mountain
Major Elements (wt. %)									
(Number of samples)	(8)	(7)	(9)	(9)	(5)	(6)	(11)	(9)	(7)
SiO_2	60·02	62·24	64·37	66·04	66·00	68·21	69·23	69·79	73·14
Al_2O_3	16·91	17·00	16·37	15·87	15·85	15·81	15·54	15·92	14·41
*Fe_2O_3	6·41	5·04	4·64	3·35	4·18	2·96	3·03	1·91	1·17
CaO	5·78	5·15	4·26	4·05	3·55	3·84	3·37	2·83	2·12
MgO	3·16	2·31	1·89	1·31	1·48	1·02	1·36	0·54	0·34
Na_2O	3·61	4·06	4·29	4·52	4·73	4·78	3·87	4·83	4·74
K_2O	1·71	1·99	1·92	1·83	2·56	1·73	2·19	1·96	2·08
TiO_2	0·74	0·65	0·49	0·37	0·42	0·35	0·39	0·27	0·20
P_2O_5	0·16	0·17	0·16	0·14	0·14	0·14	0·11	0·13	0·12
Trace Elements (p.p.m)									
(Number of samples)	(6)	(4)	(6)	(7)	(5)	(5)	(7)	(6)	(6)
Cu	51	67	45	33	43	35	47	19	8
Zn	74	60	45	39	19	33	30	29	28
Mn	692	574	430	415	119	332	328	370	231
Ni	33	27	20	12	7	8	10	5	5
Co	13	12	11	8	5	8	6	5	4
V	83	49	39	34	25	26	40	13	15
(Number of samples)	(3)	(4)	(6)	(4)	(5)	(3)	(4)	(2)	(3)
S	380	373	394	415	426	334	317	321	375
Ba	500	306	500	560	535	550	600	520	600
Rb	50	50	48	43	61	36	117	35	35
Sr	468	735	747	693	509	653	491	588	601
Ratios									
K/Rb	299	298	404	326	320	376	166	395	450
Rb/Sr	0·14	0·06	0·05	0·05	0·06	0·06	0·20	0·05	0·05
Ca/Sr	95	59	52	44	36	46	42	32	28

*Total Fe as Fe_2O_3

Most of the porphyry copper deposits are localized within rocks of the Bethlehem, Skeena, Bethsaida, and Gnawed Mountain Phases (Fig. 1).

Geochemistry

Results of partial chemical analyses are presented as means for major and trace elements in Table 1. SiO_2, Al_2O_3, P_2O_5, and TiO_2 were determined by X-ray fluorescence on fused sample powders, and Rb, Sr, and S on briquetted unfused powders. Instrumental settings and techniques are described by Olade (1974). Fe, Mg, K, Na, Ca, Cu, Zn, Mn, Ag, Pb, Ni, Co, and Cd were determined by atomic absorption spectrophotometry, and Mo, Ti, V, Ba, Sn, Bi, W, and Ga by semi-quantitative emission spectroscopy. Analytical procedures have been presented elsewhere (Olade 1974). Analytical precision at the 95% confidence level are as follows: Rb ± 2%, Sr ± 1%, S ± 15%, all major elements are generally better than ±8%, and trace elements by atomic absorption are better than ±30%.

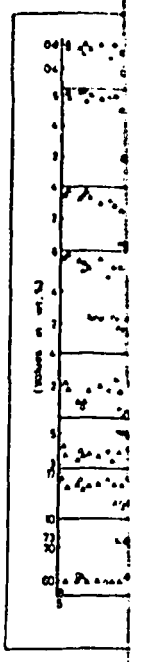

FIG. 3. V
showing maj
Larsen differe

Major Elem

Major el
functions o
(LDI = ⅓Si
FeO)) in F
concentratic
accordance
deduced fro
1969). Thus,
more felsic
youngest. R
show the g
which is con
characteristi

Chemical
that SiO_2 an
increasing d
total Fe as F
a concomita
able change
the Witches
siderable en
the aforemer
of K_2O in t
from 0.21–2.
These values
value of 3.04

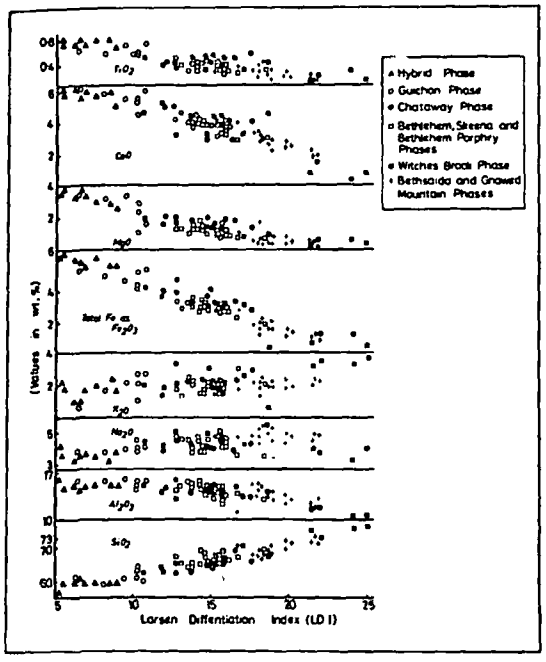

FIG. 3. Variation diagrams in Guichon Creek rocks showing major element concentrations (wt. %) versus Larsen differentiation index.

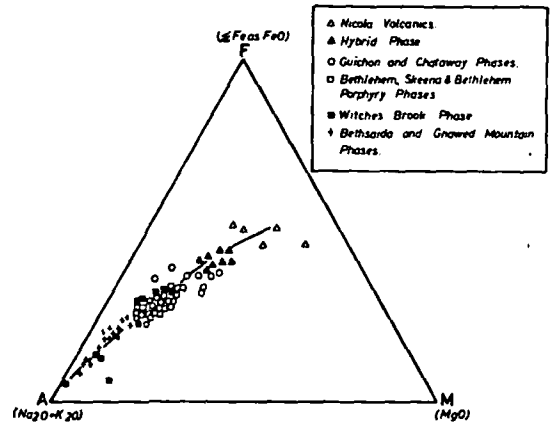

FIG. 4. AFM variation diagram for rocks of Guichon Creek batholith.

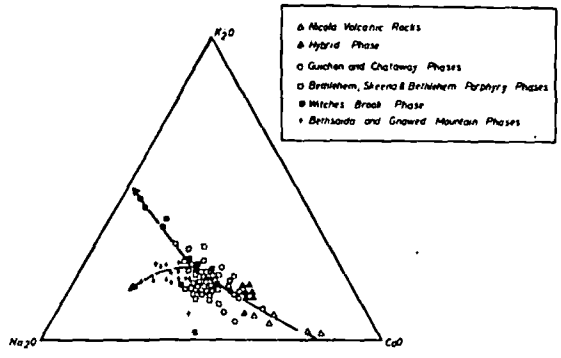

FIG. 5. CaO–Na_2O–K_2O variations for rocks of Guichon Creek batholith.

Major Element Geochemistry

Major element abundances are presented as functions of the Larsen Differentiation Index ($LDI = \frac{1}{3}SiO_2 + K_2O - (CaO + MgO + Fe\ as\ FeO)$) in Fig. 3. As shown in Table 1, mean concentrations of most major elements vary in accordance with relative ages of the rock units as deduced from contact relationships (Northcote 1969). Thus, the intrusive units generally become more felsic from the relatively oldest to the youngest. Rocks of the Witches Brook Phase show the greatest variation in element values which is consistent with their known petrographic characteristics (Northcote 1969).

Chemical variation diagrams (Fig. 3) show that SiO_2 and Na_2O concentrations increase with increasing differentiation, whereas MgO, CaO, total Fe as Fe_2O_3, TiO_2, Al_2O_3, and P_2O_5 show a concomitant decrease. K_2O shows no appreciable change with LDI, except for dike rocks of the Witches Brook Phase, which exhibit considerable enrichment. Furthermore, excluding the aforementioned K-rich rocks, concentrations of K_2O in the remainder of the batholith range from 0.21–2.89%, with a mean value of 1.85%. These values are low compared to the average value of 3.04%, quoted by Turekian and Wedepohl (1961) for high-Ca granites. A conspicuous lack of K-enrichment in the younger and more differentiated units is consistent with the rather uniform K-feldspar content, and decreasing values of modal biotite with increasing fractionation (Northcote 1969).

On an AFM diagram (Fig. 4), enrichment of total alkalis relative to MgO and FeO is evident. This trend is similar to those found in typical calc-alkaline volcanic–plutonic complexes (Nockolds and Allen 1953). However, on the CaO Na_2O–K_2O variation diagram (Fig. 5), two trends are apparent. The first, manifested by dike rocks of the Witches Brook Phase, shows enrichment in K_2O relative to CaO and Na_2O (normal calc-alkaline trend), whereas the other trend is toward Na_2O enrichment. According to Larsen and Poldervaart (1961) and Taubeneck (1967), the latter trend is commonly characteristic of petrochemical differentiation in rocks of trondhjemitic affinity.

In both the AFM and CaO–Na_2O–K_2O diagrams, 5 analyses of Nicola volcanic country rocks plot along the same 'liquid line of descent' as rocks of the Guichon Creek batholith.

Minor and Trace Element Geochemistry

Abundance data for minor and trace elements are summarized in Table 1. In describing the geochemical data, elements are grouped according to the classification of Goldschmidt (1954): chalcophile elements (Cu and S); siderophile elements (Zn, Mn, Ni, Co, and V); and lithophile elements (Rb, Sr, and Ba). Concentrations of Mo, Ag, Pb, W, Bi, and Sn are generally below the detection limits of the analytical methods; consequently, their results are not discussed further.

Chalcophile Elements (Cu, S)

With the exception of rocks from the Witches Brook and Bethlehem Porphyry Phases, mean Cu contents generally decrease from the relatively older units at the outer margins, to relatively younger at the core (Table 1). Brabec and White (1971) reported a similar distribution for aqua-regia-extractable Cu in 300 samples from the batholith. A plot of Cu values versus LDI shows a considerable scatter, although a trend towards decreasing Cu as LDI increases is evident (Fig. 6).

Geochemical behavior of Cu in silicate melts during magmatic fractionation is not well understood (Al-Hashimi and Brownlow 1970). Wager and Mitchell (1951) in their classical study of Skaergaard intrusion, found that, during the early and main phases of magmatic differentiation, Cu contents of the constituent minerals and whole rock increased, whereas after 90% solidification (Wager and Brown 1967), most minerals were suddenly depleted in Cu. Simultaneously, whole-rock S showed a sharp increase, although whole-rock Cu did not change appreciably. The redistribution of Cu and increase in S were attributed to a separation of an immiscible sulphide phase, which occurred near the end of the fractionation process. Similar, though less extensive studies on the porphyry-copper-bearing Laramide intrusions of Arizona (Graybeal 1973), and other differentiated plutonic rocks, broadly confirm the pattern observed for the Skaergaard (Cornwall and Rose, 1957; McDougall and Lovering 1963).

In the Guichon Creek batholith, the tendency

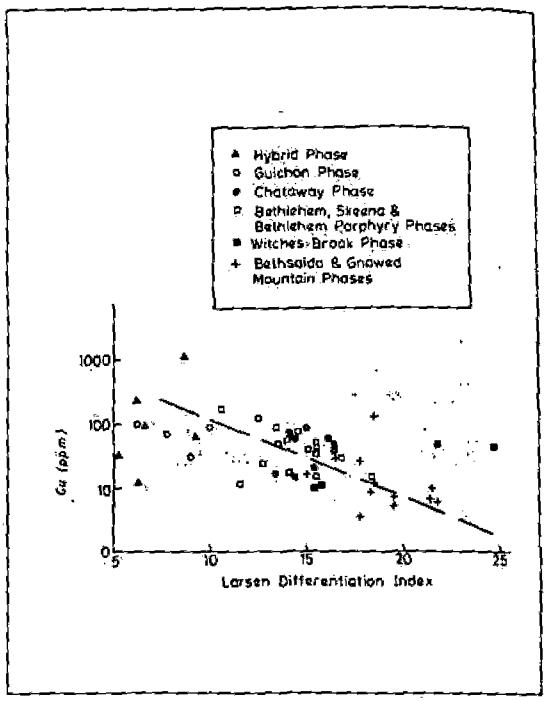

FIG. 6. Distribution of copper in relation to Larsen differentiation index (legend as for Fig. 5).

for Cu to decrease generally with increasing fractionation (Fig. 6) parallels the behavior of Fe and Mg (Fig. 3). Cu shows a relatively weak but significant correlation with Fe ($r = 0.41$), which suggests that Cu^{++} (0.72 Å) may to some extent substitute for Fe^{++} (0.74 Å) in silicates and oxides. However, from theoretical considerations, Curtis (1964) pointed out that crystal-field effects could result in the exclusion of Cu from crystal structures, in preference for Fe. Cu is strongly chalcophile, and generally combines with S to form sulfide grains. These commonly occur as inclusions in silicates, especially micas, or may even concentrate as ore deposits. On this basis, Zlobin *et al.* (1967) concluded that the positive correlations between Cu and Fe reflect only similarity in geochemical behavior rather than ionic substitution.

S concentrations range from 247 to 751 ppm and average 390 ppm for the whole batholith. This is similar to the value of 300 ppm cited as the world average for S in high-Ca granitic rocks (Turekian and Wedepohl 1961). No significant difference is apparent in mean S among the constituent intrusive units, although rocks of the Bethlehem Porphyry Phase contain slightly higher mean S value (Table 1). This may be

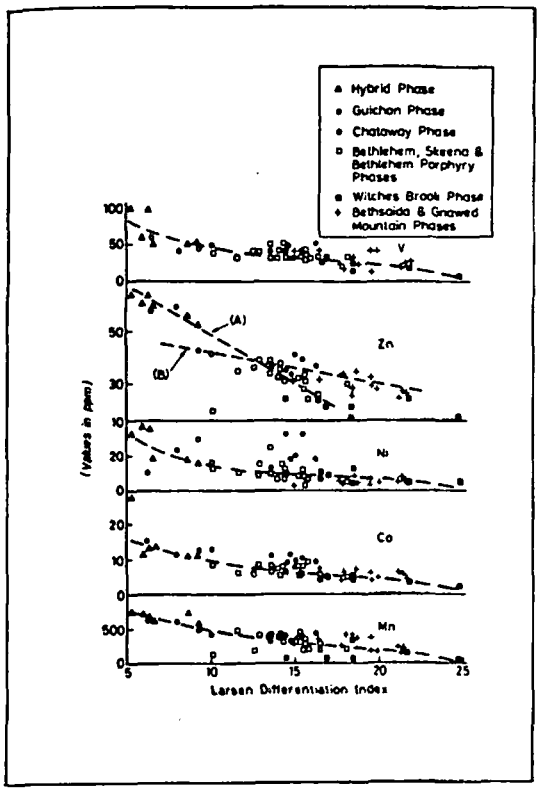

FIG. 7. Variation diagrams of Guichon Creek rocks, showing femic trace elements plotted against Larsen differentiation index.

attributed to the close spatial association of these porphyries with sulfide mineralization in the northern part of the batholith. The lack of an overall significant positive correlation between S and Cu in the batholith ($r = 0.28$) suggests that S might occur in other sulfide forms, such as pyrite.

Siderophile Elements (Zn, Mn, Ni, Co, V)

Zn levels generally decrease from an average of 74 ppm in the Hybrid Phase to a mean value of 28 ppm in the relatively younger Bethsaida and Gnawed Mountain Phases. A similar distribution was reported by Brabec and White (1971) for aqua-regia-extractable Zn. Although a plot of Zn versus LDI shows considerable scatter, two trends with no obvious genetic significance are evident (Fig. 7). The first trend (A) has a relatively steep slope and includes rocks of the Hybrid, Guichon, and Witches Brook Phases. The second trend (B), which is considered normal, joins rocks of the other phases. The former trend is attributed to extensive contamination of the Hybrid Phase and part of Guichon Phase by relative Zn-rich volcanic country rocks, and strong depletion of Zn in the K-rich dike rocks of the Witches Brook Phase. During magmatic processes, Zn^{++} generally substitutes for Fe^{++} in silicates and oxides because of similarity in ionic properties. This relationship is demonstrated by a strong positive correlation between Zn and Fe ($r = 0.89$). Comparable results have been reported for other granitic rocks (Blaxland 1971). Results of partial extraction techniques also indicate that Zn, unlike Cu, is principally associated with the silicate fraction (Brabec 1971; Olade and Fletcher 1974).

Mn distribution shows the same trends as Zn. Values generally decrease from more than 600 ppm in the more mafic Hybrid and Guichon Phases, to less than 200 ppm in the Bethsaida and Gnawed Mountain Phases. Ni, Co, and V are also characterized by comparably well-developed trends, and the group as a whole shows a strong correlation with Fe and Mg (Ni and Fe, $r = 0.78$; Ni and Mg, $r = 0.73$; Co and Fe, $r = 0.84$; Co and Mg, $r = 0.83$).

Lithophile Elements (Ba, Rb, K/Rb, Sr, Ca/Sr, Rb/Sr)

Ba levels range from 200 to 800 ppm and average 504 ppm for the batholith. No systematic variations are apparent among the intrusive units, although rocks of the Guichon Phase are noticeably depleted in Ba (Table 1).

Rb concentrations in 34 samples range from 4 to 132 ppm, and average 50 ppm for the whole batholith. Compared with the average value of 110 ppm for high-Ca granitic rocks, the Guichon Creek batholith is impoverished in Rb, although values are comparable to those reported for plutons from Mesozoic island arc systems (Kistler *et al.* 1971). When rock units of the batholith are compared, there is, surprisingly, no consistent difference in mean values (Table 1), although the K-rich rocks of the Witches Brook Phase are noticeably enriched in Rb. Geochemical behavior of Rb is influenced by the abundance of K (Nockolds and Allen 1953; Goldschmidt 1954), for which Rb substitutes in alkali feldspars and micas (Heier and Adams 1964). The strong positive correlation between K and Rb ($r = 0.77$) reflects their geochemical coherence. Thus, absence of appreciable variations in Rb levels may be closely related to a similar behavior by K (Fig. 3).

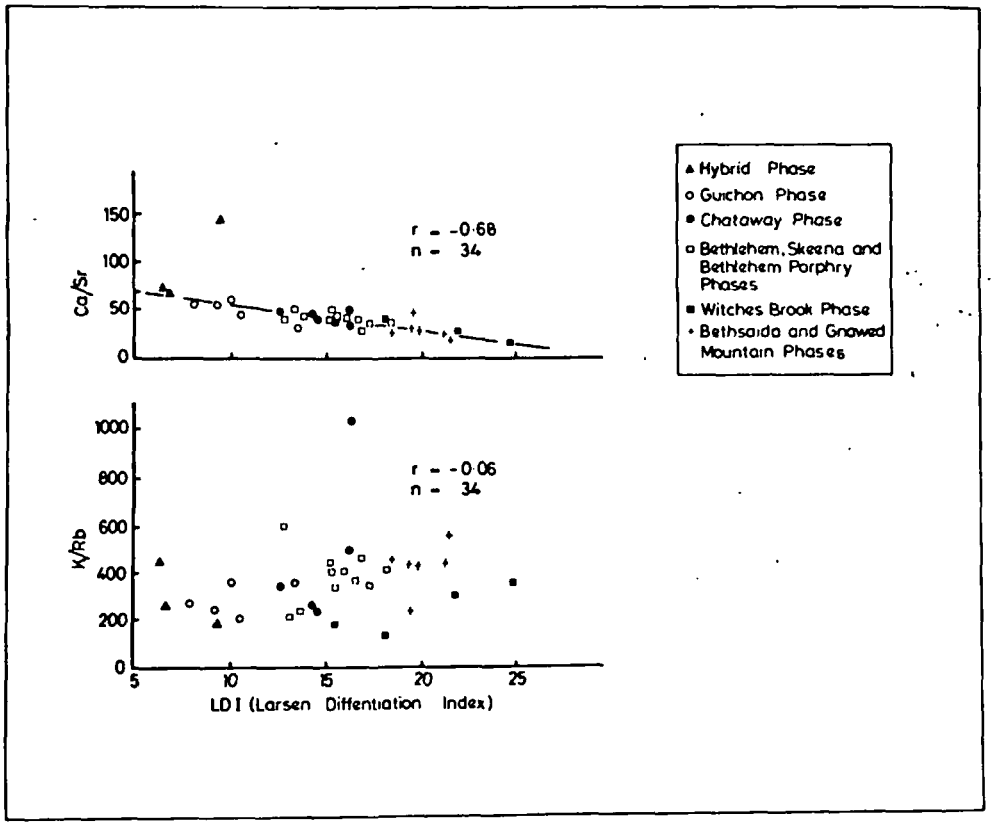

FIG. 8. Plots of K/Rb and Ca/Sr ratios *vs.* Larsen differentiation index.

The K/Rb ratio is generally considered as a reliable index of the degree of fractionation in most igneous suites (Taubeneck 1965). However, for the Guichon Creek batholith, K/Rb ratios show no consistent patterns when plotted against LDI (Fig. 8). This is attributed to the relatively low and near-uniform concentrations of both elements in the intrusive units. Moreover, K/Rb ratios range from 132 to 1030, and average 368 for the batholith. The majority of these values lie outside the limit considered normal for rocks of granitic composition (K/Rb = 150–300) (Fig. 9), and may suggest a subcrustal origin for the Guichon Creek batholith.

Sr concentrations range from 249 to 1000 ppm and average 686 ppm. These values are high, relative to the average of 440 ppm cited by Turekian and Wedepohl (1961) for high-Ca granitic rocks. Except for the contaminated Hybrid Phase, mean Sr values for the constituent units show a subtle but not significant decrease with increasing fractionation (Table 1). During magmatic processes, Sr tends to substitute for Ca and

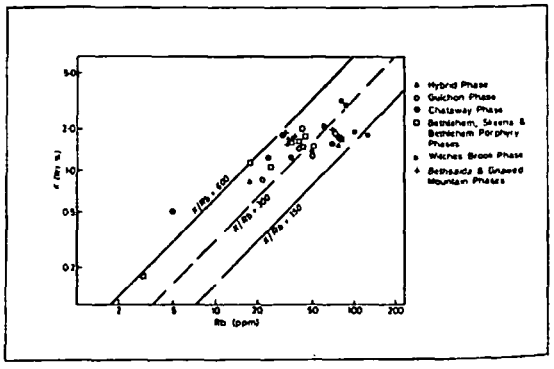

FIG. 9. Plots of K versus Rb and K/Rb ratios in rocks of Guichon Creek batholith (Normal K/Rb ratios = 150–300).

K in feldspars. Thus, the apparent decrease of mean Sr with increasing differentiation might reflect a corresponding decrease in Ca levels. A plot of Ca/Sr ratios against LDI indicates a decrease with increasing fractionation (Fig. 8). This relationship suggests that Sr is enriched relative to Ca in the more felsic rocks.

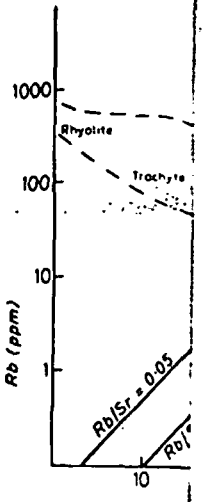

FIG. 10. Plot of
(generalized geoche
certain types of roc
Hedge 1966).

Rb/Sr ratios
and most of th
basalts and and
the ratio of 0.
(Faure and Hu
batholith has
might reflect the
of the Guichon

Petrochemical
compositional
Guichon Creek
of fractional c
intermediate co
tionation of horn
Hornblende and
enrich Si and alk
and Ti levels
plagioclase fract
content of residu

The most strik
evolution of the
enrichment in
relatively young
Gnawed Mount
and lack of terr
that the pluton

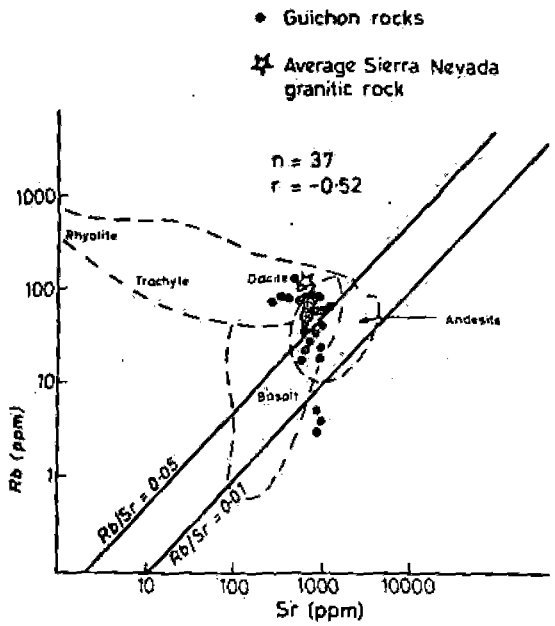

FIG. 10. Plot of Rb *vs.* Sr in Guichon Creek batholith (generalized geochemical relationships of Rb and Sr in certain types of rocks are shown for comparison; *after* Hedge 1966).

Rb/Sr ratios average 0.051 for the batholith, and most of the values plot in the region of basalts and andesites (Fig. 10). Compared with the ratio of 0.25 for typical continental sial (Faure and Hurley 1964), the Guichon Creek batholith has very low Rb/Sr ratios, which might reflect the nature of the source materials of the Guichon Creek magma (Culbert 1972).

Discussion

Petrochemical trends suggest that zonal and compositional variations exhibited by rocks of Guichon Creek batholith conform with a model of fractional crystallization of a magma of intermediate composition by progressive fractionation of hornblende, biotite, and plagioclase. Hornblende and biotite fractionation tends to enrich Si and alkali content, and deplete Fe, Mg, and Ti levels of derivative liquids; whereas, plagioclase fractionation generally depletes Ca content of residual fluids (Smith 1974).

The most striking aspect of the petrochemical evolution of the batholith is absence of K_2O enrichment in the most differentiated and relatively youngest rocks—the Bethsaida and Gnawed Mountain Phases. Low values of K_2O and lack of terminal enrichment suggest either that the pluton is not highly differentiated or that the parental magma is relatively K-poor. The latter is probably the case, because field and petrographic evidence (Northcote 1969) and petrochemical variation diagrams (Figs. 3 and 4) support magmatic fractionation. This contention is further buttressed by the tendency for Na_2O to increase with increasing differentiation (Fig. 5). This 'trondhjemitic trend' is commonly characteristic of K-poor magmas (Larsen and Poldervaart 1961; Taubeneck 1965).

The K/Rb ratio is perhaps the most important and significant element ratio in igneous petrogenesis. Absolute and relative values are generally interpreted in relation to differentiation history and nature of source materials (Shaw 1968; Erlank 1968; Hurley 1968; Culbert 1972). In rocks of Guichon Creek batholith, crystallization-fractionation did not result in a decrease of K/Rb ratios. Thus, K/Rb ratios may not reflect differentiation processes in K-poor granitoids; rather, Ca/Sr ratios constitute a more reliable index of differentiation.

The relatively low K, Rb, and Rb/Sr values, and high K/Rb and Sr levels in rocks of the Guichon Creek batholith are not due principally to mineral fractionation, but suggest derivation of the batholith from a source region depleted in alkalis and enriched in Sr, most probably subducted oceanic crust or upper mantle. This interpretation is consistent with the primitive initial Sr^{87}/Sr^{86} ratio (0.7037) reported by Chrismas *et al.* (1969), and plate tectonic models proposed for the Canadian Cordillera (Dercourt 1973; Monger *et al.* 1972; Peto 1974).

Petrochemical evidence suggests that the K-rich dike rocks of the Witches Brook Phase are distinct from the remainder of the batholith. This may be related to their 'high-level' mode of emplacement, culminating in the enrichment in alkalis (Northcote 1969).

Trace element distribution in igneous rocks is generally controlled by abundance of major elements and the ability of trace elements to enter appropriate lattices. Trace elements capable of entering the structures of rock-forming minerals can be removed from the magma, and thus eliminated from any further possibility of concentration into ore deposits (Levinson 1974). The behavior of Cu suggests that it does not readily enter into crystal lattices of femic silicates in felsic rocks. Because of its strongly chalcophile nature, Cu fractionates into the residual melt to combine with S (Wager and Brown 1967). With

increasing differentiation and volatile content, and an adequate supply of S, copper sulfides might concentrate as ore deposits if the magma is Cu-rich. However, the enrichment of Cu in such magmas is generally accompanied by enhanced levels in whole rocks and constituent minerals as demonstrated by studies on porphyry-Cu-bearing Laramide intrusions in Arizona (Graybeal 1973), and the Skaergaard (Wager and Mitchell 1951; Wager and Brown 1967). Several authors (*e.g.*, Putman and Burnham 1963; Lovering *et al.* 1970) have also reported that intrusive units that are associated with copper mineralization are characterized by high Cu contents in either fresh rocks or mineral fractions, especially biotites.

The tendency for Cu to decrease with increasing fractionation in the Guichon Creek batholith parallels that of the femic elements (Zn, Ni, Co, Mn, and V), and represents normal differentiation trends. Thus, the lack of positive correlation between copper mineralization and the Cu contents of fresh Guichon Creek rocks and mineral fractions, as earlier noted by Brabec (1970) and Brabec and White (1971), is probably explicable if mineralization is regarded as an independent by-product of magma generation, rather than the result of differentiation processes (Noble 1970; Sheraton and Black 1973). This is consistent with the fact that many of the porphyry copper deposits in the pluton (*e.g.*, Bethlehem mines, Krain, Trojan) are not associated with the most differentiated intrusive units—Bethsaida and Gnawed Mountain Phases (Hylands 1972).

Zn, Mn, Ni, Co, and V are less chalcophile than Cu and more readily enter lattices of ferromagnesian minerals. Consequently they are removed from the magma during differentiation. Low abundances of Mo, Pb, Ag, and Sn in rocks of the batholith might reflect their initial concentrations in the magma.

Conclusions

Geochemical evolution of the Guichon Creek batholith is consistent with a model of crystallization-fractionation of a calc-alkaline dioritic magma generated by partial melting of subducted oceanic crust at relatively shallow depths. The apparent negative correlation between Cu contents and ore potential of intrusive units in the Guichon Creek batholith suggests that not all Cu-bearing plutons need be enriched in Cu. Close relationships between trace metal values and degree of fractionation emphasize the need for assigning different background values to each intrusive unit during geochemical exploration.

Further research work is, however, required in establishing the relationship between ore potential and concentrations of K, Rb, Sr, K/Rb, and Rb/Sr ratios in Mesozoic calc-alkaline plutonic rocks in the Intermontane Belt of the Canadian Cordillera.

Acknowledgments

This paper constitutes part of a Ph.D. thesis completed at the University of British Columbia under the supervision of Dr. W. K. Fletcher, to whom the writer is highly indebted. I thank D. Marshall, M. Waskett-Myers, A. Dhillon, and A. Baxter for technical assistance. Financial support for the project was provided by grants from the National Research Council of Canada (PRAI P-7303 and NRC 67–7714), and a Killam Pre-Doctoral Fellowship, which supported the writer.

AGER, C. A., ULRYCH, T. J., and MCMILLAN, W. J. 1973. A gravity model for the Guichon Creek batholith, south-central British Columbia. Can. J. Earth. Sci. 10, pp. 920–935.

AL-HASHIMI, A. R. K. and BROWNLOW, A. H. 1970. Copper content of biotites from the Boulder batholith. Montana. Econ. Geol. 65, pp. 985–992.

BLAXLAND, A. B. 1971. Occurrence of Zn in granitic biotites. Mineral. Deposita. 6, pp. 313–320.

BRABEC, D. 1970. A geochemical study of the Guichon Creek batholith, British Columbia. Unpubl. PhD thesis. Univ. British Columbia, Vancouver, 146 p.

——— 1971. Aqua regia extractable *vs*. total copper and zinc content of granitic rocks. Soc. Min. Eng. Trans. 250, pp. 94–97.

BRABEC, D. and WHITE, W. H. 1971. Distribution of copper and zinc in rocks of Guichon Creek batholith. *In*: Geochemical Exploration. CIM Spec. Vol. 11, pp. 291–297.

CARR, J. M. 1966. Geology of the Bethlehem and Craigmont copper deposits. *In*: Tectonic History and Mineral Deposits of the Western Cordillera. CIM Spec. Vol. 8, pp. 321–328.

CHRISMAS, L., BAADSGAARD, H., FOLINSBEE, R. E., FRITZ, P., KROUSE, H. R., and SASAKI, A. 1969. Rb/Sr. S. and O isotope analyses indicating source and date of contact metasomatic copper deposits, Craigmont, British Columbia, Canada. Econ. Geol. 64, pp. 479–488.

CORNWALL, H. R., and ROSE, H. J. 1957. Minor elements in .Keeweenawan lavas, Michigan. Geochim. Cosmochim. Acta. 12, pp. 209–224.

CULBERT, R. R. 1972. Abnormalities in the distribution of K, Rb and Sr in the Coast Mountain batholith, British Columbia. Geochim. Cosmochim. Acta, 36, pp. 1091–1100.

CURTIS, C. D. 1964. Application of the crystal-field theory to the inclusion of transition elements in minerals during

magmatic differentiation. Geochim. Cosmochim. Acta, 28, pp. 389–403.

DERCOURT, J. 1972. The Canadian Cordillera, the Hellenides, and the sea-floor spreading theory. Can. J. Earth Sci. 9, pp. 709–743.

ERLANK, A. J. 1968. The terrestrial abundance relationship between potassium and rubidium. *In*: Origin and Distribution of the Elements. (X.X. Ahrens, *Ed.*) Pergamon Press, Oxford, pp. 871–888.

FAURE, G., and HURLEY, P. M. 1964. The isotopic compositions of strontium in oceanic and continental basalts; Application to the origin of igneous rocks. J. Petrol. 4, pp. 31–50.

GOLDSCHMIDT, V. M. 1954. Geochemistry. Oxford University Press, Cambridge. 750 p.

GRAYBEAL, F. T. 1973. Copper, manganese and zinc in coexisting mafic minerals from Laramide intrusive rocks in Arizona. Econ. Geol. 68, pp. 785–798.

HEDGE, C. E. 1966. Variations in radiogenic strontium found in volcanic rocks. J. Geophys. Res. 71, pp. 6119–6126.

HEIER, K. S., and ADAMS, J. A. S. 1964. The geochemistry of the alkali metals. Phys. Chem. Earth, 5, pp. 253–381.

HURLEY, P. M. 1968. Absolute abundances and distribution of Rb, K and Sr in the earth. Geochim. Cosmochim. Acta, 32, pp. 273–283.

HYLANDS, J. 1972. Porphyry copper deposits of the Guichon Creek batholith, B.C. Proc. 24th Int. Geol. Cong. 4, pp. 241–250.

KISTLER, R. W., EVERNDEN, J. F., and SHAW, H. R. 1971. Sierra Nevada plutonic cycle: Part 1, Origin of composite granitic batholith. Geol. Soc. Am. Bull. 82, pp. 853–868.

LARSEN, E. S. J., and POLDERVAART, A. 1961. Petrologic study of Bald Rock batholith, near Baldwell Bar, California. Geol. Soc. Am. Bull. 72, pp. 69–92.

LEVINSON, A. A. 1974. Introduction to Exploration Geochemistry. Applied Publishing Ltd., Calgary.

LOVERING, T. G., COOPER, J. R., DREWES, H., and CONE, G. C. 1970. Copper in biotites from igneous rocks in Southern Arizona as an ore indicator. U.S. Geol. Surv. Prof. Pap. 700B, pp. 1–8.

MCDOUGALL, I. and LOVERING, J. F. 1963. Fractionation of Cr, Ni, Co and Cu in differentiated dolerite–lamprophyre sequence at Red Hill, Tasmania. Geol. Soc. Aust. J. 10, pp. 325–338.

MCMILLAN, W. J. 1972. The Highland Valley porphyry copper district. Guidebook 9, 24th Intern. Geol. Cong., pp. 53–69.

——— 1973. Geological Map of the Highland Valley. Brit. Col. Dept. Mines Rep. (in press).

MONGER, J. W., SOUTHER, J. G., and GABRIELSE, H. 1972. Evolution of the Canadian Cordillera: A plate tectonic model. Am. J. Sci. 272, pp. 577–602.

NOBLE, J. A. 1970. Metal provinces of the western United States. Geol. Soc. Amer. Bull. 81, pp. 1607–1624.

NOCKOLDS, S. R. and ALLEN, R. 1953. The geochemistry of some igneous rock series. Geochim. Cosmochim. Acta, 4, pp. 105–142.

NORTHCOTE, K. E. 1969. Geology and geochronology of the Guichon Creek batholith. B. C. Dep. Mines Bull. 56, 73p.

OLADE, M. A. 1974. Bedrock geochemistry of porphyry copper deposits, Highland Valley, British Columbia, Canada. Unpubl. PhD thesis, Univ. British Columbia, Vancouver, British Columbia. 495 p.

OLADE, M. A. and FLETCHER, K. 1974. Potassium chlorate–hydrochloric acid: A sulphide selective leach for bedrock geochemistry. J. Geochem. Explor. 3, pp. 337–344.

PETO, P. 1974. Plutonic evolution of the Canadian Cordillera. Geol. Soc. Am. Bull. 85, pp. 1269–1276.

PUTMAN, G. W., and BURNHAM, S. J. 1963. Trace elements in igneous rocks, northwestern and central Arizona. Geochim. Cosmochim. Acta, 27, pp. 53–106.

SHAW, D. M. 1968. A review of K–Rb fractionation trends by covariance analysis. Geochim. Cosmochim. Acta, 32, pp. 573–601.

SHERATON, J. W., and BLACK, L. P. 1973. Geochemistry of mineralized granitic rocks of Northeast Queensland. J. Geochem. Explor. 2, pp. 331–348.

SMITH, T. E. 1974. The geochemistry of the granitic rocks of Halifax County, Nova Scotia. Can. J. Earth Sci. 11, pp. 650–656.

TAUBENBECK, W. H. 1965. An apparaisal of some potassium–rubidium ratios in igneous rocks. J. Geophys. Res. 70, pp. 475–478.

——— 1967. Petrology of Cornucopia Tonalite Unit, Cornucopia stock, Wallowa Mountains, northeastern Oregon. Geol. Soc. Am. Spec. Pap. 91, 56 p.

TUREKIAN, W. H. and WEDEPOHL, K. 1961. Distribution of the elements in some major units of the Earth's crust. Geol. Soc. Am. Bull. 72, pp. 641–664.

WAGER, L. R. and BROWN, G. M. 1967. Layered igneous rocks. Oliver and Boyd, Edinburgh and London, 588 p.

WAGER, L. R., and MITCHELL, R. L. 1951. The distribution of trace elements during strong fractionation of basic magma–a further study of the Skaergaard intrusion, East Greenland. Geochim. Cosmochim. Acta 1, pp. 129–208.

WHITE, W. H., THOMPSON, R. M., and MCTAGGART, K. C. 1957. The geology and mineral deposits of Highland Valley, B.C. Can. Inst. Min. Metall. Trans. 60, pp. 273–289.

ZLOBIN, B. I. *et al.* 1967. Copper in intrusions of the central part of northern Tian-Shan as related to the problems of metallogeny. Geol. Rudn. Mestorozd. 1, pp. 45–56 (in Russian).

J. Ganguly

stals, and applications to solid solutions
ds 28, 2225–2237 (1967)
ıry. Oxford 1970
:clogites and eclogites: their differences

n aluminum-substituted yttrium iron
ff. Aerospace Res. Doc. AFCRL-70-0215
ls, 1, Ortho- and Ring-silicates. London:

s with garnet structures. Acta Cryst. 19,

solid solution 1. Mixing of the alumino-
148 (1974)
eralogist 44, 445–446 (1959)
xcess functions from the intracrystalline
Cosmochim. Acta 38, 1527–1548 (1974)
olland 1967
radite (var-colophonite) and uvarovite.

I, Philips Res. Rep. 5, 333–356 (1950)
II, Philips Res. Rep. 6, 183–210 (1951)
eochim. Cosmochim. Acta 26, 581–598

logist 57, 300–316 (1972)
rale am Beispiel der Chromfärbungen.

kdown of albite at depths in the Earth.

garnets. Am. Mineralogist 56, 791–825

ies at low pressures. Am. Mineralogist

Longmans 1954
olutions. Berlin-Heidelberg-New York:

ides and fluorides. Acta Cryst. B 25,

t group. Am. Mineralogist 41, 428–436

Contrib. Mineral. Petrol. 55, 91–104 (1976)

Contributions to Mineralogy and Petrology

The Significance of Garnet and Cordierite from the Sioux Lookout Region of the English River Gneiss Belt, Northern Ontario

Nigel B.W. Harris

Department of Geology, University of Toronto, 170 College Street, Toronto, Ontario, Canada

Abstract. Garnet and cordierite bearing Archean gneisses are a common rock-type in the English River gneiss belt of the Superior Province, northern Ontario. Bulk compositions of such gneisses are found to be depleted in potassium with respect to the garnet and/or cordierite-free biotite gneisses. The mineral assemblages of the garnet and cordierite gneisses indicate that they have equilibrated at higher metamorphic grades than the garnet and/or cordierite-free biotite gneisses. These observations suggest that anatexis has occurred in the garnetiferous regions of the gneiss belt resulting in a granite melt which had migrated from the source rocks, thereby depleting the garnetiferous restite in potassium.

1. Introduction

The English River gneiss belt is a 650 kilometre long region of granites and granitic gneisses within the Superior Province of the Canadian Shiled. It extends from Lake Winnipeg in the west to the James Bay lowlands in the east, and its width varies between 80 and 120 kilometres. It is distinguished from the metavolcanic belts lying to the north and south by its abundance of biotite granitic gneisses and paucity of amphibolites, by its low aeromagnetic anomalies and by its peculier crustal structure [1].

The samples discussed in this paper are taken from a 160 by 120 kilometre area of the gneiss belt, which lies to the northeast of Sioux Lookout, mapped by Skinner in 1969 [2].

2. General Geology

This region of the gneiss belt is underlain by foliated tonalitic-granodioritic plutonic rock, massive, cross-cutting granodioritic-granitic plutons, and fine-grained gneissic metasediments. Amphibolites are rare and underlie less than 5%

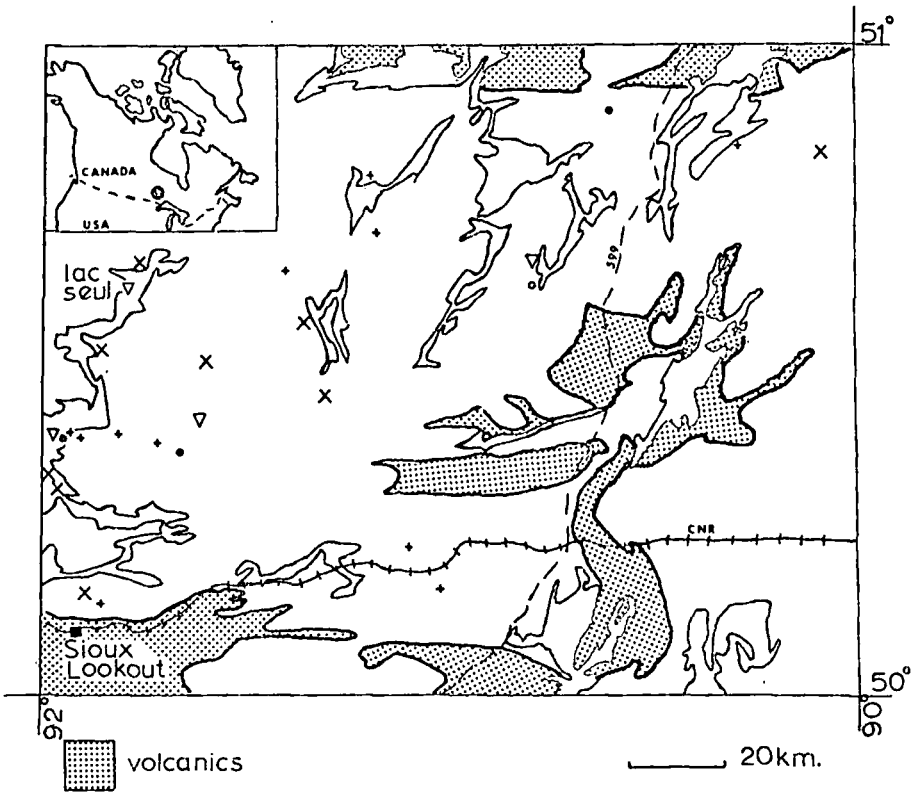

Fig. 1. Location map of analysed samples. × biotite gneiss, + biotite-garnet gneiss, ● biotite-garnet-cordierite gneiss, o biotite-cordierite-sillimanite gneiss, ▽ garnet pegmatite

of the region. The plutonic rocks are characterised by quartz, plagioclase, biotite ± microcline ± hornblende. This assemblage is insensitive to significant changes in metamorphic conditions. However the more pelitic nature of the metasediments leads to the formation of garnet, cordierite and, rarely, sillimanite, which provide some information on the metamorphic history of the belt.

The mineralogy of the sedimentary gneisses is represented by biotite (B), quartz (Q), plagioclase (P), microcline (K), garnet (G), cordierite (C), muscovite (M) and sillimanite (S). Accessory iron oxides occur in both garnet-bearing and garnet-free gneisses. In the few sections which show chloritisation of biotite and saussuritisation of plagioclase, iron oxides are associated with biotite and appear to be a retrograde breakdown of an iron-rich biotite.

Cordierite and/or garnet gneisses occur throughout the metasediments of the region (Fig. 1), although many metasediments contain biotite as the only ferromagnesian phase. There are five mineral assemblages in which these phases occur:

(i) B+C+G+K±M

(ii) B+C+G±M

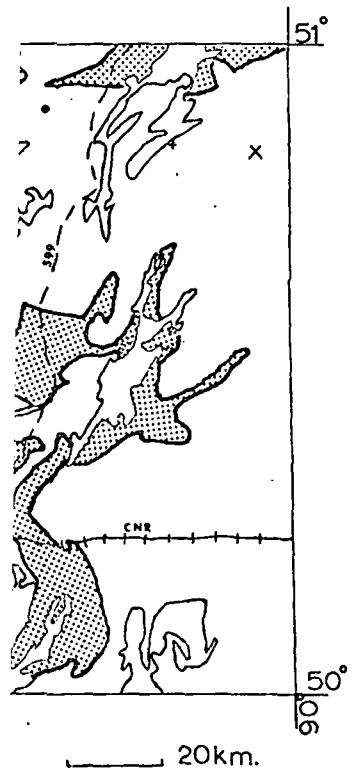

biotite-garnet gneiss, ● biotite-garnet-
rnet pegmatite

d by quartz, plagioclase, biotite
nsensitive to significant changes
pelitic nature of the metasedi-
: and, rarely, sillimanite, which
istory of the belt.
is represented by biotite (B),
t (G), cordierite (C), muscovite
occur in both garnet-bearing
h show chloritisation of biotite
are associated with biotite and
-rich biotite.
oughout the metasediments of
nts contain biotite as the only
emblages in which these phases

(iii) B+C+S+K

(iv) B+G+K±M

(v) B+G.

Quartz and plagioclase coexist with all five assemblages. Muscovite can generally be identified as a retrograde phase which is associated with sericitisation of feldspar, chloritisation of biotite and pinitisation of cordierite, where present.

Electron microprobe analyses of the feldspars from the gneisses indicate that plagioclase varies in composition from Ab_{99}–Ab_{73} and microcline from Or_{85}–Or_{90}.

Garnet is also found in pegmatites and granites intruding the garnetiferous gneisses. Garnet-bearing pegmatites or granites have not been found within garnet-free gneisses.

3. Previous Metamorphic Studies in the English River Gneiss Belt

Several previous surveys have estimated the metamorphic grade of assemblages from the English River gneiss belt. Dwibedi [3] surveyed a locality in the Manitoba region of the gneiss belt, and concluded that metamorphism reached the almandine-amphibolite facies. This conclusion was based on microcline triclinicity and the presence of sillimanite. Jones [4], from a metamorphic study of the same region, concluded that metamorphic grade increased gradually from lower amphibolite facies, along the northern and southern margins of the belt, to sporadic localities of granulite facies around the centre of the belt. This was based on the anorthite content of plagioclase. A recent helicopter survey of the region west of Armstrong [5] concludes that diagnostic metamorphic phases were lacking but a metamorphic grade in the middle to upper amphibolite facies was suspected. The most detailed metamorphic study made to date [6] discussed the observed assemblages garnet + sillimanite + biotite, and garnet + cordierite + sillimanite in the A-F-M ternary system and concludes that the metamorphic grade various from greenschist up to upper amphibolite (4 kilobars, 700° C) and that metamorphism is of the high temperature–low pressure Abukuma type. However the phase analysis does not consider the effect of the potassic component on the system, nor the effects of a liquid or vapour phase on the mineral assemblages.

4. Compositions of Ferromagnesian Phases

Electron microprobe analyses were made on garnet cordierite and biotite phases from the gneisses (Fig. 2), and garnet from the pegmatites.

The garnets analysed contain less than 6% spessartine and less than 3% grossular, and are essentially part of the almandine-pyrope solid solution series (Table 1). The almandine component varies between 70–80% and zoning does not exceed 2%. Cordierite compositions lie between 64 and 70% of the magne-

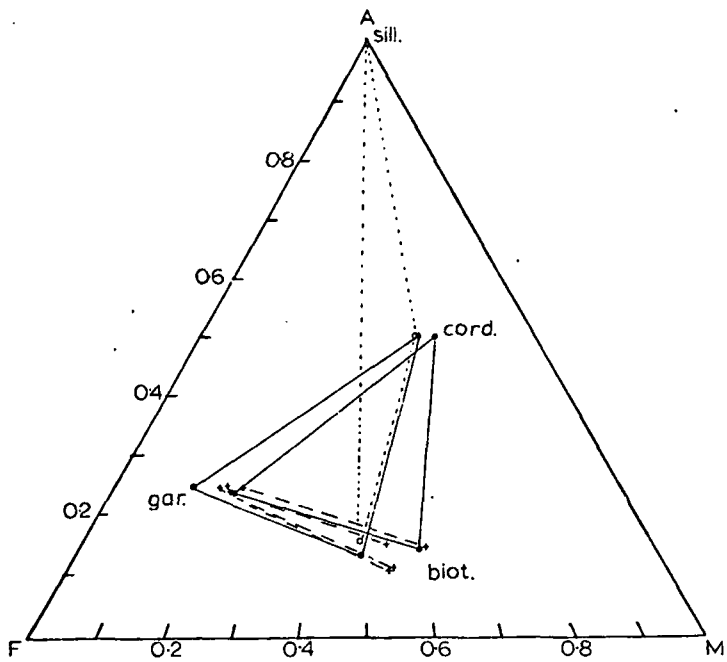

Fig. 2. A–F–M plot for biotite, cordierite, garnet phases. $A=(Al_2O_3-K_2O)/(Al_2O_3-K_2O+FeO+MgO)$, $M=MgO/(MgO+FeO)$. Legend as for Fig. 1

sium end-member (Table 2). Biotite compositions lie between 48 and 60% of the magnesium end-member, and their high alumina content indicate that they fall in the siderophyllite field (Table 3).

In the following phase analysis it is assumed that the observed coexisting phases are in equilibrium. Three observations support this assumption:

(i) Compositions of ferromagnesian phases are not found to be zoned.

(ii) Evidence of textural disequilibrium has not been observed in the gneisses.

(iii) Tie-lines between composition plots of coexisting phases (Fig. 2) do not intersect.

The compositions of coexisting cordierite and garnet have a sufficiently high Mg/Fe ratio to lie in the 'Regional assemblage' field defined by Chinner [7]. This implies that these assemblages equilibrated under conditions of regional rather than thermal metamorphism. The distribution coefficient of iron and magnesium between garnet and biotite (K_D) given by $K_D=$ Fe/Mg (Garnet) – Fe/Mg (biotite), varies between 3.8 and 5.6. More quantitative studies on the use of iron-magnesium distribution between garnet and cordierite [8] are applicable only to garnet-cordierite-sillimanite assemblages, and these three phases do not coexist in the assemblages discussed in this paper. Moreover such grade indicators are also dependent on P_{H_2O} which is an unknown parameter in these assemblages.

Table 1. Garnet analyses

	Cord.+Gnt.+ Biot. gneiss		Gnt.+Biot. gneiss				Gnt. pegmatite
	126	393	1	174	176	199	223
SiO_2	36.93	37.71	37.99	39.55	37.67	38.48	37.14
TiO_2	0.03	0.00	0.01	0.07	0.00	0.01	0.21
Al_2O_3	20.34	21.28	21.75	22.68	21.64	21.48	21.90
FeO	36.13	33.80	33.63	30.93	33.20	34.49	35.67
MnO	2.85	1.25	1.86	1.17	1.25	1.43	2.32
MgO	3.37	5.73	5.21	5.73	5.57	5.23	2.73
CaO	0.32	1.12	0.96	1.03	1.14	1.11	0.46
K_2O	0.00	0.00	0.00	0.01	0.00	0.00	0.02
Na_2O	0.02	0.08	0.04	0.03	0.08	0.03	0.02
Total	99.99	100.97	101.45	101.20	100.55	102.26	100.47
Number of ions per formula unit (assuming 12 oxygens)							
Si	3.00	2.97	2.98	2.98	2.97	2.99	2.92
Ti	0.00	0.00	0.00	0.00	0.00	0.00	0.01
Al	1.94	1.97	2.01	2.02	2.01	1.97	2.04
Fe	2.45	2.22	2.24	1.95	2.19	2.25	2.34
Mn	0.19	0.08	0.12	0.07	0.09	0.09	0.15
Mg	0.40	0.67	0.63	0.64	0.65	0.61	0.39
Ca	0.02	0.09	0.08	0.08	0.09	0.09	0.05
K	0.00	0.00	0.00	0.00	0.00	0.00	0.00
Na	0.00	0.01	0.01	0.01	0.00	0.00	0.00
Garnet molecule in per cent of end-members							
Alm.	80	70	73	71	73	74	80
Pyr.	13	23	20	23	21	20	13
Spess.	6	2	4	3	3	3	5
Gross.	1	3	3	3	3	3	2

5. Bulk Chemical Analyses of Garnet and Cordierite Bearing Assemblages

X−R−F bulk analyses (Table 4) of cordierite and/or garnet gneisses, biotite gneisses (garnet-free) and garnet pegmatites have been plotted in the A−K−F and A−F−M ternary systems (Figs. 3 and 4). The A−K−F plot of these analyses indicates that the garnet and/or cordierite gneisses and the garnet-free biotite gneisses fall into two distinct fields separated by the biotite-muscovite or the biotite-sillimanite tie-line. Since none of the garnet-free biotite gneisses contain sillimanite, and many contain muscovite, it is assumed that it is the biotite-muscovite tie-line that controlled the presence or absence of the garnet/cordierite phases. This implies that the formation of garnet or cordierite is controlled by low potash in the bulk composition. It can also be seen from the A−K−F plot (Fig. 3) that within the low potash field the presence of cordierite is controlled by a high Al/(Fe+Mg) ratio. If the tie-lines from biotite to each of the other phases are constructed then the biotite-muscovite-microcline,

Table 2. Cordierite analyses

	Cord. + Gnt. + Biot. gneiss		Cord. + Sill. + Biot. gneiss
	126	393	225
SiO_2	48.45	49.80	49.57
TiO_2	0.00	0.02	0.02
Al_2O_3	32.27	34.19	34.22
FeO	8.26	7.21	8.61
MnO	0.18	0.16	0.36
MgO	8.20	9.33	8.64
CaO	0.03	0.02	0.01
K_2O	0.00	0.00	0.02
Na_2O	0.14	0.24	0.06
Total	97.53	100.97	101.51
Number of ions per formula unit (assuming 18 oxygens)			
Si	5.04	4.96	4.95
Ti	0.00	0.00	0.00
Al	3.96	4.02	4.03
Fe	0.71	0.60	0.72
Mn	0.01	0.01	0.03
Mg	1.27	1.38	1.29
Ca	0.00	0.00	0.00
K	0.00	0.00	0.00
Na	0.02	0.02	0.01

Table 3. Biotite analyses

	Gnt. + Biot. gneiss				Cord. + Gnt. + Biot. gneiss		Cord. + Sill. + Biot. gneiss
	1	174	176	199	126	393	225
SiO_2	35.79	36.82	35.70	36.14	35.03	37.05	35.69
TiO_2	3.07	3.59	4.95	3.54	3.50	2.40	2.24
Al_2O_3	19.21	19.18	17.16	17.26	18.85	19.96	20.83
FeO	17.43	14.38	16.76	18.06	18.80	16.16	19.51
MnO	0.01	0.10	0.02	0.00	0.02	0.14	0.18
MgO	10.85	12.40	11.14	11.35	9.97	12.72	10.21
CaO	0.03	0.03	0.02	0.03	0.03	0.02	0.01
K_2O	10.15	10.21	9.80	9.63	9.81	9.67	9.67
Na_2O	0.02	0.01	0.06	0.12	0.21	0.34	0.08
Total	96.55	96.72	95.61	96.12	96.22	98.46	98.42
Number of ions per formula unit (assuming 22 oxygens)							
Si	5.34	5.34	5.38	5.43	5.29	5.36	5.25
Ti	0.34	0.39	0.56	0.40	0.40	0.26	0.25
Al	3.48	3.26	3.06	3.05	3.36	3.40	3.61
Fe	2.17	1.73	2.11	2.26	2.37	1.95	2.40
Mn	0.00	0.01	0.00	0.00	0.00	0.02	0.02
Mg	2.41	2.66	2.50	2.54	2.24	2.74	2.24
Ca	0.00	0.00	0.00	0.00	0.00	0.00	0.00
K	1.93	1.87	1.88	1.85	1.89	1.78	1.81
Na	0.00	0.00	0.02	0.03	0.06	0.10	0.02

Table 4. Mean bulk compositions

	Biot.+Gnt. gneiss	Biot.+Gnt.+ Cord. gneiss	Biot.+Cord.+ Sill. gneiss	Biot. gneiss	Gnt. pegmatite
	$n=6$	$n=2$	$n=1$	$n=9$	$n=4$
SiO_2	63.96	58.72	70.50	69.22	72.96
TiO_2	0.65	0.81	0.33	0.35	0.02
Al_2O_3	16.50	17.98	15.70	16.23	14.94
FeO	5.87	7.55	2.46	2.11	1.00
MnO	0.09	0.12	0.03	0.04	0.04
MgO	2.74	3.82	1.70	1.03	0.33
CaO	2.76	1.93	2.27	2.72	0.97
K_2O	2.32	3.28	1.26	2.53	5.76
Na_2O	3.53	2.92	3.57	4.14	2.85
H_2O	0.73	1.40	0.41	0.57	0.37
Total	99.15	98.53	98.23	98.94	99.24

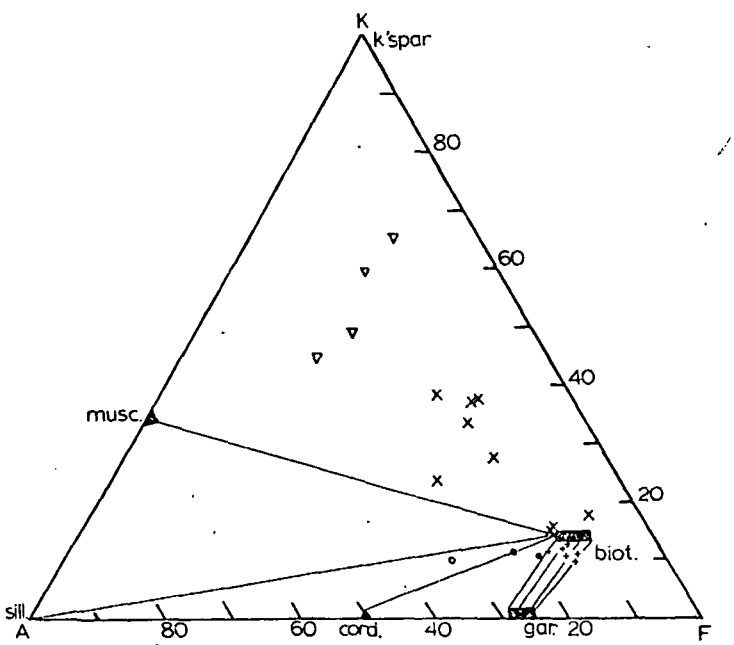

Fig. 3. A – K – F plot for bulk chemical compositions. $A=Al_2O_3-(K_2O+Na_2O+CaO)$, $K=K_2O$, $F=FeO+MgO+MnO$. Legend as for Fig. 1

biotite-sillimanite-cordierite, biotite-cordierite-garnet, and biotite-garnet fields are appropriately defined with respect to the observed assemblages. However the fields defined by these tie-lines do not account for microcline coexisting with many garnet and cordierite assemblages.

The A – F – M plot of these analyses (Fig. 4) does not indicate distinct fields for garnet-free and garnet and/or cordierite bearing assemblages. However the plot does demonstrate that cordierite bearing assemblages have a higher alumina

›rd.+Gnt.+ ›t. gneiss		Cord.+Sill.+ Biot. gneiss
6	393	225
.03	37.05	35.69
.50	2.40	2.24
.85	19.96	20.83
.80	16.16	19.51
.02	0.14	0.18
.97	12.72	10.21
.03	0.02	0.01
.81	9.67	9.67
.21	0.34	0.08
.22	98.46	98.42
.29	5.36	5.25
.40	0.26	0.25
.36	3.40	3.61
.37	1.95	2.40
.00	0.02	0.02
.24	2.74	2.24
.00	0.00	0.00
.89	1.78	1.81
.06	0.10	0.02

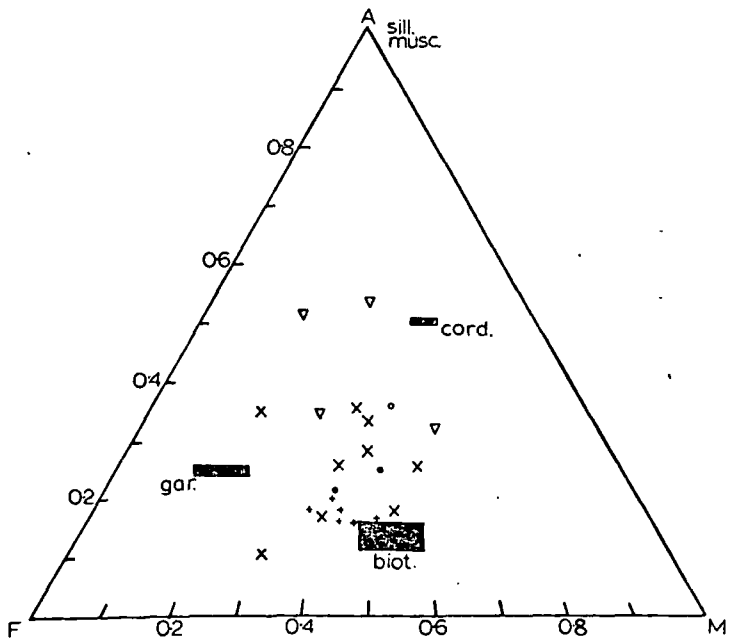

Fig. 4. A – F – M plot for bulk chemical compositions. $A = (Al_2O_3 - Na_2O - K_2O - CaO)/(Al_2O_3 - Na_2O - K_2O - CaO + FeO + MgO)$, $M = MgO/(MgO + FeO)$. Legend as for Fig. 1

content than those garnet bearing assemblages which are cordierite-free. The overlap between the composition fields of garnet-bearing and garnet-free gneisses in the A – F – M plot, and the difficulty in explaining garnet/cordierite and microcline assemblages in the A – K – F diagram imply that the assemblages should be considered in the A – F – M – K tetrahedron.

It can be seen from Fig. 3 that the muscovite-biotite tie-line effectively separates the fields of garnet and cordierite bearing assemblages from fields in which these phase are absent. Phase relations between microcline muscovite, sillimanite, biotite, garnet and cordierite are indicated in Fig. 5(i), under conditions below the muscovite + quartz breakdown. It can be seen that while the muscovite-biotite tie-line exists the assemblages biotite-garnet-microcline and biotite-garnet-microcline-muscovite (assemblage iv) are only stable for a limited rock composition field, since biotite, garnet, muscovite and microcline are nearly co-planar in A – F – M – K space at low grades. This observation is inconsistent with the widespread distribution of assemblages (iv). Moreover, under these conditions, the assemblages biotite, cordierite, sillimanite and microcline (assemblage iii) and the assemblage biotite, cordierite, garnet and microcline (assemblages i) are unstable.

The effect of increasing grade on the equilibrium assemblages is now considered. It should be noted that grade variation will not only rearrange tie-lines between coexisting phases, but also change the compositions of solid solution phases: with increase in grade biotite increases its Mg/Fe ratio, garnet increases its magnesium content, and cordierite decreases its iron content.

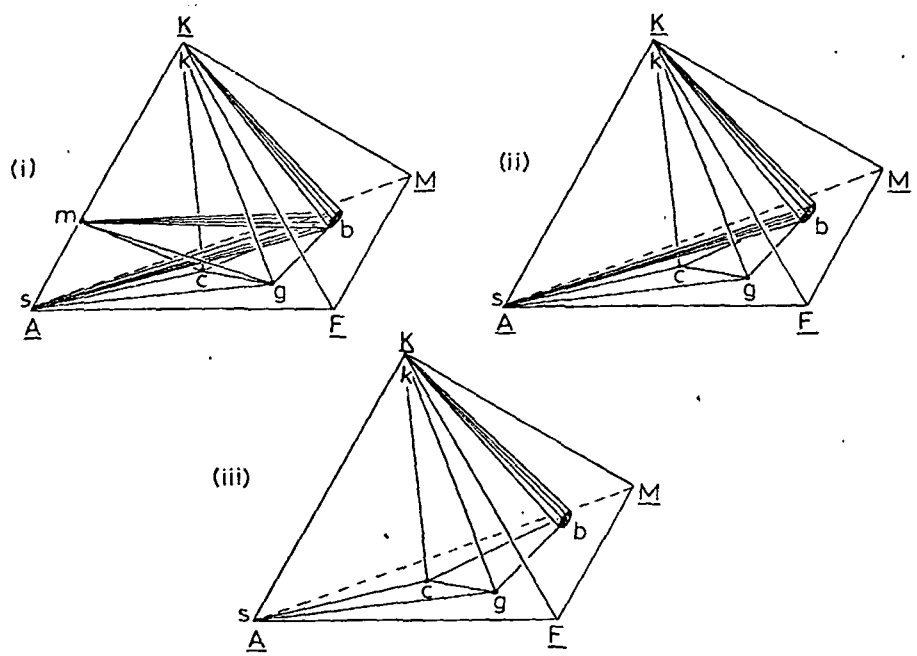

Fig. 5. Phase relations between microcline (*K*), muscovite (*M*), biotite (*B*), cordierite (*C*), garnet (*G*), sillimanite (*S*) in the A–K–M–F tetrahedron: (i) Below muscovite + quartz reaction: (ii) Above muscovite + quartz reaction, below biotite + sillimanite reaction: (iii) Above biotite + sillimanite reaction

With increase in grade, the following discontinuous reaction will occur:

(a) Muscovite + Quartz = Sillimanite + Microcline + H_2O.

These conditions are defined by Fig. 5(ii). Now biotite, sillimanite, cordierite, microcline is a stable assemblages (assemblage iii). Garnet, microcline and biotite may now coexist, but now with sillimanite rather than muscovite which is not observed with these phases. Biotite, cordierite and garnet are still unstable in the presence of microcline. Biotite, garnet and microcline are still only stable for a limited rock composition field.

With further increase in grade, the reaction

(b) Biotite + Sillimanite + Quartz = Cordierite + Garnet + Microcline + H_2O

will occur, resulting in the assemblages defined in Fig. 5(iii). Now the critical assemblage is cordierite, garnet and microcline, but biotite remains since sillimanite was consumed in the last reaction.

Rocks with more Al than garnet-biotite-microcline contain first muscovite, then sillimanite, then cordierite with increasing grade. It is therefore apparent that the observed biotite-cordierite-garnet assemblages can be used as general indicators of metamorphic grade. Assemblage (iii) is indicative of conditions above the muscovite and quartz breakdown and below the reaction between biotite and sillimanite. Assemblage (i) is stable above the biotite and sillimanite reaction.

Assemblage (iv) is stable above the biotite-sillimanite reaction and only stable below this reaction for a limited rock composition field. The use of the garnet-biotite-microcline assemblage as an indicator of relatively high grades is supported by the association in the field between assemblage (iv) with assemblages (i) and (iii). Furthermore, since microcline is not present in the low grade biotite-muscovite gneisses, its appearance in the garnet gneisses (which have been shown to be depleted in potassium with respect to the biotite-muscovite gneisses) implies that it has been derived from a mica breakdown reaction. Microcline-free assemblages (ii) and (v) may be stable throughout the metamorphic range of these reactions and do not help to define the metamorphic grade.

The presence of garnet in pegmatites which contain no biotite implies that either the pegmatite has crystallised under conditions which were unstable for biotite formation, or that garnet is not in equilibrium with the other phases. There is no evidence that a high Fe/Mg ratio has caused the crystallisation of garnet rather than biotite in the pegmatite (Fig. 4). It is improbable that granitic pegmatites have crystallised at temperatures too high for biotite stability since the granite composition and high vapour pressure, characteristic of pegmatites, indicate solidus temperatures around 650–700° C. Even under conditions defined by the crystallisation of dry granitic magma, grossular-poor garnets are thought to be unstable, and have been attributed to refractory remnants surviving the anatexis of pelitic rocks [9]. Furthermore the microtexture of some garnet pegmatites indicates that garnet is reacting with microcline to form biotite and muscovite. Finally the rigorous spatial association between garnet pegmatites and garnet gneisses, and the similarity of garnet compositions from these two rock types (Table 1), indicate a common source for the garnets. It is concluded that the pegmatite garnets are derived from the gneisses, possibly as restite crystals after the partial melting of the gneisses as discussed in the following section.

6. Physical Conditions during Metamorphism

It has been established that the coexistence of garnet or cordierite with microcline is only possible below the muscovite-quartz and biotite-sillimanite breakdown reactions for a narrow rock composition field (Fig. 5). The widespread occurrence of this association for rocks of varying compositions suggest they have equilibrated at metamorphic grades above the muscovite-quartz and biotite-sillimanite breakdown reactions. However the biotite gneisses have not been subjected to such high grades since muscovite and quartz are frequently observed to coexist in these gneisses, and since their bulk compositions (Fig. 3) would imply the stability of sillimanite, or cordierite, or garnet under such metamorphic conditions. Therefore the garnet and/or cordierite gneisses have been subject to higher metamorphic grades than the biotite gneisses. Independent evidence for the relatively high grade of the garnet gneisses comes from interbedded mafic gneisses. In the garnetiferous regions, such gneisses contain varying proportions of ortho and clino pyroxene, indicating the beginning of the granulite

nanite reaction and only stable
on field. The use of the garnet-
latively high grades is supported
blage (iv) with assemblages (i)
resent in the low grade biotite-
neisses (which have been shown
otite-muscovite gneisses) implies
down reaction. Microcline-free
out the metamorphic range of
tamorphic grade.
contain no biotite implies that
litions which were unstable for
librium with the other phases.
has caused the crystallisation
(Fig. 4). It is improbable that
res too high for biotite stability
essure, characteristic of pegma-
700° C. Even under conditions
nagma, grossular-poor garnets
ibuted to refractory remnants
thermore the microtexture of
is reacting with microcline to
us spatial association between
nilarity of garnet compositions
ommon source for the garnets.
ved from the gneisses, possibly
ie gneisses as discussed in the

et or cordierite with microcline
biotite-sillimanite breakdown
Fig. 5). The widespread occur-
ompositions suggest they have
muscovite-quartz and biotite-
iotite gneisses have not been
quartz are frequently observed
compositions (Fig. 3) would
arnet under such metamorphic
te gneisses have been subject
neisses. Independent evidence
sses comes from interbedded
gneisses contain varying pro-
the beginning of the granulite

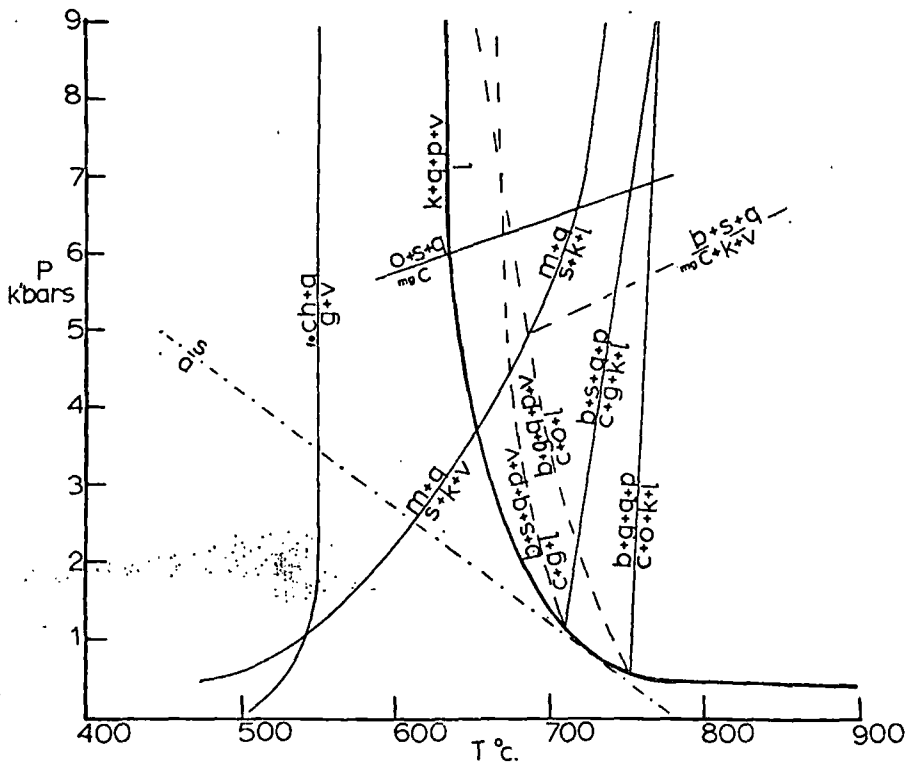

Fig. 6. Pressure/temperature fields for reactions between quartz (*q*), plagioclase (*p*), microcline (*k*), garnet (*g*), cordierite (*c*), biotite (*b*), muscovite (*m*), sillimanite (*s*), andalusite (*a*), chlorite (*ch*), orthopyroxene (*o*), liquid (*l*), vapour (*v*). Sillimanite/andalusite inversion (*13*), Fe-chlorite breakdown (*6*), Mg-cordierite + microcline reaction (*14*), Mg-cordierite breakdown (*15*), other reactions (*12*). Dashed lines imply that reactants include vapour phase

facies. Outside the garnetiferous regions, hornblende is stable in the absence of pyroxene, indicating sub-granulite conditions.

Why have potash-poor gneisses (now cordierite or garnet bearing) been subject to higher grades than potash-rich biotite gneisses? It is suggested that it is the higher metamorphic grade which has caused potash-loss and the consequent formation of garnet and/or cordierite. This may be understood by considering the position of the muscovite-quartz breakdown in P/T space. It is found to cross the wet granite solidus at about 650° C and 3.5 kb (Fig. 6). Above this point the reaction would be accompanied by melting of quartz, plagiocaase and potassium feldspar from the muscovite breakdown. Migration of this granitic liquid would leave behind a restite impoverished in both H_2O and potassium. Hence it is suggested that those gneisses containing garnet and/or cordierite are in fact restites from semi-pelitic sediment which have lost potassium and an aqueous phase to a granitic liquid. Moreover garnet and/or cordierite bearing gneisses have a significantly higher-mafics/felsics ratio which is consistent with the theory that felsic phases have been lost by anatexis in the garnetiferous regions. Lenticular lit-par-lit leucosomes are observed in the garnet gneisses,

and their conformable contacts, mafic selvedges and granitic compositions indicate an anatectic origin [10], and are therefore further evidence of some melting in the garnet gneisses.

The second reaction invoked for the garnet gneisses involves biotite and sillimanite. It is more difficult to place this reaction in P/T space for two reasons.

(i) Biotite stability is affected by P_{O_2}. For example the stability of iron-rich biotite and garnet is reduced by a high P_{O_2} [11].

(ii) The reaction is highly dependant on P_{H_2O}.

The reaction is plotted from Grant [12] and indicates the approximate positions for the reaction in the presence of vapour and also in the dry system. It is likely that the system was dry during this stage of metamorphism since the anatexis resulting from muscovite breakdown would tend to remove available vapour by solution in the melt. The vapour-absent biotite and sillimanite reaction would occur at about 100° C above the muscovite and quartz breakdown, assuming Grant's interpretation of the position of this reaction in P/T space is correct. It should be noted that although garnet + microcline assemblages are attributed to conditions above the biotite-sillimanite breakdown this does not preclude the possibility of some garnet being initially formed at lower temperatures, for example on the chlorite-quartz breakdown curve.

The maximum grade for the observed assemblages is given by the reaction:

(c) Biotite + Garnet + Plagioclase = Microcline + Cordierite + Pyroxene + Liquid.

The absence of pyroxene in biotite-garnet gneisses indicates that the grade was insufficient for this reaction to occur, and infers a maximum temperature of about 750° C, in the dry system, and 700° C in the wet system.

The upper pressure limit for the assemblages is also vapour dependent. In the wet system, the breakdown of magnesium cordierite and microcline would give an upper pressure of about 5.5 kb for temperatures up to 750° C [15]. In the dry system magnesium cordierite is stable up to about 6.5 kb at these temperatures [14]. The pressures of both these reactions would be reduced by the iron content of the cordierite, so the maximum pressure at which the cordierite assemblages equilibrated is about 6 kb.

7. Conclusions

The garnet or cordierite gneisses which also contain microcline represent regions of relatively high metamorphic grades within the gneiss belt, and have been subject to temperature between 650° C and 750° C and pressures between 3.5 and 6.0 kb. Under these conditions some anatexis has occurred, producing a granitic liquid and a garnet and/or cordierite bearing restite. The geothermal gradient implied is 40–60° C/km.

These conditions are similar to those defined by McRitchie [6] from assemblages in the Manitoba region of the belt 250 kilometres to the west; the greater

l granitic compositions indi-
ıer evidence of some melting

neisses involves biotite and
:tion in P/T space for two

ıple the stability of iron-rich

iicates the approximate posi-
and also in the dry system.
age of metamorphism since
ould tend to remove available
iotite and sillimanite reaction
ıd quartz breakdown, assum-
ıction in P/T space is correct.
ne assemblages are attributed
lown this does not preclude
med at lower temperatures,
ve.
ıges is given by the reaction:

Cordierite + Pyroxene +

isses indicates that the grade
fers a maximum temperature
the wet system.
s is also vapour dependent.
m cordierite and microcline
r temperatures up to 750° C
stable up to about 6.5 kb at
e reactions would be reduced
:imum pressure at which the

n microcline represent regions
e gneiss belt, and have been
C and pressures between 3.5
is has occurred, producing a
aring restite. The geothermal

y McRitchie [6] from assemb-
ıetres to the west; the greater

grade defined by the present study is a result of considering the possibility of vapour-absent reactions. The similarity of metamorphic grade between the Manitoba region and the Sioux Lookout region of the belt is at variance with Dwibedi's postulate [3] that metamorphic grade in the gneiss belt increases from West to East.

The distribution of garnet and cordierite over the region as a whole (Fig. 1) does not appear significant. However a more detailed study by the author of the garnet distribution in the Lac Seul areas of the Sioux Lookout region indicates that garnets are not generally found within ten kilometres of the southern margin of the gneiss belt (Harris *et al.*, in preparation). This is consistent with the theory that metamorphic grade decreases towards the margins of the gneiss belt [4], and with the author's observation that metamorphic grade falls to the greenschist facies as the soutern limit of the gneiss belt is approached. The garnetiferous regions in the Lac Seul area are identifiable on aeromagnetic linear highs (Ontario Department of Mines, aeromagnetic maps 1148G, 1139G). If the garnets do represent regions of incipient melting within the gneiss belt, then it may be possible to identify localities of anatexis from aeromagnetic studies.

Acknowledgements. I thank Dr. A.M. Goodwin for encouragement and discussion, Dr. J.J. Fawcett for critically reading the manuscript and the Canadian Department of Energy, Mines and Resources for research grant No. 1135-D13-4-22/74 which supported this study. I am indebted to Dr. R. Skinner and the Geological Survey of Canada for collecting some of the rock samples, to Dr. P. Palonen and the Ontario Department of Mines at Sioux Lookout for assistance in field work, to Dr. O.P. Malik for some of the microprobe analyses, and to Mr. J. Escobar for the X−R−F analyses.

References

1. Hall, D.H., Hajnal, Z.: Crustal structure of North-West Ontario. Can. J. Earth Sci. 6, 81–99 (1969)
2. Skinner, R.: Geology of Sioux Lookout map-area, Ontario. Geol. Surv. Canada. Paper 68–45 (1969)
3. Dwibedi, K.: Petrology of the English River gneissic belt, North-West Ontario and South-East Manitoba. Ph. D. Dissertation. University of Manitoba (1967)
4. Jones, R.D.: Metamorphism of the English River gneissic belt along the Red Lake road. M.Sc. Dissertation, University of Manitoba (1973)
5. Sage, R.P., Breakes, F.W., Stott, G.M., McWilliams, G.M., Bowen, R.P.: Operation Ignace-Armstrong, Caribou Lake-Pashkakogan Lake sheet. Ontario Department of Mines, Prelim. Map P962 (1973)
6. McRitchie, W.D., Weber, W.: Metamorphism and deformation in the Manigotagan gneissic belt, South-East Manitoba. Manitoba Mines Branch, Publication 71-1, 235–284 (1971)
7. Chinner, G.A.: Garnet-cordierite parageneses. Yearbook, Carnegie Inst. Washington 58, 112–115 (1959)
8. Hensen, B.J.: Cordierite-garnet equilibrium as a function of pressure-temperature and Fe-Mg ratio. Yearbook, Carnegie Inst. Washington 71, 418–421 (1972)
9. Hensen, B.J., Green, D.H.: Experimental study of the stability of cordierite and garnet in pelitic compositions at high pressures and temperatures. Contrib. Mineral. Petrol. 38, 151–167 (1973)

10. Harris, N.B.W.: Some migmatite types and their origins, from the Barousse Massif, Central Pyrenees. Geol. Mag. **111**, 319–328 (1974)
11. Chinner, G.A.: Pelitic gneisses with varying ferrous/ferric ratios from Glen Clova, Angus, Scotland. J. Petrol. **1**, 178–217 (1960)
12. Grant, J.A.: Phase equilibria in high grade metamorphism and partial melting in pelitic rocks. Am. J. Sci. **273**, 289–317 (1973)
13. Holdaway, M.J.: Stability of andalusite and the aluminium silicate phase diagram. Am. J. Sci. **271**, 97–131 (1971)
14. Newton, R.C., Charlu, T.V., Kleppa, O.J.: A calorimetric investigation of the stability of anhydrous Mg-cordierite with application to granulite facies metamorphism. Contrib. Mineral. Petrol. **44**, 295–311 (1974)
15. Schreyer, W., Siefert, F.: Compatibility relations of the aluminium silicates in the systems MgO-Al_2O_3-SiO_2-H_2O and K_2O-MgO-Al_2O_3-SiO_2-H_2O at high pressure. Am. J. Sci. **267A**, 407–443 (1969)

Received April 16, 1975 / Accepted October 15, 1975

Stable isotope study of coexisting metamorphic minerals from the Esplanade Range, British Columbia

JAMES R. O'NEIL *U.S. Geological Survey, 345 Middlefield Road, Menlo Park, California 94025*
EDWARD D. GHENT *Department of Geology, University of Calgary, Calgary, Alberta T2N 1N4 Canada*

ABSTRACT

Hydrogen, carbon, and oxygen isotope analyses have been made of coexisting minerals from regionally metamorphosed rocks of the Esplanade Range, British Columbia. Regularities in oxygen and hydrogen isotope compositions imply attainment of isotopic equilibrium. Temperatures, determined on the basis of oxygen isotope fractionations between quartz and ilmenite (magnetite), range from 460°C (biotite-chloritoid zone) to 540°C (staurolite-biotite zone) and are in good agreement with temperatures estimated from comparison of experimental phase equilibria with the mineral assemblages. The isotope data are comparable to results obtained by other workers studying Barrovian-type metamorphism in different areas.

The relatively narrow ranges of δO^{18} values for quartz and δD values of biotite and hornblende from a wide range of protoliths suggest either that there was good oxygen and hydrogen isotope communication between these rocks or that they exchanged with a large reservoir having fixed isotope ratios. A single orthoamphibolite, however, has oxygen and hydrogen isotope compositions that show that it was not in communication with the other rocks.

The carbonates in the Esplanade Range are unusually enriched in C^{13} relative to similar metamorphic rocks in other localities. Values of δC^{13} become more positive with increasing grade and range from −2.5 to +9.8. *Key words: metamorphic petrology, stable isotopes.*

INTRODUCTION

Oxygen and hydrogen isotope analyses have been made of separates of coexisting metamorphic minerals from seven carefully selected rocks from a single metamorphic area, the Esplanade Range in southeastern British Columbia (Fig. 1). Oxygen and carbon isotope analyses were made of an additional six rocks that contained carbonate minerals.

The Esplanade Range is one of several metamorphic highs along the Omineca crystalline belt of the eastern Canadian Cordillera (Wheeler, 1966). The metamorphism occurred in late Mesozoic time as indicated by radiometric ages. The area is underlain by Proterozoic metasedimentary rocks and minor metabasalt units that range in metamorphic grade from the biotite-chloritoid zone to the staurolite-biotite zone (Barrovian-type facies series of Hietanen, 1967). Petrologic, geochemical, and structural studies on these rocks provide a framework within which the results of isotope analyses can be interpreted (Ghent and others, 1970; De Vries and others, 1971; Jones and Ghent, 1971; Ghent and De Vries, 1972; Ghent and E. H. McKee, in prep.; Ghent, in prep.).

Detailed field relationships, locations, petrography, and mineral assemblages for the samples employed in the present study are given in Ghent and De Vries (1972) and Ghent (unpub. data). A brief summary of the mineral assemblages and references to electron-microprobe analyses are given in Appendix Table 1. Previous estimates of P_s (load pressure), T (temperature), and fluid composition attending metamorphism were made from experimental and computed phase equilibria (Ghent and others, 1970; Ghent and De Vries, 1972; Ghent, in prep.).

ANALYTICAL TECHNIQUES

Mineral separations were made by standard techniques using magnetic separation and heavy liquids. In several cases, the final separates were hand-picked under the microscope. Quartz separates were treated with HF to remove minor impurities. Oxygen was liberated from silicate minerals by reaction with BrF_5 at 550°C (Clayton and Mayeda, 1963) and then converted to CO_2 and analyzed on a mass spectrometer. CO_2 for isotopic analysis was liberated from carbonate samples by reaction with 100 percent H_3PO_4 (McCrea, 1950). For hydrogen isotope analyses, the mineral separates were heated in a vacuum at 150°C for at least 2 hr to remove any extraneous water and then decomposed by induction heating. Liberated water was then passed over uranium metal at 800°C to produce molecular hydrogen for mass spectrometric analysis (Bigeleisen and others, 1952).

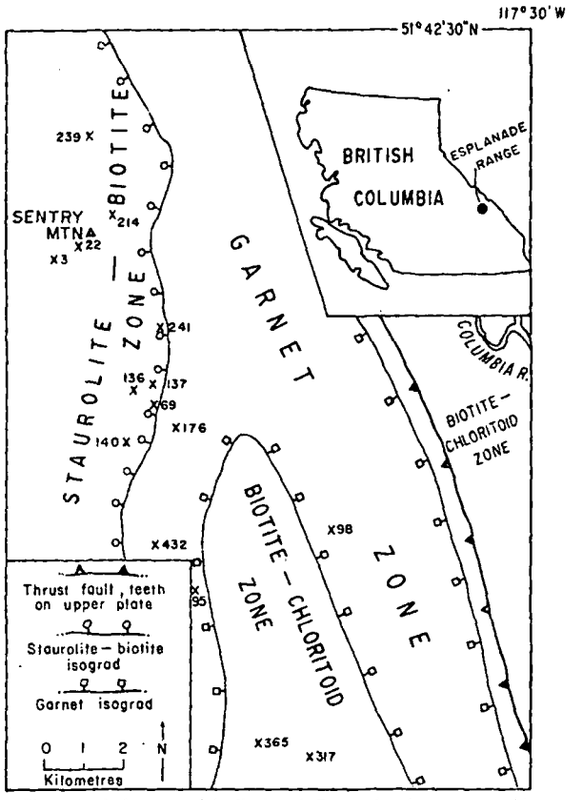

Figure 1. Index map of the Esplanade Range showing metamorphic zonation and sample locations.

Geological Society of America Bulletin, v. 86, p. 1708–1712, 3 figs., December 1975, Doc. no. 51208.

MINERAL DEVELOPMENTS AND POTENTIAL OF SASKATCHEWAN METAVOLCANIC BELTS

by

A. J. Gracie

Prospectors and Developers Convention, March 1972.

Toronto

SUMMARY

This paper discusses the nature and distribution of Saskatchewan's metavolcanic belts. A historical outline of mineral developments and exploration activity is presented with a description of present day exploration activity and the mining potential of the metavolcanic belts. An encouraging recent case history from a well prospected area is also described.

NATURE AND DISTRIBUTION OF THE METAVOLCANIC BELTS

Using principally the Saskatchewan Department of Mineral Resources geological maps for the Precambrian area, it is possible to divide the metavolcanic belts into two groups, on the basis of the percentage of metavolcanic rocks they contain. Group (A) consists of those parts of the shield containing more than 50 per cent metavolcanic rocks. Group (B) comprises those areas with less than 50 per cent. These are approximate divisions, as are shown in Figure 1.

Metavolcanic rocks are the metamorphosed derivatives of rhyolites, dacites, andesites and basalts together with pyroclastic rocks such as tuffs and agglomerates. Metamorphosed intrusive rocks such as granites, diorites and gabbros are common to both metasedimentary and metavolcanic belts. Metasedimentary rocks make up the remainder of Group (A) whereas in Group (B), metasedimentary rocks predominate.

The three traditional "greenstone" belts in the province's Precambrian area belong to Group (A). These are the Flin Flon-Amisk Lake Belt, the La Ronge-Reindeer Belt and the Stony Rapids Belt (Figure 1). In the Flin Flon area the belt has been divided into a predominantly volcanic Amisk Group which is overlain in part by the predominantly metasedimentary Missi Group.

A much greater area of the shield may be assigned to Group (B) (Figure 1). Metavolcanic rocks occur discontinuously from Flin Flon to La Ronge along the southern edge of the shield. The Stony Rapids metasedimentary-metavolcanic belt, which also contains extensive and economically significant norite bodies, may extend under the Athabasca Sandstone and join the Virgin River Belt. In the latter, however, rocks of definite metavolcanic origin are not common. Within the Lynn Lake-La Ronge-Flin Flon triangle the total area underlain by assemblages containing metavolcanic rocks is greater than the total area of the traditional 'greenstone' belts.

HISTORICAL OUTLINE: PRIOR TO 1964 (Figures 1 and 2).

The earliest discovery in any of the Saskatchewan metavolcanic belts, which led directly to a producing mine, was that by Tom Creighton and the Mosher and Dion brothers in 1914. Opened in 1930, the Hudson Bay Mining and Smelting Flin Flon Mine (Cu, Zn, Au, Ag) is still the main centre of production for the area under consideration.

GOLD. Gold was the main exploration target until approximately 1950. This resulted in a large number of quartz-vein gold showings being found in all parts of the metavolcanic belts, especially in the traditional greenstone areas. Quartz-vein gold occurrences may carry free gold, arsenopyrite, pyrite or ankerite. The small Prince Albert, New Cor and Henning Maloney Mines were brought into production for short intervals in the pre-war years in the Amisk Lake area. At the Studer Mines Sulphide Lake property near La Ronge, reserves were estimated, in 1961, at 18,000 tons, grading 0.42 ounces Au per ton. In the Fond du Lac area, gold was discovered around Thompson Island and Sucker Bay. On the Ela claims in this region a prospect shaft was sunk in the 1930's

by Goldfields Uranium. During the 1940's Consolidated Mining and Smelting closely examined five gold properties in the La Ronge-Reindeer Belt but none of these was brought into production.

URANIUM. Pitchblende occurrences are not preferentially related to the metavolcanic belts, although the favourable "linear belts" distinguished by Beck (1969) include metasedimentary and metavolcanic rocks.

As far as the metavolcanic belts discussed in this paper are concerned, showings were first discovered at Black Lake in 1948 and underground development took place at the Canadian Nisto Mines property on the Black Lake fault (Figure 1). About 500 tons of high-grade ore were mined and shipped to Uranium City.

The only other uranium showings associated with the metasedimentary and metavolcanic belts discussed in this paper are radioactive pegmatites. Numerous uraninite-bearing pegmatites were outlined in the Charlebois Lake area on the eastern flank of the Stony Rapids Belt and in the Drope Lake-Nunn Lake area near Lac La Ronge. The Lac La Ronge pegmatites were extensively explored in the 1950's by airborne surveys, diamond drilling, and underground development. A small pilot mill was started but grades proved too low for economic development of the deposits.

COPPER, ZINC. With regard to base metal development, I have already mentioned that the Flin Flon Mine was the first producer. Sulphide deposits in the Flin Flon area have been divided by Byers, Kirkland and Pearson (1965) into two groups. The first is a barren group composed of disseminated to massive pyrite and pyrrhotite with little or no base metal sulphides. The second is an ore-bearing group composed of bodies of disseminated to massive pyrite and

pyrrhotite containing economic quantities of chalcopyrite and/or sphalerite. This classification is generally useful in the search for new base metal bearing orebodies in all parts of Saskatchewan's metavolcanic belts.

In the case of many "barren" sulphide deposits tested to date, their barren nature has not been fully appreciated until after a costly drilling and sampling program has been carried out. Clearly a mineralogical or geochemical method of distinguishing between the two groups would be of great value and is suggested as a worthwhile and practical research subject.

J. Brain's FLASH claims first staked in 1949 were developed into two orebodies. The Birch Lake Mine yielded 300,000 tons of ore averaging 6.2% Cu, during 1957-1960. The Flexar Mine was put into production in 1970 and is still in operation. Nearby, the Coronation Mine was discovered by Hudson Bay Exploration and Development Co. Ltd. in 1952 by a ground electromagnetic survey. Diamond drilling indicated 545,000 tons of ore to a depth of 600' grading 0.055 oz/ton Au, 0.23 oz/ton Ag, 5.37% Cu and 0.5% Zn. The mine was made the subject of comprehensive geological and geochemical studies (Byers 1968).

In 1914 in the La Ronge area, the Hall brothers discovered what is now the Anglo-Rouyn Mine. The showings were trenched and drilled in 1929 by Consolidated Mining and Smelting. In 1956 a shaft was sunk by Anglo-Rouyn Mines but work was halted. In 1957 reserves were estimated at 2,445,000 tons grading 1.95% Cu. The mine was not finally put into production until 1965. Records concerning a shaft sunk on the Pitching Lake copper property 50 miles northeast, by Glenn Uranium, on a large scale northeast plunging syncline have been dispersed and the on-site drill records were destroyed by a forest fire. Other interesting copper showings are found on the Tabbernor Fault (Figure 1).

The 'MacKenzie' Cu-Zn orebody at Brabant Lake was discovered by an Indian trapper in 1956 and development of this property has indicated 4,330,000 tons, grading 0.64% Cu and 4.43% Zn.

NICKEL. Considerable exploration has been conducted in the La Ronge-Reindeer and Stony Rapids Belts for nickel and copper-nickel deposits associated with small basic intrusives. Work on Studer Mines Reef Lake Cu-Ni find is an example of this. Work on nickel mineralization associated with a large scale norite intrusive began at Axis Lake in the Stony Rapids Belt in 1929. This early work gave interesting values of Ni, Cu and Co. Numerous nickel showings, generally associated with small scale norite bodies, occur in the Reeve-Tantato-Father Lakes area, north of the main norite body. A pyroxenite plug with Ni-Cu values at its north contact with granite was found at Nemeiben Lake near La Ronge and first drilled by Consolidated Mining and Smelting in 1945. The area was also covered by a magnetometer survey at that time.

THE PROVINCIAL GOVERNMENT. The Saskatchewan Department of Mineral Resources ran a prospectors school and prospectors assistance plan from 1948 to 1964. Resident Geologists were first maintained at Uranium City and Prince Albert. The Prince Albert Office was moved to La Ronge permanently in 1965 with the completion of the Precambrian Geological Laboratory. Mining records are maintained at Uranium City and La Ronge. An average of six geological field parties have been sent out each year since 1948 to map 15' quadrangles in the Precambrian area for publication at the scale of 1 inch to 1 mile. Aeromagnetic coverage at the scale of 1 inch to 1 mile is now complete for the whole of the Precambrian area. Selected areas were covered by magnetic or magnetic and electromagnetic surveys on a scale of 1 inch to ½ mile in 1957 and 1958.

CURRENT ACTIVITY (1964-1972) (Figures 1-3).

An important aspect of the present situation in mineral exploration is a direct result of a provincial Precambrian Incentive Program. This provided 50 per cent government participation on approved programs up to a fixed amount on a given property. It was run between 1966 and 1969. At first the program was applied to groups of claims, claim blocks and a few permits. This resulted in an intensification of exploration work in the metavolcanic areas previously outlined. Selco flew a large area in the Flin Flon-La Ronge area partially covered by Palaeozoic limestones. Favourable anomalies were detailed on the ground and were drilled. The Scurry-Rainbow Gochager Lake nickel discovery in 1967-1968 was made under the Precambrian Incentive Program and although it has so far proved uneconomic it did attract considerable claim block staking within the La Ronge-Reindeer Belt. This triggered a rapid increase in the number of airborne and ground follow-up programs. Airborne programs were also run by Canico and Sherritt Gordon at this time. Canico have renewed their efforts on the belt again in the past few years.

The staking activity resulting from the Scurry-Rainbow find in the La Ronge area acted as a prelude for the property rush generated by the Gulf Minerals Rabbit Lake discovery. After the Gulf Minerals discovery, land was taken out in Mineral Prospecting Permits. In general these were not issued in areas of heavy mineral claim and claim block staking. Figure 2 shows the permits issued in the Lynn Lake-La Ronge-Flin Flon triangle during the period 1969-1972. Most of these permits lie in areas where metavolcanic rocks do not form a high percentage of the shield and they appear to be principally related to the Tabbernor Lake Fault. One permit has been taken out in an area of Palaeozoic cover just south of Hanson Lake. Parts of the Precambrian area

covered by these permits were previously flown with magnetic and electromagnetic equipment in 1957 by Mansa Exploration. All of the Stony Rapids metavolcanic and metasedimentary belt was covered with permits until very recently.

In many instances, permits during the period 1969-1972 were flown with electromagnetic, magnetic, and four channel radiometric spectrometer equipment. Anomalies were ground-checked on cut grids by magnetic, electromagnetic and scintillometer surveys. Favourable anomalies were drilled. Geochemical surveys of overburden, soil, and stream sediments were made on a few permits. All stages of exploration mentioned were not carried out on every permit, however. The area around the old Nunn Lake-Lac La Ronge uraninite showing was re-examined using a 4 channel spectrometer. Emphasis on prospecting for uranium minerals was marked in the Stony Rapids Belt.

To date these various programs have not resulted in any new mines in the area under consideration, but much of the work has been on a rather broad scale.

During the period 1965-1972, two base metal mines were closed and one has depleted ore reserves. These are, Western Nuclear Mines at Hanson Lake, a Cu-Zn producer which was active from July, 1967 to July, 1969 and Hudson Bay's Coronation copper mine which operated from 1960 to 1965. Reserves at Anglo-Rouyn will be exhausted by October, 1972. Promising copper properties of Uranium Valley Mines Ltd., at Nemeiben Lake and Strauss Exploration at Mokoman Lake have not yet been developed. Uranium Valley Mines has indicated reserves of 1.5 million tons grading 1.56% Cu.

Government effort in the north is directed to geological mapping, recording services and the geological laboratory at La Ronge, built in 1965. The basic purpose of the laboratory is the collection and dissemination of geological information. Facilities include assessment files for the La Ronge and Reindeer Districts, a technical library, a core examination laboratory

and core storage facilities with core selected from interesting mineralized zones and stratigraphic sections. The laboratory is also the base for equipment and supply of the D.M.R. field parties. A prospectors' school and a new prospectors' assistance plan is to be run starting in 1972.

POTENTIAL OF THE METAVOLCANIC BELTS

In assessing the potential of the metavolcanic rocks, it is relevant to point out that on a regional basis the La Ronge-Reindeer belt is continuous with that metavolcanic belt which in Manitoba contains Sherritt Gordon's Lynn Lake (Ni-Cu-Co) mine, its Fox Lake (Cu-Zn) mine and the new Ruttan Lake (Cu-Zn) deposit. The Lynn Lake area also contains the Royal Agassiz Mines Ltd. gold property. The Amisk group of rocks is continuous with similar rocks in Manitoba which extend to the Snow Lake-Wekusko Lake group of mines. Apart from volcanic rocks, extensive norite exists in the Stony Rapids Belt.

Transportation is an important factor when assessing the potential of regions such as this and it is significant that road access to the southern greenstone belts in Saskatchewan is much improved. Road connections now exist between La Ronge, Reindeer Lake and Flin Flon and access is available to Pelican Narrows.

The potential of the metavolcanic belts is being assessed in a number of ways.

Firstly "grass-roots" prospecting is being encouraged. The Provincial Government intends to reactivate a prospectors' school and a prospectors' assistance plan. Many of the people attending the school will be of Indian and Metis ancestry, from remote communities in Northern Saskatchewan.

Large scale geochemical prospecting combined with airborne geophysical surveys on a permit area (36 to 300 square miles) represents a second general method. This is large budget prospecting and is preferably undertaken in an area which is not heavily staked in smaller dispositions. Such surveys have been carried out around the south end of Reindeer Lake and in the southwest section of the La Ronge-Reindeer Belt.

A third method is to attempt to add to existing tonnages of ore on known properties by property re-examination and further drilling. Properties favourable to such an examination would perhaps be the Axis Lake, Nemeiben Lake, Clam Lake and Brownell Lake Cu-Ni deposits. The Brabant Lake Cu-Zn and the Dead Lake Pb-Zn prospect might be other targets. National Nickel have already attempted a program of this kind on the Nemeiben Lake Ni-Cu orebody.

In the fourth method, in essence an extension of method (1), the prospector who has located a discovery by his own efforts options it to a larger and better financed company. A recent discovery by Mr. J. Brain in the Amisk Lake area, the oldest and best explored section of the province's metavolcanic belts, is an example of this. I am indebted for my information on the property to Mr. L. E. W. Hogg, of Northland Exploration Ltd., Regina and it is presented with his kind permission. The property referred to is basically ML 5055 and ML 5065 held by Mr. Joe Brain on the west side of Missi Island in the north half of Amisk Lake (Figure 2). The discovery area has been under disposition by Mr. Brain for the last 20 years, during which time several mining companies both large and small have held options on part or all of the ground. No significant results were obtained. This had involved five previous geophysical surveys. These were a vertical loop in 1954, magnetometer and

frequency domain induced polarization surveys in 1962. Crone and Ronka EM surveys were also conducted in 1971 by Northland Explorations.

In September, 1971 Joe Brain drilled four holes on his property for assessment work purposes. Three holes were drilled to pass beneath a series of trenches which contain low grade chalcopyrite-molybdenite mineralization. The third hole drilled under the trenches encountered massive pyrite-chalcopyrite mineralization across 25', assays of which average 2.5% Cu, 0.108% Mo and 0.10% oz/ton of Ag. The prospector optioned the northern and southern halves of his property to different companies: to Hudson Bay Mining and Smelting in the north and Flin Flon Mines in the south. In October, 1971 a sixth geophysical survey was conducted by R. G. Agarwal, consulting geophysicist in association with Flin Flon Mines Ltd. This was a Time-Domain induced polarization survey. This survey located the massive sulphides already discovered in the hole drilled by J. Brain. The position of the drill holes with respect to the I.P. anomalies is shown in Figure 3. It is believed that the failure of the geophysical instruments except for the Time-Domain I.P. survey operating at maximum power is due to the highly siliceous country rocks which produce high resistivities and acted as insulators to the mineralized zones. The example is intended to illustrate that new and significant discoveries are not impossible, even in what are generally considered classical and well worked metavolcanic areas.

REFERENCES

Beck, L. S. 1959: Mineral Occurrences in the Precambrian of Northern Saskatchewan; Sask. Dept. Mineral Resources Report 36.

Beck, L. S. 1969: Uranium Deposits of the Athabasca Region, Saskatchewan; Sask. Dept. Mineral Resources Report 126.

Byers, A. R., Kirkland, S. J. T. and Pearson, W. J. 1965: Geology and Mineral Deposits of the Flin Flon Area: Sask. Dept. Mineral Resources Report 62.

Byers, A. R. (editor): Coronation Mine Symposium, G.S.C. paper 68-5.

Fuzesy, M. A.: Index to Assessment Work in the La Ronge Mining District, 1970; Sask. Dept. Mineral Resources. Unnumbered report.

Fuzesy, M. A.: Index to Assessment Work in the Reindeer Mining District of Saskatchewan, 1971; Sask. Dept. Mineral Resources. Unnumbered report.

Key to Locations, Figure 1

MINES

Base Metal:		1)	Hudson Bay - Flin Flon
		2)	Hudson Bay - Flexar
		3)	Anglo Rouyn - Waden Bay
	(closed)	4)	Hudson Bay - Birch Lake
		5)	Hudson Bay - Coronation
		6)	Western Nuclear - Hanson Lake
Nickel:	(closed)	7)	Rottenstone Mines - Rottenstone Lake
Uranium:		8)	Eldorado Nuclear - Ace-Fay
		9)	Eldorado Nuclear - Hab
	(under construction)	10)	Gulf Minerals - Rabbit Lake
	(closed)	11)	Gunnar, many others - Uranium city area

PROSPECTS

Base Metal:	12)	Canadian Javelin - Brabant Lake
	13)	Uranium Valley - Nemeiben Lake
	14)	Joe Brain - Missi Island
	15)	Strauss Exploration - Mokoman Lake
Nickel, Copper-Nickel:	16)	National Nickel - Nemeiben Lake
	17)	Scurry Rainbow - Forbes Lake
	18)	Reef Lake
	19)	Canadian Nickel - Brownell Lake
	20)	Reeve - Tanato - Father Lakes
	21)	Inexco - Axis Lake
Uranium:	22)	Drope Lake
	23)	Charlebois Lake
	24)	Haymac Mines - Nisto Lake
Gold:	25)	Sucker Bay
	26)	Studer Mines - Sulphide Lake
	27)	Waddy Lake
	28)	Henning Maloney Shaft
	29)	Prince Albert Mine

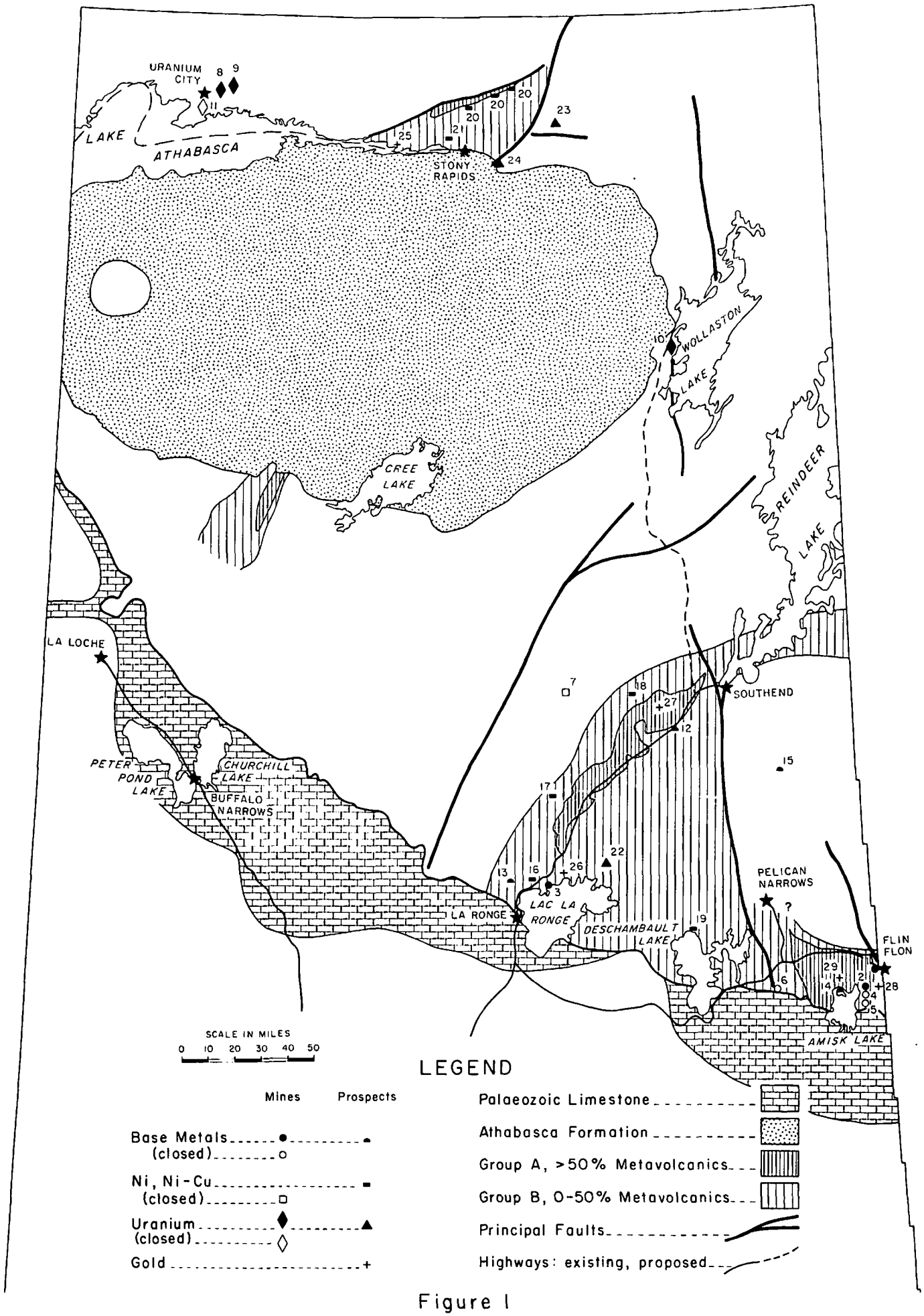

Figure 1

LOCATION OF METAVOLCANIC BELTS, MINES AND PROSPECTS

NORTHERN SASKATCHEWAN

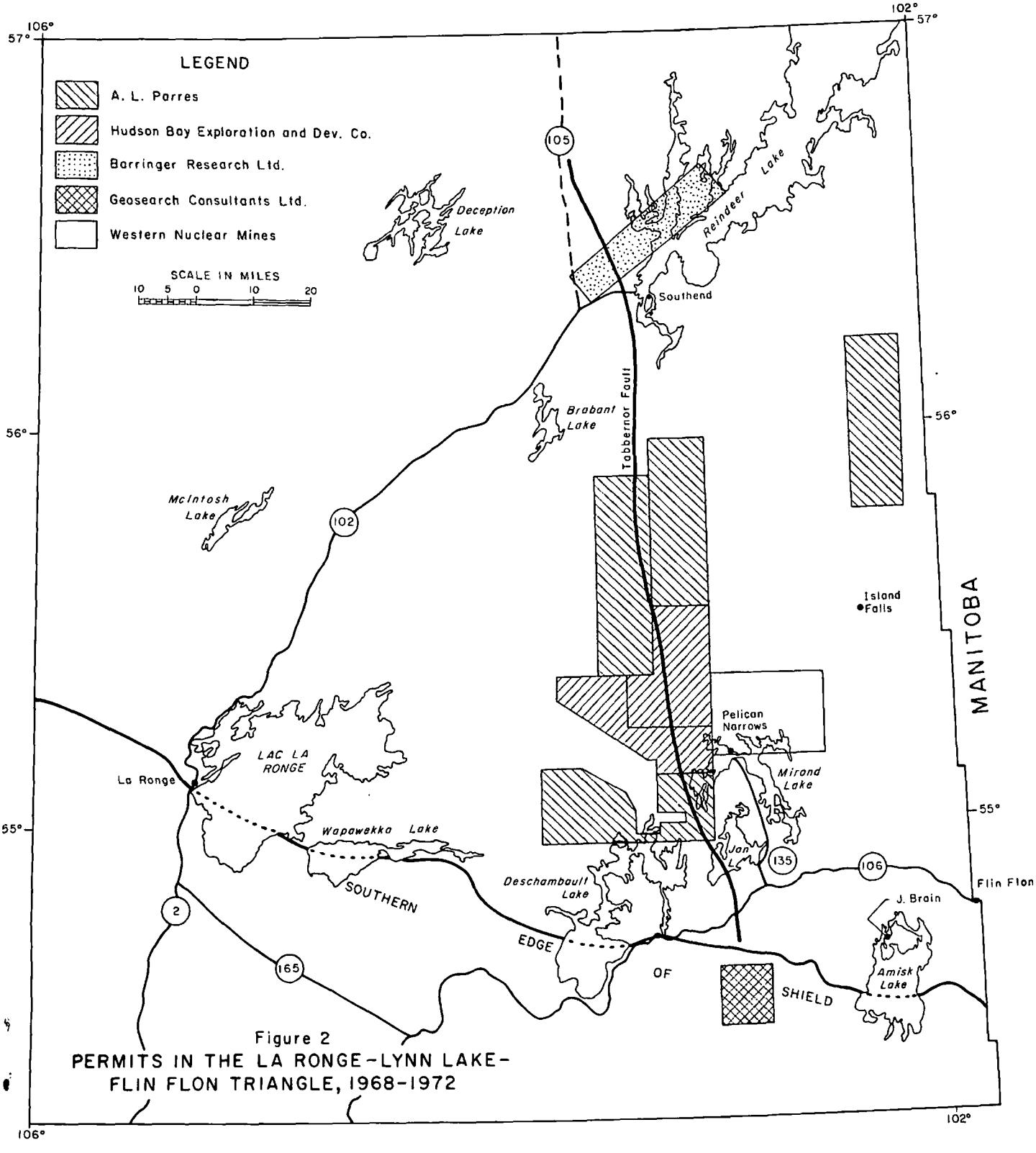

Figure 2
PERMITS IN THE LA RONGE-LYNN LAKE-
FLIN FLON TRIANGLE, 1968-1972

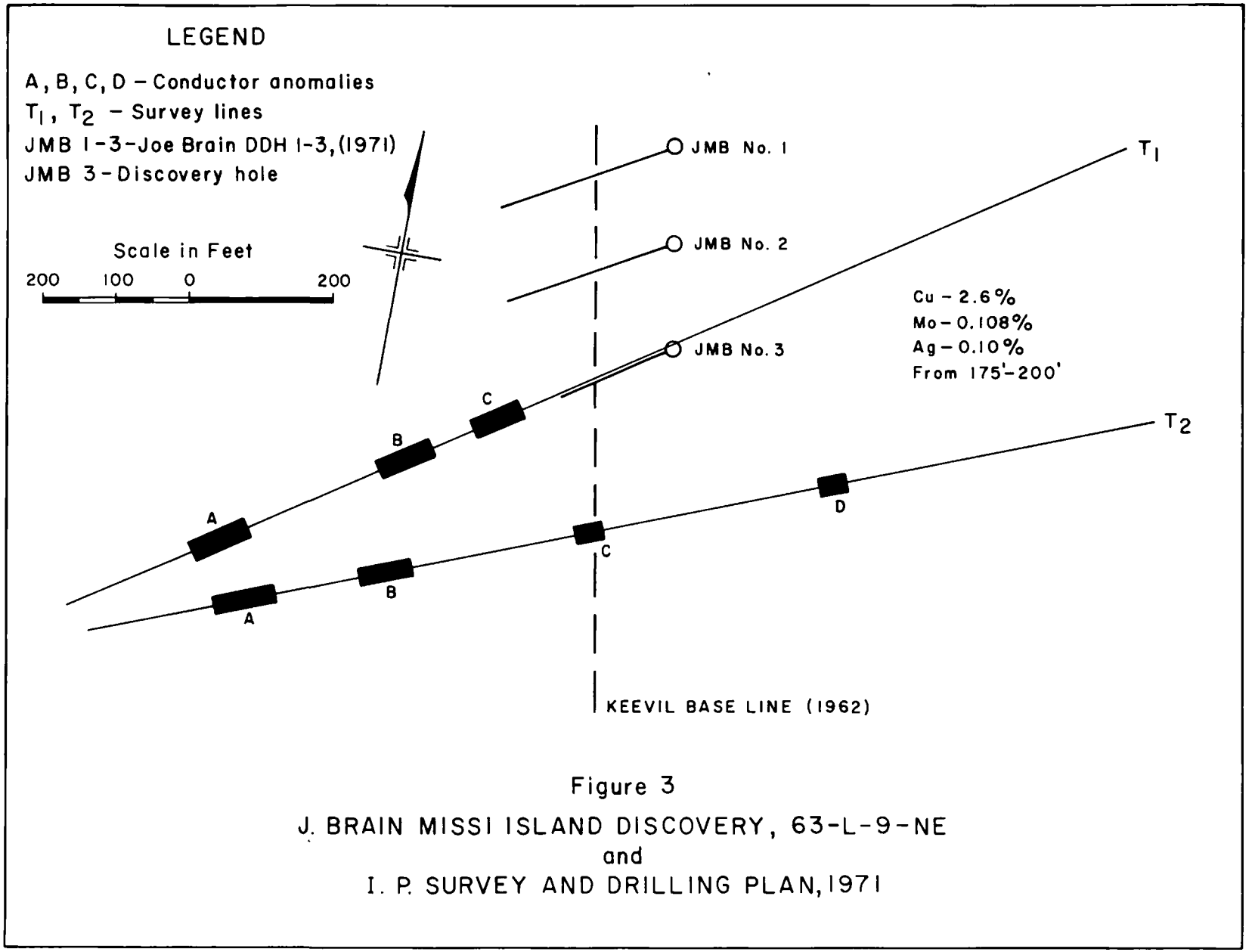

Figure 3

J. BRAIN MISSI ISLAND DISCOVERY, 63-L-9-NE
and
I. P. SURVEY AND DRILLING PLAN, 1971

GEOTHERMAL MEASUREMENTS IN NORTHERN CANADA

ALAN JUDGE[1]

ABSTRACT

Information on underground temperatures and temperature gradients is particularly important in northern Canada from a practical point of view because of the presence of permafrost and the problems created thereby. Permafrost thicknesses and temperatures are important in many phases of the petroleum industry, ranging from geophysical interpretations to the eventual design of a production well. In the mining industry it is important in slope stability of open pits, in explosive charge design, in underground ventilation design and drift and stope stability. Determination of the thermal properties of subsurface rocks penetrated enables calculation of the terrestrial heat flow which can be used to make permafrost thickness predictions and is important in an understanding of the geological processes which are acting to create the lithosphere of northern Canada.

RESUME

Les problèmes causés par le pergélisol rendent particulièrement importantes les informations sur la température et sur les gradients de température du sous-sol du Nord canadien. L'industrie pétrolière doit tenir compte de la température et de l'épaisseur du pergélisol, à partir de l'interprétation géophysique jusqu'à la conception des puits de production. L'industrie minière doit étudier l'influence de ces deux facteurs sur la stabilité des pentes des exploitations à ciel ouvert, sur les types d'explosif à utiliser, sur la ventilation souterraine et sur la stabilité des galeries et des chantiers d'abatage. La connaissance des propriétés thermiques des roches du sous-sol permet de calculer leur flux thermique et ainsi, de prédire l'épaisseur du pergélisol. Elle permet également une plus grand compréhension des processus géologiques impliqués dans la formation de la lithosphère du Nord canadien.

[1]Department of Energy, Mines and Resources, Ottawa.

GEOTHERMAL MEASUREMENTS IN NORTHERN CANADA

Geothermal Measurements in the Arctic Islands

Geothermal research in northern Canada was hampered for many years by the great expense involved in operating a drill-rig, and the lack of interest in the nature of the underground thermal regime other than for pure science. In the early fifties Bremner (1955) from the Dominion Observatory carried out a drilling programme at Resolute Bay on Cornwallis Island and subsequently the holes were instrumented with multi-sensor cables. Misener (1955) was able to determine a heat flow value for that location and the resulting high value caused Lachenbruch (1957) to consider theoretically the effect of a shoreline on the underground thermal regime. However, the difficulties encountered in drilling through permafrost and the expense involved discouraged further work. As a result, Brown's (1967) map of permafrost distribution in Canada lists thicknesses for only two sites in the Arctic Islands; the second one being the Dome Petroleum wildcat well at Winter Harbour which was preserved and instrumented by the United States Geological Survey in 1962.

The discovery of the Mould Bay geomagnetic anomaly and its suggested high temperature origin (Whitham 1963) led Law et al (1965) to design and construct a thermal gradiometer to be used in the bottom sediments of the shallow straits and channels around the Mould Bay area. In 1968 this programme was expanded to include several lakes and fiords on Ellesmere Island in order to investigate a second geomagnetic anomaly. Plans were also made to investigate systematically each of the deeper water areas of the archipelago as a means of making reconnaissance studies of the variation of terrestrial heat flow. Also involved were long-term studies of the variation of bottom-water temperatures. The latter is the upper boundary condition for the heat flow and its possible instability is of prime concern. In terms of the thermal regime of the permafrost on land such heat flow measurements could provide little more than background information for permafrost thickness prediction.

A regional study of the sub-surface thermal regime in northern Canada has become feasible in the past few years because of greatly increased drilling activity associated with the current search for oil and gas and gradually increasing mining activity.

With substantial assistance from industry in the preservation of boreholes and logistic support from the Polar Continental Shelf Project, the Earth Physics Branch of the Department of Energy, Mines and Resources has been making temperature measurements to depths of 300 metres or more at 30 sites in northern Canada, 17 of them in the Arctic Islands. These sites are shown in Figure 1. Shallow measurements in holes of 60

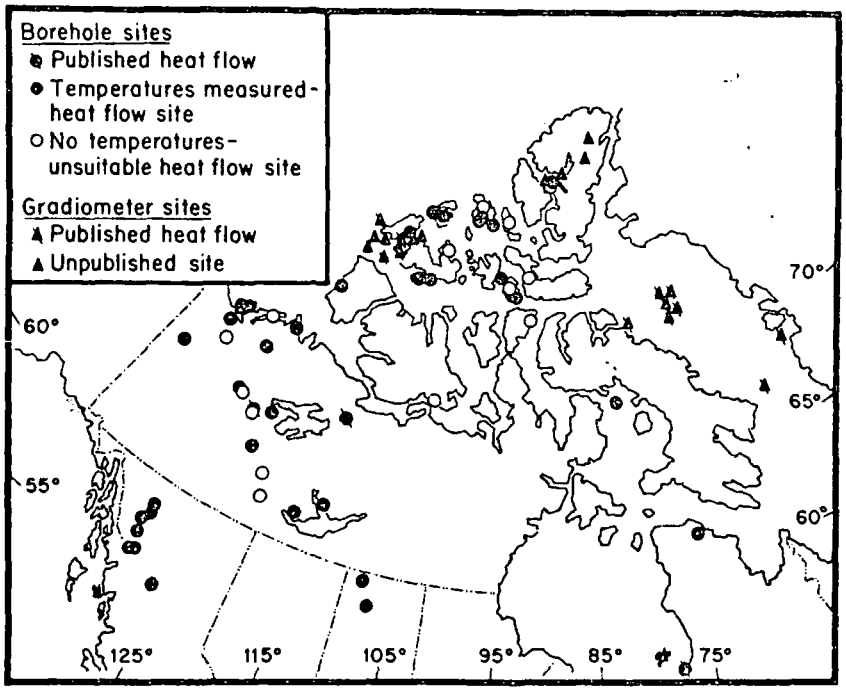

Fig. 1. Heat flow sites in northern Canada.

metres or less have been made in cooperation with the Geological Survey of Canada along the Mackenzie Valley. In Figure 1 open circles represent either sites at which temperature determinations have not yet been made or sites not suitable for heat flow determination although temperature measurements have been made.

Preservation of Boreholes

There are many problems involved in obtaining temperature measurements in northern boreholes. Perhaps the most difficult one to overcome is that of preserving an open hole, or instrumenting it with a multisensor cable, and yet fulfilling the abandonment requirements of the regulatory agencies. This is necessary because of the length of time that a borehole takes to return to equilibrium. Other problems arise from the cost and difficulty of access to many of the sites. The simplest way to keep open a borehole is to abandon it below the base of the surface casing and to displace the drilling mud within the surface casing by diesel fuel. There are however several disadvantages to this method. Diesel fuel is very expensive to fly into remote locations. The bore fluid may convect in large diameter boreholes (24 cm) particularly in formations with a high

geothermal gradient such as in the Sverdrup Basin and MacKenzie Valley. Unarmoured multisensor cables installed directly in the drilling mud in cased boreholes generally do not survive freeze-back. Probably the best solution, although expensive, would appear to be that of strapping multisensor cables to the surface casing during its installation. Multisensor cables installed directly into small diameter, uncased mining exploration holes appear to survive the freezing back process. More detailed aspects of the methods of preserving boreholes are described in Judge (1973b).

Measurement of Temperature

All borehole temperature measurements are made using either thermistors built in to multithermistor cables or a single thermistor on a portable cable. The portable cable system used in open holes has a probe containing a single thermistor which is lowered in steps to obtain a series of temperature readings down the hole. The multithermistor cable is usually lowered into the borehole on completion of the drilling and is left as a permanent or semipermanent installation. Advantages and disadvantages exist with either method, and these have been discussed else-

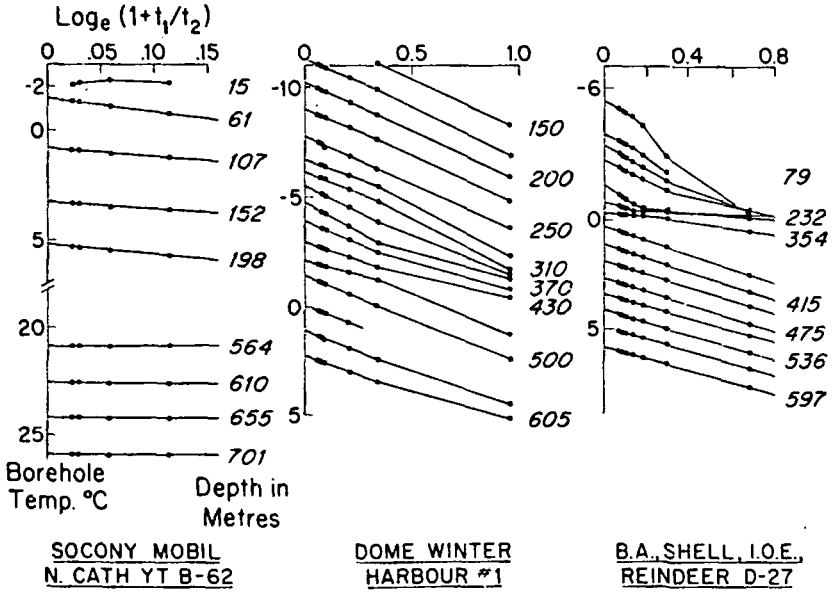

Fig. 2. Borehole return to equilibrium — three northern boreholes.

where (Judge 1973b, c). Thermistor resistance, with either system, is read using a portable Wheatstone bridge constructed to have a precision of 0.01°C over a wide range of ambient temperatures. It is capable of discriminating temperature differences of 0.003°C in a single thermistor.

Return to Equilibrium of a Borehole

Several authors have discussed the temperature disturbance caused by the drilling process to the rocks surrounding a borehole. The length of time necessary to reestablish equilibrium conditions is dependant on the length of a time of drilling, the volume of drilling fluid circulated, the difference between drilling fluid and undisturbed formation temperatures and the fluid loss rate due to formation permeability (Jaeger 1961; Cheremensky 1962). The return of sections of the borehole within the permafrost may be prolonged over that for a borehole in southern Canada if, during drilling, the formations surrounding the hole are within the permafrost, have a high ice content and that ice is thawed (Jessop 1970; Judge 1973b). Three examples of this return to equilibrium are shown in Figure 2 for northern holes drilled in different lengths of time and in rocks of differing porosities. All three wells were completed in a similar fashion, being abandoned below and up to the base of the surface casing and the mud above displaced with arctic diesel fuel. The figure shows the change of temperature at a specific depth with time since the completion of the hole: t_1 is the drilling time below the depth under consideration and t_2 the time interval between a temperature measurement and the time that a particular depth was reached. The intercept on the vertical axis is the probable equilibrium temperature.

Both the Winter Harbour and Reindeer wells were drilled to approximately 3800 metres in 180 to 190 days. Four months after drilling, when the cable was installed in the Winter Harbour well, the temperatures in the permafrost section were already below 0°C and the geothermal gradient partly reestablished. This was not true however of the Reindeer well. When a cable was installed in this well six months after its completion, temperatures in the entire section of the hole between 18 metres and 323 metres, i.e. most of the permafrost section, were between -0.1°C and -0.4°C. The difference between the two wells lies in the high rock porosity in the Reindeer well. Below the permafrost section the return to equilibrium in the Reindeer well is similar to that in the entire Winter Harbour well. Neither well will be within 0.05°C of equilibrium until after the year 2000. Other boreholes in the north which took less time to drill to shallower depths and in rocks of low porosity have returned to equilibrium much more rapidly. The North Cath well shown was completed in 43 days to a total depth of 2100 metres through low porosity rocks.

Permafrost Thickness and Distribution

Brown (1967) summarised permafrost thicknesses measured in Canada prior to 1967 and Ferriens (1965) made a similar compilation for Alaska prior to 1965. Figure 3 summarizes, in metres, the new measurements added to theirs. Some of the previously reported results were based on observations of the presence of visible ice in recovered samples or on the loss of drilling fluid rather than temperature alone, on which the new observations are based. Very few of these measurements are based on observed equilibrium temperatures but are reasonable estimates based on extrapolation to equilibrium as mentioned in the previous section.

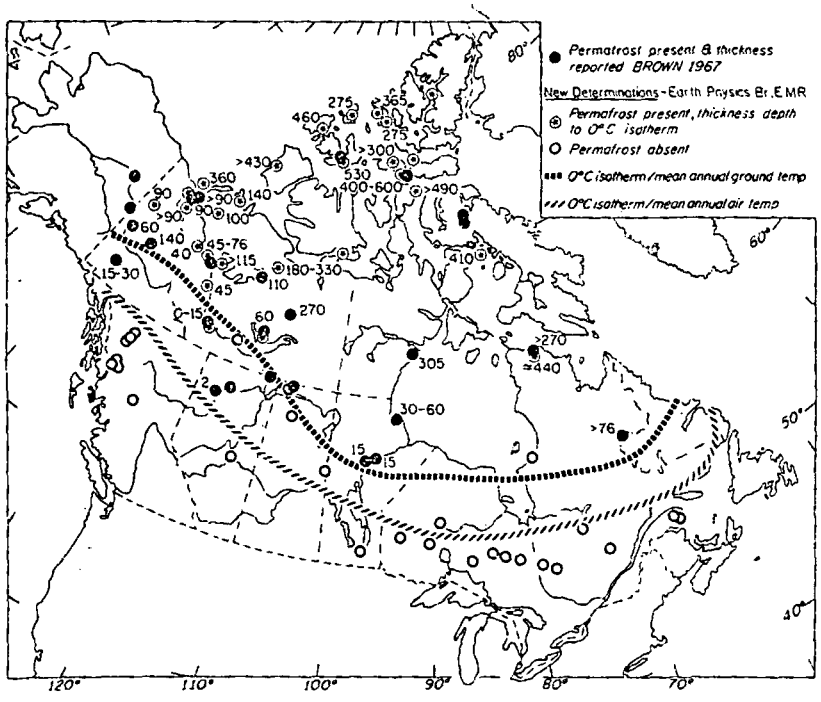

Fig. 3. Permafrost thickness in Canada.

At present the thickest permafrost measured in Canada is 530 metres at Winter Harbour in a well only 1000 metres from the present shoreline. The maximum observed thickness in North America is 600 metres measured by Lachenbruch (1972) at Prudhoe Bay in Alaska. Presently determined onshore thicknesses in the Arctic Islands range from 200 metres within a few tens of metres of a shoreline to 530 metres. Thinner permafrost, or none, is to be expected beneath the waters of the Arctic

channels and thicker permafrost, perhaps as high as 1000 metres, on the Arctic Platform, in view of its low heat flows, low surface temperatures and high thermal conductivities. It is also apparent that thick permafrost is not confined to the Arctic Islands. A thickness of 400 metres is projected in northern Quebec based on temperatures measured to 260 metres, a thickness of 360 metres measured at two sites on Richards Island in the Mackenzie Delta and a thickness of 330 metres at the Muskox Intrusion south of Coppermine.

In more southerly areas, such as along the Mackenzie Valley, the distribution of the thinner permafrost is very complex. Small lateral changes of surface temperature due to changes in vegetation cover, moisture content and snow cover cause wide variations in permafrost thickness and temperatures. This is discussed in more detail in Judge (1973c).

Distribution of Terrestrial Heat Flow

Published terrestrial heat flow values in Canada vary from 0.6 to 2.1 μcal cm^{-2} sec^{-1} uncorrected for the effects of the Pleistocene ice-sheets. Although 33 borehole values have been published for Canada, only 4 of these are in the north. The published sea-bottom measurements in the Western Queen Elizabeth Islands augment these measurements, although assuming the values to be undisturbed is questionable. Judge (1973a) has shown all these values both uncorrected and corrected for Pleistocene effects. Corrected values for the Canadian Shield lie between 0.6 and 1.3 with a mean of 1.0 ± 0.2. In contrast with this result, values over the Great Plains and Cordillera of western Canada vary from 1.6 to 2.0 and from Maritime Canada from 1.0 to 1.7. Further subdivision of the published variations reveals very little difference between the exposed Grenville and Superior provinces of the Shield, with the exception of northern Quebec where heat flows are low. However, the few measurements from the Churchill province suggest a heat flow 25% higher than that of the Grenville and Superior provinces. Judge (1972) found no significant difference between the heat flow on exposed rocks of the Grenville province and those covered by 1500 metres of Paleozoic sedimentary rocks, whereas Garland and Lennox (1962) measured a heat flow near Edmonton, where 3 kilometres of sediments are present above the basement, some 25% higher than on the exposed basement.

Polyak and Smirnov (1968) and Roy et al (1968) have suggested heat flow to be typical of certain regions. Verma and Hamza (1969) have suggested that a relationship exists between heat flow and the age of basement rocks. In a crude fashion the divisions of the Shield, both exposed and unexposed, can be transferred to the Arctic Platform, composed of Precambrian rocks either exposed or overlapped by a thin as-

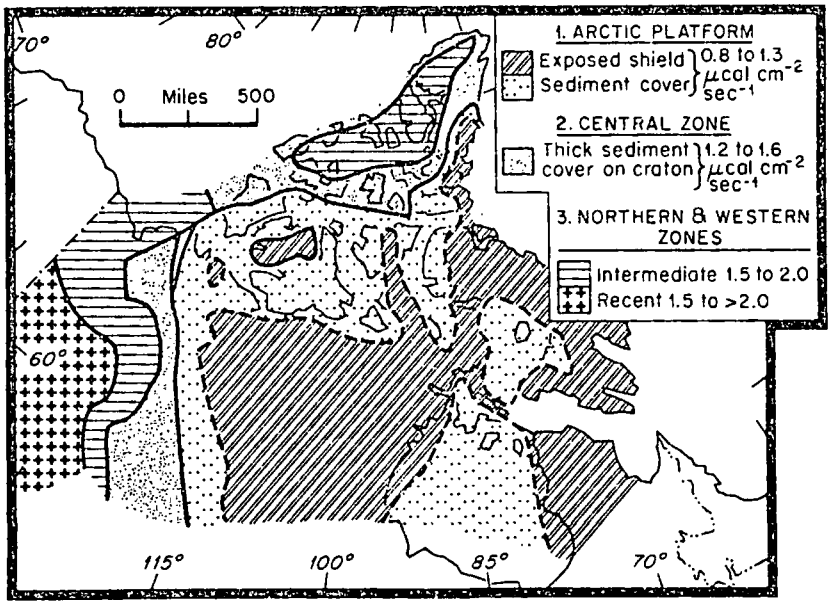

Fig. 4. Suggested regional heat-flow distribution in northern Canada.

semblage of lower and middle Paleozoic rocks. Similarly, using Thorsteinsson and Tozer's (1969) description of the tectonic framework of the north, comparisons may be made with other parts of Canada. The suggested regional heat flow distribution is shown in Figure 4.

The heat flow is expected to be lowest on the Arctic Platform where the basement has not been reactivated since Precambrian time and highest in the Sverdrup Basin where there is evidence of Tertiary igneous activity. Values probably vary from 0.8 to 1.3 on the Arctic Platform, 1.2 to 1.6 along the bounding sedimentary basin, and 1.5 to 2.0 in the Sverdrup Basin.

Tests of Validity of Proposed Heat Flow Distribution

Published values of heat flow in the north are 1.3 at Coppermine and Eldorado on the exposed shield platform, 1.3 at Resolute on the bounding basin and 2.0 at Norman Wells in the western region. The sea-bottom values in the vicinity of Mould Bay vary from 0.6 to 1.7 at the boundary of the Sverdrup Basin and the Central Zone. The low values towards Banks Island may represent an extension of the Arctic Platform.

Judge (1973a) suggested that, in a simple fashion, knowledge of the surface temperature, the subsurface lithology and the heat flow at a location could be used to predict permafrost thickness and distribution. This

argument can be turned around and the permafrost thickness, if undisturbed by a nearby shoreline, used to determine a local geothermal gradient. If some knowledge is possessed of the lithology of the formations penetrated, their thermal properties may be estimated and a rough heat flow calculated. These arguments are only applicable to regions with low surface temperatures or thick permafrost. In regions of thin permafrost such as the Mackenzie Valley, lateral variations of a few degrees in surface temperatures and recent changes of climate confuse the picture considerably.

Measurements completed to date suggest that the permafrost thickness in the Sverdrup Basin is at least 30% less, on average, than that in the Central Zone. Average thermal conductivities of the carbonates and sandstones of the Central Zone are probably not greatly different to those of the frozen clastics in the Sverdrup Basin. Thus the results are consistent with the proposed distribution. Likewise the measured thicknesses on the northern Shield and Arctic Platform are consistent with the proposed distribution.

Recently heat flow measurements have been completed at four sites on the mainland of north-western Canada. (Judge, in preparation). The values found were close to 2.0 in the northern Yukon, the Anderson Plain and Cape Bathurst east of the Mackenzie Valley. These results reinforce the suggested general distribution but also narrow the Central Zone on the western mainland.

Further holes are being acquired when possible and the programme of measuring temperatures and conductivities continued in an attempt not only to measure the thickness of permafrost but also to understand its genesis and distribution in relation to heat flow, thermal conductivity and surface temperature history.

Bibliography

Bremner, P. C., 1955, Diamond drilling in permafrost at Resolute Bay, N.W.T.: Dom. Obs. Canada, Pub. 16, p. 365-390.

Brown, R. J. E., 1967, Permafrost map of Canada: Canada, Nat. Res. Council, Div. Bldng. Res., Pub. No. 9769.

Cheremensky, G. A., 1962, The time of re-establishing the thermal conditions disturbed by drilling a borehole: Akad. Nauk SSSR, Izv., Ser. Geofiz., p. 1801-1805.

Ferriens, O. J., 1965, Permafrost map of Alaska: U.S. Geol. Surv., Misc. Geol. Invest., Map I-445.

Garland, G. D., and Lennox, D. H., 1962, Heat flow in western Canada: Geophys. Jour., v. 6, p. 245-262.

Jaeger, J. C., 1961, The effect of the drilling fluid on temperatures measured in boreholes: Jour. Geophys. Res., v. 66, p. 563-569.

Jessop, A. M., 1970, How to beat permafrost problems: Oilweek, Jan. 12, 1970, p. 22-25.

Judge, A. S., 1972, Geothermal measurements in a sedimentary basin: Ph.D. Thesis, University of Western Ontario.

——, 1973a, The prediction of permafrost thickness: Can. Geotech. Jour., v. 10, p. 1-11.

——, 1973b, Deep temperature observations in the Canadian North: Proc. Second. Int. Permafrost Conf., Yakutsk; Nat. Acad. Sci. (U.S.A.).

——, 1973c, The thermal regime of the Mackenzie Valley: observation of the natural state; Government of Canada, internal report to the Environmental — Social Committee on Northern Pipelines, 170 p.

Lachenbruch, A. H., 1957, Thermal effects of the ocean on permafrost: Bull. Geol. Soc. Amer., v. 68, p. 1515-1530.

——, 1972, Geological Survey research 1971 — geothermal studies: U.S. Geol. Surv., Prof. Paper 750-A, p. 111.

Law, L. K., Paterson, W. S. B., and Whitham, K., 1965, Heat flow determinations in the Canadian Arctic Archipelago: Can. Jour. Earth Sci., v. 2, p. 59-71.

Misener, A. D., 1955, Heat flow and depth of permafrost at Resolute Bay, Cornwallis Island, N.W.T.: Trans. Amer. Geophys. Union, v. 36, p. 1055-1060.

Polyak, B. G., and Smirnow, Ya. B., 1968, Relationship between terrestrial heat flow and tectonics of continents: Geotectonics, v. 4, p. 205-214.

Roy, R. F., Blackwell, D. D., and Birch, F., 1968, Heat generation of plutonic rocks and continental heat flow provinces: Earth Planet. Sci. Let., v. 5, p. 1-12.

Thorsteinsson, R., and Tozer, E. T., 1969, Geology of the Arctic Archipelago, *in* Douglas, R. J. W., *ed.*, Geology and economic minerals of Canada: Geol. Surv. Canada, Econ. Geol. Rept. no. 1, 5th ed., chap. 10.

Verma, V. M. and Hamza, R. K., 1969, The relationship of heat flow with age of basement rocks: Bull. Vulcanol., v. 33, p. 123-152.

Whitham, K., 1963, An anomaly in geomagnetic variations at Mould Bay in the Arctic Archipelago of Canada: Geophys. Jour., v. 8, p. 26-45.

Judge, A. S., 1972, Geothermal measurements in a sedimentary basin: Ph.D. Thesis, University of Western Ontario.

——, 1973a, The prediction of permafrost thickness: Can. Geotech. Jour., v. 10, p. 1-11.

——, 1973b, Deep temperature observations in the Canadian North: Proc. Second. Int. Permafrost Conf., Yakutsk; Nat. Acad. Sci. (U.S.A.).

——, 1973c, The thermal regime of the Mackenzie Valley: observation of the natural state; Government of Canada, internal report to the Environmental — Social Committee on Northern Pipelines, 170 p.

Lachenbruch, A. H., 1957, Thermal effects of the ocean on permafrost: Bull. Geol. Soc. Amer., v. 68, p. 1515-1530.

——, 1972, Geological Survey research 1971 — geothermal studies: U.S. Geol. Surv., Prof. Paper 750-A, p. 111.

Law, L. K., Paterson, W. S. B., and Whitham, K., 1965, Heat flow determinations in the Canadian Arctic Archipelago: Can. Jour. Earth Sci., v. 2, p. 59-71.

Misener, A. D., 1955, Heat flow and depth of permafrost at Resolute Bay, Cornwallis Island, N.W.T.: Trans. Amer. Geophys. Union, v. 36, p. 1055-1060.

Polyak, B. G., and Smirnow, Ya. B., 1968, Relationship between terrestrial heat flow and tectonics of continents: Geotectonics, v. 4, p. 205-214.

Roy, R. F., Blackwell, D. D., and Birch, F., 1968, Heat generation of plutonic rocks and continental heat flow provinces: Earth Planet. Sci. Let., v. 5, p. 1-12.

Thorsteinsson, R., and Tozer, E. T., 1969, Geology of the Arctic Archipelago, *in* Douglas, R. J. W., *ed.*, Geology and economic minerals of Canada: Geol. Surv. Canada, Econ. Geol. Rept. no. 1, 5th ed., chap. 10.

Verma, V. M. and Hamza, R. K., 1969, The relationship of heat flow with age of basement rocks: Bull. Vulcanol., v. 33, p. 123-152.

Whitham, K., 1963, An anomaly in geomagnetic variations at Mould Bay in the Arctic Archipelago of Canada: Geophys. Jour., v. 8, p. 26-45.